

PAN-EUROPEAN SOIL EROSION RISK ASSESSMENT

Contract no. QLK5-CT-1999-01323
Third Annual Report (1 Apr '02 - 1 Apr '03)

Edited by Anne Gobin and Gerard Govers



Laboratory for Experimental Geomorphology
Katholieke Universiteit Leuven



School of geography
University of Leeds



Estacion Experimental de Zonas Aridas, Almeria
Consejo Superior de Investigaciones Cientificas



Unité de Science du Sol, Orléans
Institut National de la Recherche Agronomique



European Soil Bureau, Environment Institute
DG - Joint Research Centre, Ispra



Agricultural University of Athens



International Soil Reference and Information Centre
Wageningen University and Research Centre

TABLE OF CONTENTS

CHAPTER 1 INTRODUCTION.....5

1.1. PREAMBLE.....5

1.2. PROJECT OBJECTIVES5

1.3. PROJECT PARTICIPANTS5

1.4. RESEARCH ACTIVITIES AND WORKPLAN7

1.5. OUTLINE9

CHAPTER 2 UNIVERSITY OF LEEDS.....11

2.1. SUMMARY OF PROGRESS IN THE REPORTING PERIOD11

2.2. INTRODUCTION11

2.3. PESERA CODE.....13

2.3.1. PESERA-RDI point code 14

2.3.2. PESERA-RDI_GRID 14

2.4. HIGH RESOLUTION CALIBRATION DATA.....18

2.4.1. Data requirements and data format for the implementation of the PESERA model at 1km and higher resolution: 20

2.5. MODEL APPLICATION21

2.5.1. Model Execution 21

2.6. INTERNET APPLICATION23

2.7. PESERA DOCUMENTATION25

2.8. SUMMARY AND ISSUES TO BE ADDRESSED CONCLUSIONS.....25

2.8.1. The PESERA model, Current Situation: 25

2.8.2. Key data requirements/considerations: 26

CHAPTER 3 ESTACION EXPERIMENTAL DE ZONAS ARIDAS (EEZA), CSIC27

3.1. OBJECTIVES27

3.2. WP2: SYNERGETIC EFFECTS OF SPATIAL AND TEMPORAL VARIATION IN LAND ATTRIBUTES.....27

3.2.1. Work carried out during the reporting period 27

3.2.2. Background and objectives 28

3.2.3. Simulation study using LISEM 30

3.2.4. Implications for the PESERA model 42

3.2.5. Conclusions 47

3.2.6. Work to be done by the end of the project 47

3.3. WP3: CALIBRATION AND VALIDATION AT RAMBLA HONDA FIELD SITE.....48

3.3.1. Work carried out during the reporting period 48

3.3.2. Evaluation of PESERA model performance	49
3.3.3. Pesera parameter estimation	55
3.4. WP4: VALIDATION AT SE SPAIN AND COMPARISON WITH CSIC-EEZA APPROACH	59
<u>CHAPTER 4 KATHOLIEKE UNIVERSITEIT LEUVEN</u>	<u>60</u>
4.1. ROLE AND CONTRIBUTION	60
4.2. WP1: LAND USE AND VEGETATION GROWTH	60
4.2.1. The plant growth model	61
4.2.2. Plant growth parameters database	62
4.2.3. Plant cover for arable crop groups	65
4.2.4. Spatialising agricultural land use and dominant arable crops	67
4.2.5. Land use scenarios	72
4.3. WP3: CALIBRATING AND VALIDATING THE PESERA MODEL WITH HIGH RESOLUTION MEASUREMENTS	73
4.3.1. Testing the PESERA approach with long-term soil erosion plot data	73
4.3.2. Validating the PESERA map with high resolution observations	77
4.4. END-USER INVOLVEMENT	80
4.4.1. The European Environment Agency	80
4.4.2. The ENRISK Project	81
4.4.3. The SOWAP Project	81
<u>CHAPTER 5 INRA-ORLÉANS</u>	<u>82</u>
5.1. ROLE AND CONTRIBUTION	82
5.2. ORIGINAL OBJECTIVE OF WP 4 AND WP5	82
5.3. RESEARCH ACTIVITIES DURING THE THIRD REPORTING PERIOD	82
5.3.1. WP5: Database development at European level	82
5.3.2. Regional approach for validation at low resolutions (WP4)	83
5.4. WORK PACKAGE MANAGEMENT ISSUES	90
5.4.1. Significant difficulties or delays experienced during the third reporting period	90
5.4.2. Sub-contracted work during the third reporting period	90
5.4.3. Deliverables	90
<u>CHAPTER 6 THE EUROPEAN SOIL BUREAU AT JRC</u>	<u>91</u>
6.1. ROLE AND CONTRIBUTION	91
6.2. SOIL WATER STORAGE CAPACITY	91
6.2.1. Soil Water Storage Capacity (SWSC)	91
6.2.2. Drainable Pore Space	92
6.2.3. Implementation	95
6.2.4. Spatial distribution of SWSC at European level	98
6.2.5. Future actions	101

<u>CHAPTER 7</u>	<u>INTERNATIONAL SOIL REFERENCE AND INFORMATION CENTRE (ISRIC).....</u>	<u>102</u>
7.1.	ROLE AND CONTRIBUTION	102
7.2.	ACTIVITIES DURING REPORTED PERIOD	102
7.2.1.	WP6: Data layers for scenario studies	102
<u>CHAPTER 8</u>	<u>AGRICULTURAL UNIVERSITY OF ATHENS.....</u>	<u>106</u>
8.1.	MAIN WORK CARRIED OUT DURING THE REPORTING PERIOD	106
8.2.	METHODOLOGY AND MAIN RESULTS OBTAINED	106
8.2.1.	WP7: Compilation of the user’s manual for the PESERA model	106
8.2.2.	WP7: End-users of the PESERA model	107
8.2.3.	WP4: Example of regional model application	108
<u>CHAPTER 9</u>	<u>CONCLUSIONS</u>	<u>114</u>
9.1.	OVERALL CONCLUSIONS.....	114
9.2.	SPECIFIC CONCLUSIONS.....	114
9.2.1.	WP1: Modelling Strategy	114
9.2.2.	WP2: Spatial and temporal resolution linkages	115
9.2.3.	WP3: Calibration and validation at high resolution	115
9.2.4.	WP4: Validation at low resolution	115
9.2.5.	WP5: Application at the European scale	116
9.2.6.	WP6: Scenario analysis	116
9.2.7.	WP7: End-user Involvement	116
9.3.	PERSONNEL, TIMEFRAME AND FINANCES.....	116
<u>CHAPTER 10</u>	<u>REFERENCES.....</u>	<u>118</u>
<u>CHAPTER 11</u>	<u>APPENDIX 1 - MODEL SPECIFICATIONS</u>	<u>121</u>
11.1.	THE VEGETATION COVER TABLE (<i>EROS022</i>)	121
11.2.	DATA REQUIREMENTS FOR THE PESERA/RDI MODEL (<i>VER. EROS022/PESERA-GRID023</i>).....	122
11.3.	RUNNING MODULAR COMPONENTS OF PESERA-RDI_GRID.....	123
11.3.1.	EXTRACTING	123
11.3.2.	PREPROCESSING	124
11.3.3.	PESERA_GRID	124
11.3.4.	POST-PROCESSING	124
11.4.	OUTPUT GRIDS.....	125
<u>CHAPTER 12</u>	<u>APPENDIX 2 – DESCRIPTION OF EUROPEAN WIDE DATASETS.....</u>	<u>126</u>

12.1. GENERAL	126
12.2. RELIEF PARAMETERS	127
12.3. METEOROLOGICAL PARAMETERS	127
12.4. SOIL PARAMETERS	130
12.5. WATER CONTENT:	130
12.6. LAND COVER PARAMETERS	131
<u>CHAPTER 13</u> <u>APPENDIX 3 – FARM STRUCTURE SURVEY</u>	133
13.1. SPATIAL LINK OF FARM STRUCTURE SURVEY (FSS) DATA	133
13.2. CLASSIFICATION	133
<u>CHAPTER 14</u> <u>APPENDIX 4 - WATER CONTENT LAYERS</u>	135
14.1. NEW CALCULATIONS	137
14.2. AWC_SUB2 DERIVED FROM TEXTURE AND SUBSOIL PACKING DENSITY	139

CHAPTER 1 INTRODUCTION

1.1. PREAMBLE

This document is the third annual report for the PESERA project, which details the specific contributions of each research group for the period 1st April 2002 to 1st April 2003. The project (QLK5-CT-1999-01323) commenced on 1 April 2000 and is scheduled to run for 36 months, with an additional cost-neutral extension of 6 months. A physically based and spatially distributed model has been developed, and calibrated to quantify soil erosion in a nested strategy of focussing on environmentally sensitive areas relevant to a European scale. The model's robustness and flexibility has been demonstrated through its performance at different resolutions and across different agro-ecological zones. During the cost-neutral extension the emphasis will be on the model's relevance to policy makers through scenario analysis and further validation.

1.2. PROJECT OBJECTIVES

The overall objectives of the project are threefold:

1. to develop a physically based and spatially distributed model for quantifying soil erosion and assess its risk across Europe, attach a prediction error to the model output, and calibrate the model with existing information on soil erosion rate measurements,
2. to validate the developed model across different agro-ecological zones at catchment, country and Pan-European level, and compare the model output to other methods for erosion risk assessment, and
3. to ensure the relevance of the approach to end-users through multiple applications and demonstrations, impact assessment, scenario analysis, and development of a user-friendly interface.

1.3. PROJECT PARTICIPANTS

The Project consortium consists of seven contractual partners, residing in seven different countries of the European Union (Table 1-1).

Table 1.1: List of participants

Participant Organisation (No-Role-Acronym)	Address of department and personnel involved
Katholieke Universiteit Leuven (P1-CO-KULEUVEN)	Laboratory for Experimental Geomorphology Redingenstraat 16, 3000 Leuven, BELGIUM Tel: (32-16)326433; Fax: (32-16)326400 anne.gobin@geo.kuleuven.ac.be olivier.cerdan@geo.kuleuven.ac.be gerard.govers@geo.kuleuven.ac.be
University of Leeds (P2-CR-UNIVLEEDS)	School of geography Woodhouse Lane, LS6 4DX Leeds, UK Tel: (44-113)2333310; Fax: (44-113)233 6758 mike@geog.leeds.ac.uk (Mike Kirkby) b.irvine@geog.leeds.ac.uk (Brian Irvine)
Institut National de la Recherche Agronomique (P3-CR-INRA)	Unité de Science du Sol BP 20619 Domaine de Limère, 45166 Olivet Cedex, FRANCE Tel: (33-2)38417845; Fax: (33-2)38417869 Dominique.King@orleans.inra.fr Yves.Le-Bissonnais@orleans.inra.fr Joel.Daroussin@orleans.inra.fr
Commission of the European Communities - DG Joint Research Centre (P4-CR-CEC/DGJRC)	European Soil Bureau, Environment Institute, TP 262, Via E. Fermi, Ispra (VA) 21020, ITALIA Tel: (39-332) 786 330; Fax: (39-332) 789 936 robert.jones@jrc.it luca.montanarella@jrc.it
Agricultural University of Athens (P5-CR-AUA)	Agricultural University of Athens Iera Odos 75, 118-55 Athena, GREECE Tel: (00301)5294821, Fax: (00301)5294832 Nyassog@hol.gr (Nicholas Yassoglou) Lsos2kok@auadec.aua.gr (Costas Kosmas)
Consejo Superior de Investigaciones Cientificas (P6-CR-CSIC)	Estacion Experimental de Zonas Aridas (EEZA) General Segura 1, 04001 Almeria, SPAIN Tel: (34-950) 276400; Fax: (34-950) 277100 Puigdefa@eeza.csic.es (Juan Puigdefabregas) Matthias.Boer@eeza.csic.es (Matthias Boer) Gabriel@eeza.csic.es (Gabriel del Barrio)
International Soil Reference and Information Centre (P7-CR-ISRIC)	International Soil Reference and Information Centre PB 353, Duivendaal 7-9, 6700AJ Wageningen, THE NETHERLANDS Tel: (31-317)471715; Fax: (31-317)471700 Vanlynden@isric.nl (Godert van Lynden) Mantel@Isric.nl (Stephan Mantel)

1.4. RESEARCH ACTIVITIES AND WORKPLAN

In order to achieve the objectives, three major phases and seven Work Packages (WP) covering the three phases were identified (Figure 1-1). A time schedule is provided in Figure 1-2.

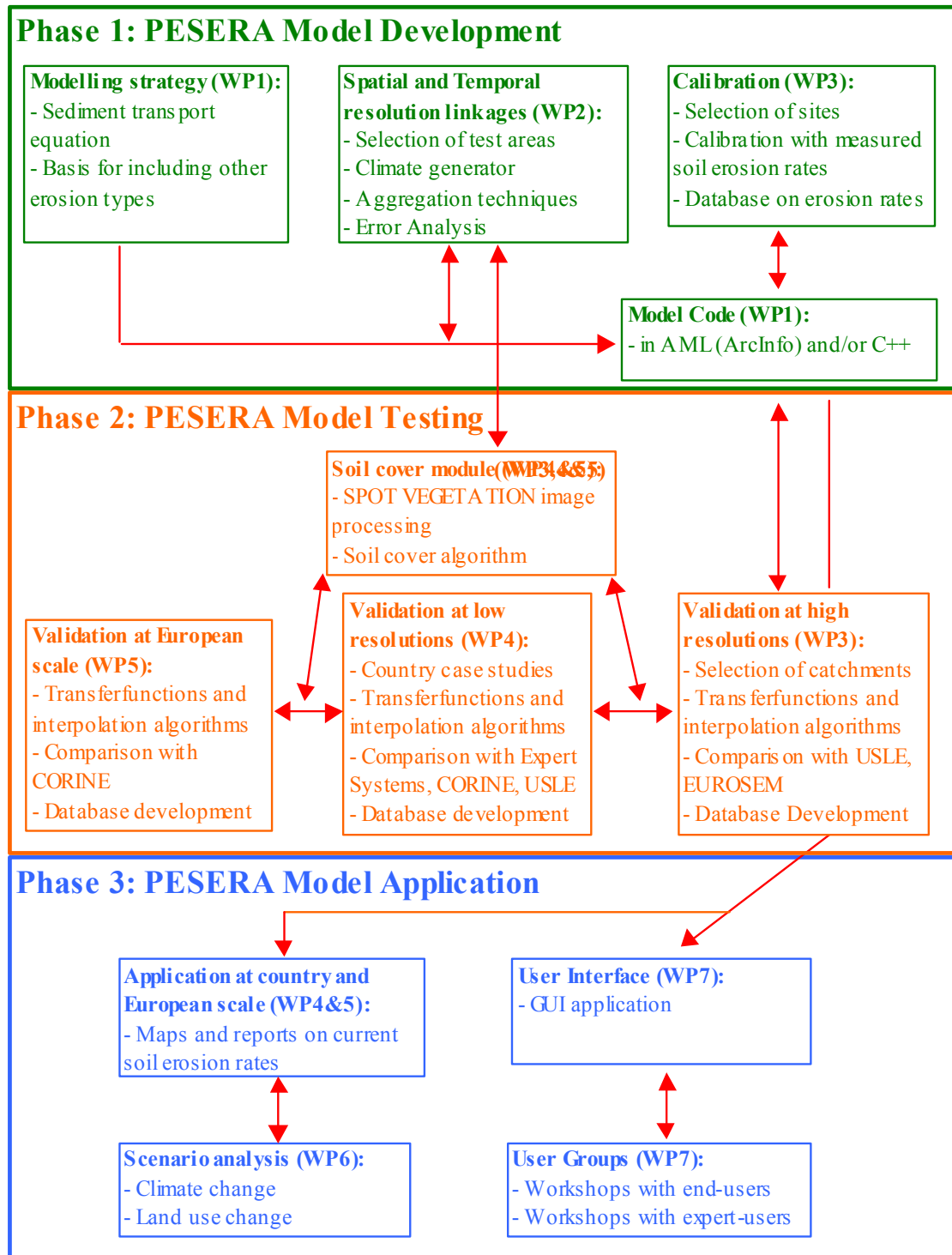


Figure 1.1: Project scientific structure

Phase 1 focuses on the development of a process-based and spatially distributed to quantify soil erosion across Europe. The model is intended as a regional diagnostic tool, replacing comparable existing methods, such as the Universal Soil Loss Equation, which lack a sound physical basis and compatibility with higher resolution models. This will entail the development of a modelling strategy, sensitivity analysis, temporal and spatial aggregation/disaggregation techniques, error analysis and calibration with the aid of soil erosion rate measurements across Europe. A database will be compiled on existing soil erosion measurements from plots and small catchments across Europe.

Phase 2 deals with validation and comparison with other erosion risk assessment methods across Europe and at three different resolutions (catchment, country and Pan-European scale). Linking existing datasets to model parameters through transfer functions, interpolation algorithms and statistical methods will demonstrate the model's flexibility and robustness. The use of 10-daily vegetation cover from NDVI and SPOT VEGETATION/HRVIR will provide seasonal variations in soil erosion. Accurate spatial databases will be compiled from existing information on factors affecting erosion in Europe (climate, soil, topography, land cover) and upgraded using satellite imagery and computational techniques.

Phase 3 deals with application of the model, development of a user-friendly interface and establishment of user-groups at both national and European level. Quantification of the erosion problem enables evaluation of the possible effects of future changes in climate and land use, scenario analysis and impact assessment according to cost-effectiveness, technical feasibility, social acceptance and implementability. End-user groups, expert-user groups and research networks will actively participate in model testing and in evaluating the Project's progress and results.

1.5. OUTLINE

Chapter 2 provides a summary of the work undertaken by the University of Leeds (Uleeds) on the development of the modelling strategy and model code. The model code for grid applications and the resulting Pan-European application at a 1 km² resolution are discussed. A web-based version has been elaborated upon.

Chapter 3 provides a summary of the work undertaken by Consejo Superior de Investigaciones Científicas (CSIC), on synergetic effects of spatial and temporal variation in land attributes on hillslope erosion rates and implications for the PESERA soil erosion model. The PESERA model has been evaluated at the Rambla Honda field site in SE Spain.

Chapter 4 provides a summary of the work undertaken by the Katholieke Universiteit Leuven (KULeuven). An extensive database was created on agricultural parameters for the PESERA model and included planting dates for different crop groups, average monthly crop covers, spatialised of agricultural land use and dominant arable land uses across Europe. The long-term erosion measurements database has been used to evaluate the runoff generation and sediment transport equation, which are at the core of the PESERA model. The 1 km² PESERA map has been validated with an erosion rate observation and measurement database. Details on co-operations are provided.

Chapter 5 provides a summary of the work undertaken by INRA-Orléans on the completion of European-wide databases with the last version of all available parameters. A regional approach has been developed for validation at low resolutions. This regional approach was demonstrated with several data resolutions available for Normandie. The PESERA model has been compared with the French expert model for evaluating soil erosion.

Chapter 6 outlines the work undertaken by the European Soil Bureau at the Environment Institute of the Joint Research Centre (ESB/EI/JRC) on the development of the soil water storage capacity.

Chapter 7 provides a summary of the work undertaken by the International Soil Reference and Information Centre (ISRIC). ISRIC has performed several test-runs of the regional model, which has led to a user-friendly version of the model. Details are provided on the acquisition of scenario layers for climate and land use.

Chapter 8 provides a summary of the work undertaken by the Agricultural University of Athens (AUA). A draft user's manual has been compiled. A regional application of the model was accomplished for the island of Lesbos. End-user contacts have been maintained at the MEDRAP workshop.

Chapter 9 outlines general conclusions, specific conclusions and some general management observations.

Four appendices have been included in the general report: (1) model specifications, data requirements and modular components of the PESERA grid version; (2) technical notes on European-wide datasets; (3) Notes on Farm Structure Survey Data; and, (4) Details on soil water content layers.

A compilation of the following Project meetings is attached to the digital file: the 5th PESERA workshop, held at Leeds, the 6th PESERA workshop, held at Ispra, and the 7th PESERA workshop, held at Wageningen.

CHAPTER 2 UNIVERSITY OF LEEDS

Mike Kirkby, Brian Irvine, Jianhui Jin, Andy Turner

School of Geography
The University, Leeds LS2 9JT, UK

2.1. SUMMARY OF PROGRESS IN THE REPORTING PERIOD

There has been very substantial progress in getting the model into a form where it can be used by other partners, and the model has been distributed in a Beta-version to those requesting it. There has also been progress with developing a web-based version, which allows the scientific public to access the model on the web, and run the model for a window of up to about 100x100 km in a reasonable time, without compromising rights of access to the licensed data, and with the opportunity to set up simple land use or climate change scenarios.

There has also been progress in using the model at other scales, both at higher resolutions, for example in Normandy (50m) and at lower resolutions (5 km) for North Africa, making use of IIASA (International Institute for Applied System Analyses) global climate data and FAO soils map of the world. Some of these and our core results have been supplied for presentation to DISMED (for North Africa) and COP6 (for UNCCD) through Denis Peter.

2.2. INTRODUCTION

The PESERA-RDI model offers a methodology to assess regional soil erosion risk, providing a tool suitable for planning and policy makers at the national and continental scale. The physical basis of the model offers the potential to enhance future land degradation predictions, distinguishing between the effects of land-use and climatic changes. As the components are explicit within the model the sensitivity of changing environments can be explored.

The Regional Degradation Indicator (RDI) model is expanded in PESERA from the concepts of both MEDALUS and MODEM. PESERA-RDI thus offers an explicit theoretical response based on a simple and conservative erosion model, making use of land-use, topographic, soil and climatic data (Kirkby and Neale 1987, de Ploey et al 1991, Kirkby & Cox 1995). The PESERA-RDI_GRID coarse scale model distributes a point-based model across Europe generating a series of physically based estimates of potential monthly erosion at 1km grid resolution.

The model estimates ground cover, surface crusting, runoff and sediment transport, to give an estimate of water and sediment delivered to stream channels. The estimates are consistent

with finer scale erosion models for flow strips, evaluated at the slope base; and are integrated across the frequency distribution of storm magnitudes. The model is based on a partition of daily precipitation into Hortonian and saturation overland flow, subsurface flow and evapotranspiration. Hortonian overland flow, which is mainly responsible for soil erosion, is generated with respect to local soil and sub-surface moisture characteristics. Allowance is also made for snow accumulation and melting. The emphasis of the PESERA-RDI model is the prediction of hillslope erosion, and the delivery of erosion products to the base of each hillslope. Channel delivery processes and channel routing are explicitly not considered.

The PESERA-RDI approach has some similarity with the Revised Universal Soil Loss Equation (RUSLE) (Renard et al, 1991; Renard et al, 1997), but differs significantly by separating the roles of soil on infiltration and resistance to erosion, which provides an improved physical basis.

Preliminary model results are available, and forecasts are now being calibrated against runoff plot and small catchment data. A map of estimated erosion is displayed in Figure 2.1.

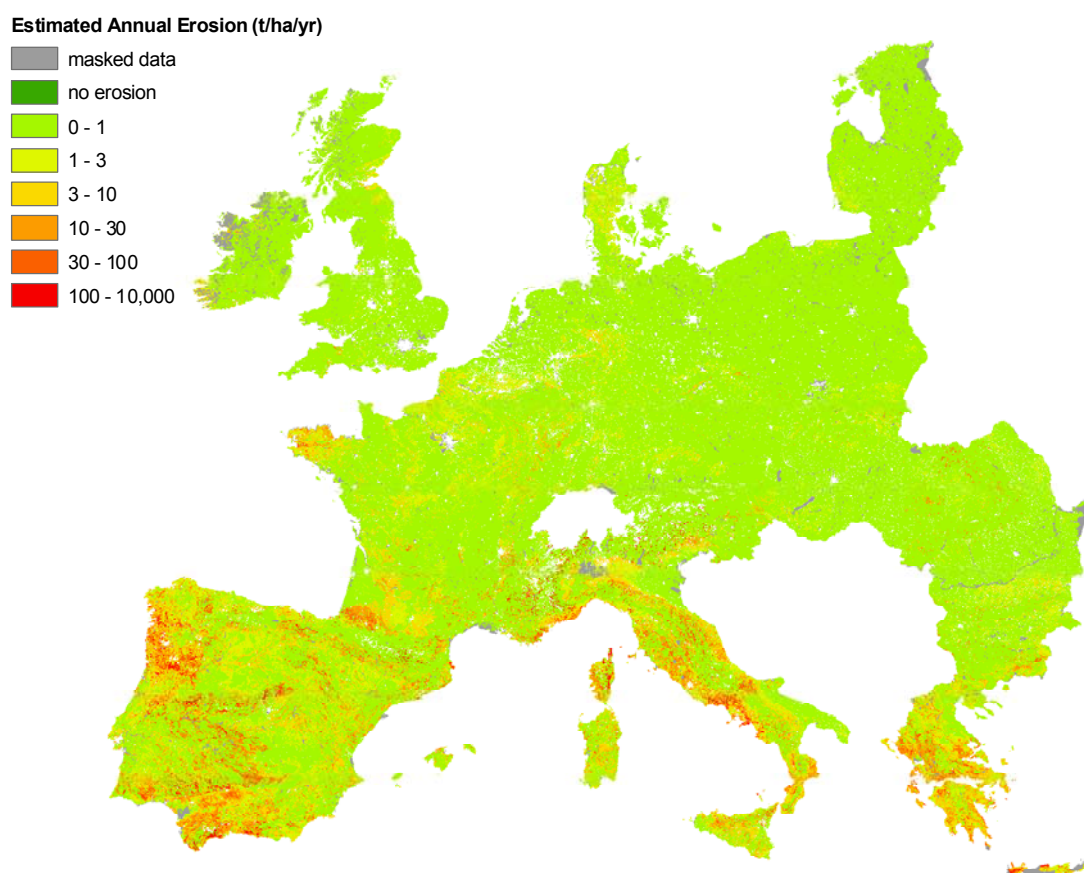


Figure 2.1: Estimated Erosion Risk for Europe at 1km resolution.

Although currently being applied at a 1 km resolution for Europe the model may be applied at other scales: at 50 - 250m to areas of particular concern and, at coarser resolution (5 - 10 km) data, globally, although with some inevitable degradation of quality.

As an addition to this work, a web–interface and model interface have been developed so that the public can run the RDI model and view the results. The web-interface can be accessed at: www.ccg.leeds.ac.uk/medact2/index

Although the model structure is set, as shown in Figure 2.2, consideration is required from other work packages before the model code is finalised.

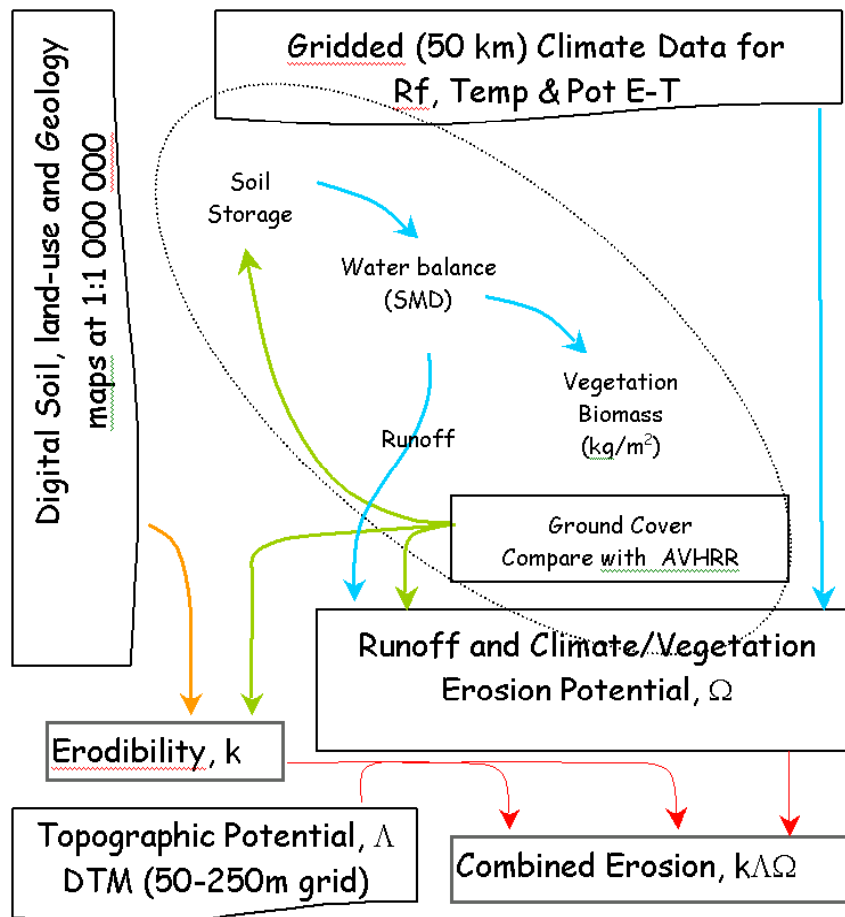


Figure 2.2: PESERA-RDI model structure, Data and Component Interaction.

2.3. PESERA CODE

The development of the PESERA-RDI model over the report period is summarised in Table 2.1.

Table 2.1: Summary of PESERA-RDI model development

Last 12 months	PESERA GRID upgraded from ver.111 to ver.032:
	Fortran development through to June/July 2002

	Optimising spatial potential October/November
	Initiated web and user interface
	Initial release (limited area)
Last 6 months	Completed/stabilised modular component
	Completed web and user interface
	RDI model update (ver. 112)
	PESERA-RDI_GRID: model update
	Preparation of calibration data where available
	Predicting future land-use: Neural Networks
	Preparations of Documentation and dissemination of model
	Dissemination of output in wider community: DISMED, COP6

2.3.1. PESERA-RDI point code

The most recent developments in the point code have been to include dual land-use, readily available water, water use efficiency, and a methodology to compare field measurements aiding high resolution validation. Final observations regarding spatial and temporal linkage and linkage between high and low resolution calibration remain to be incorporated.

2.3.2. PESERA-RDI_GRID

The PESERA-RDI_GRID code distributes point code across a spatial grid, enabling regional and continental estimates for soil erosion and derived intermediate components:

- available soil storage
- soil deficit
- snow accumulation and
- runoff (overland flow)
- vegetation cover

The modular version has been successfully applied in Athens and Wageningen. Although the model is not yet finalised European erosion surfaces and maps have been derived and disseminated. Calibration data has been derived for Hautie-Normandie and Southern Italy. High-resolution grids have been produced for Lesvos. Coding requirements that are identified from the point-code calibration and high resolution data will be incorporated in the GRID version. Additional, calibration data is proposed based on local data for Northern Italy, Almeria and Flanders.

2.3.2.1. Intermediate Outputs

The current version of the model relies on vegetation look-up tables. It is hoped to produce erosion surfaces and maps based on 'grown' vegetation allowing a fuller assessment of the performance of the vegetation growth model

Incorporating Land-use and Crop Growth

Current land-use categories are shown in Table 2.2. At its simplest the model will take crown cover from ‘look-up’ tables but the potential for growing crops to consider future scenarios is not fulfilled. The cover table may be acceptable under some land-use, (see Appendix 1).

Table 2.2: Land-use Categories

Code	Land-use	Covertime\$	Management	Cover\$
100	Artificial	-	-	
210	Arable	O (C)*	tillage	B, S, W*
221	Vines	O	-	
222	Fruit trees	O	-	
223	Olives	O	-	
231	Pastures	X	-	
240	Heterogeneous agriculture	O	-	
310	Forest	O	-	
320	Scrub	O	-	
330	Bare	Z	-	
334	Degraded natural land	O	-	
400	Water bodies	-	-	

*Where C is Cereal-Dry Farmed, S is Spring Sown Arable, W is Winter Sown Arable, and B is Both Spring and Winter Sown Arable Crops (in 1 year).

However, where crop types and management practice are available the model can be extended to incorporate such input. Such data is required to apply the proposed crop factor, Figure 2.3, which requires a planting date.

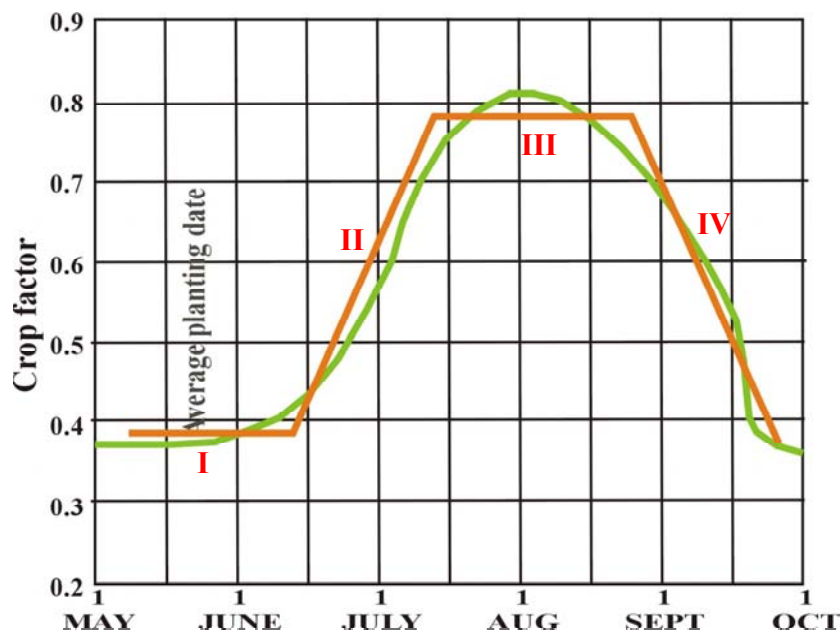


Figure 2.3: Variation of maize factor during the growing season (green) and simplified plant characteristic curve according to the different growth stages (initial stage: I / crop development: II / mid-season: III / late season: IV), expressed in actual days of year for Iowa, USA. (Gobin, 2002)

Assuming a prior knowledge of crop type and planting/harvesting regimes the GrowVeg routine simulates vegetation growth for the purpose of erosion estimates. AVHRR or VEGETATION data, where available, can be used to calibrate the performance of the GrowVeg output.

Although arable crops may appear to pose the greatest challenge, the incorporation of varying cultivation techniques in other crops, i.e vines, olives, may have an influence on erosion estimates. However, the application in the model may be simplified to an estimate of secondary cover. The influence of physical techniques, contour ploughing and terracing is not explicit in the model.

The intermediate outputs remain valid for further use beyond the output of PESERA. Soil deficit and runoff are shown in Figure 2.4. Soil moisture deficit predictions suggest that the drainage parameter (zm) should be re-evaluated in the GRID version as the influence of slope on drainage is not considered.

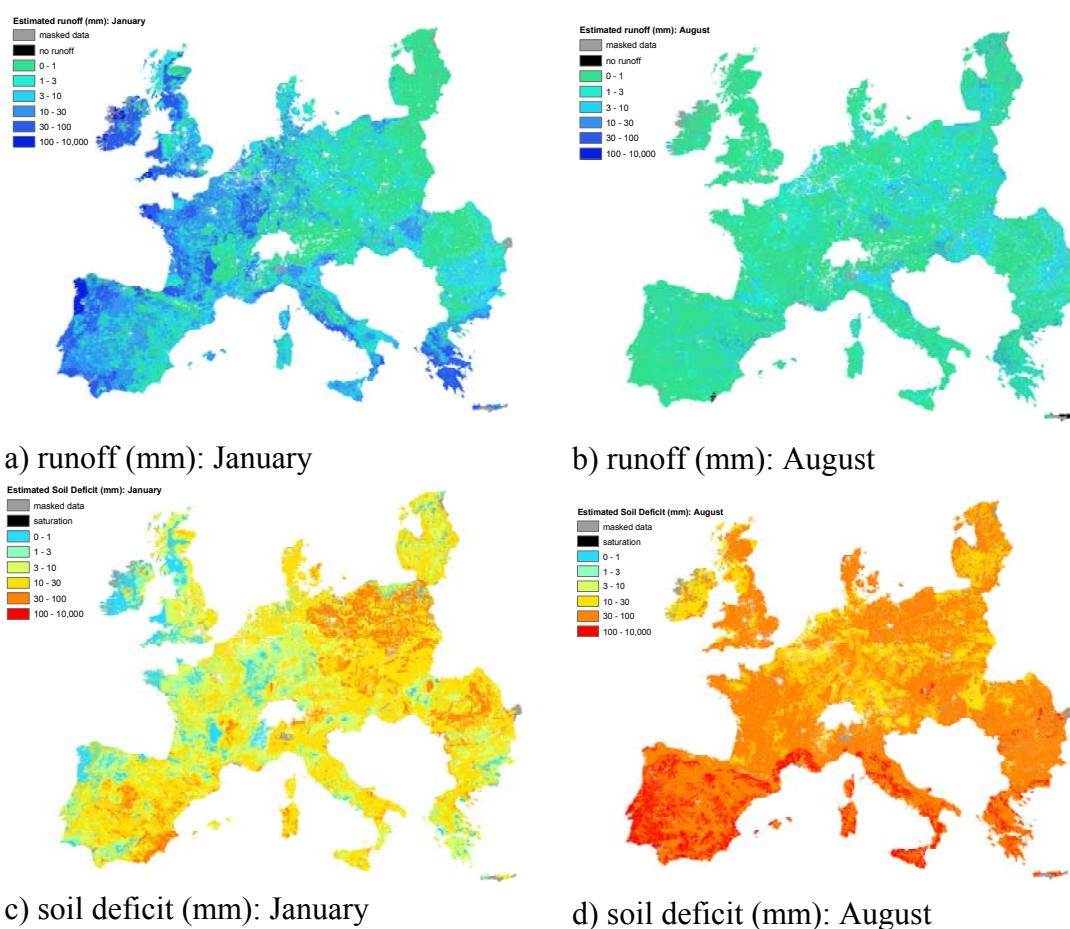


Figure 2.4: Intermediate Output from PESERA-RDI_GRID

Fortran Code Development

The core of the PESERA_RDI-GRID model is developed in Fortran90, accommodating additional complexities of 1-D PESERA-RDI (eros022 & eros112) and is likely to be available to run on both UNIX and DOS platforms. Data extraction, pre-processing and output modules are required to facilitate the execution of the model code. Such extraction and output modules were not initially considered as an integral part of the PESERA-RDI_GRID model, nor was the use of the execution of the code on a DOS platform.

Therefore, additional to the core model development, the following points were identified and actioned.

the development of a user interface (identified through discussions with ISRIC) and the need to reduce memory demand to lower system requirements for running the model.

Run times have not been radically reduced but flexibility to spread the computational load has been radical allowing the code to run on more modest machines enabling European grids to run ‘overnight’.

The coding of the PERERA/GRID coarse scale model in Fortran90 was considered primarily an exercise in iteration management on a cell by cell basis and maintaining spatial continuity through data management. However, considerable investment has been made to ensure the code could operate on any reasonable platform. Both UNIX and DOS versions of the code can now be made available.

Input grids are combined into a single table with each row containing the required ‘cell’ data set, currently 93 values. The length of the table is relatively unrestricted. The reduced demand on RAM ensures the model operates on a greater number of machines allowing processing time to be split between available processors when considering the European scale.

The current single processor run time can be approximated by the percentage data cover of a tile multiplied by the observed reference tile value (9 / 7502 hrs.km⁻²) and the respective tile area. This approximates to 48hours for the European grid. Split between three processors a run can be achieved ‘overnight’. In general, high resolution grids, c.50m, have higher run times than the European grid as there is less ‘breaks’ in the data.

It is envisaged that these run times will be faster when applied to processors greater than 1.6GB

Consideration has been given to the potential for running the code over the internet. This is being applied within the framework of DesertLinks, Medaction and PESERA.

Preliminary results from the PESERA-RDI_GRID model are presented with no explicit calibration carried out.

The PESERA_GRID model has recently been updated to include the water use efficiency (WUE) and soil water storage capacity (SWSC). The SWSC grid has been prepared based on the calculation of SWSC, Equation 10, Jones et al (2002). On defining planting dates the WUE grids are readily constructed.

2.4. HIGH RESOLUTION CALIBRATION DATA

High resolution erosion surfaces and maps have been prepared where data has been available based on eros022.xls. Figures 2.5, 2.6 and 2.7 show erosion maps for Normandie (50m), Lesvos (100m) and Southern Italy (250m) respectively.

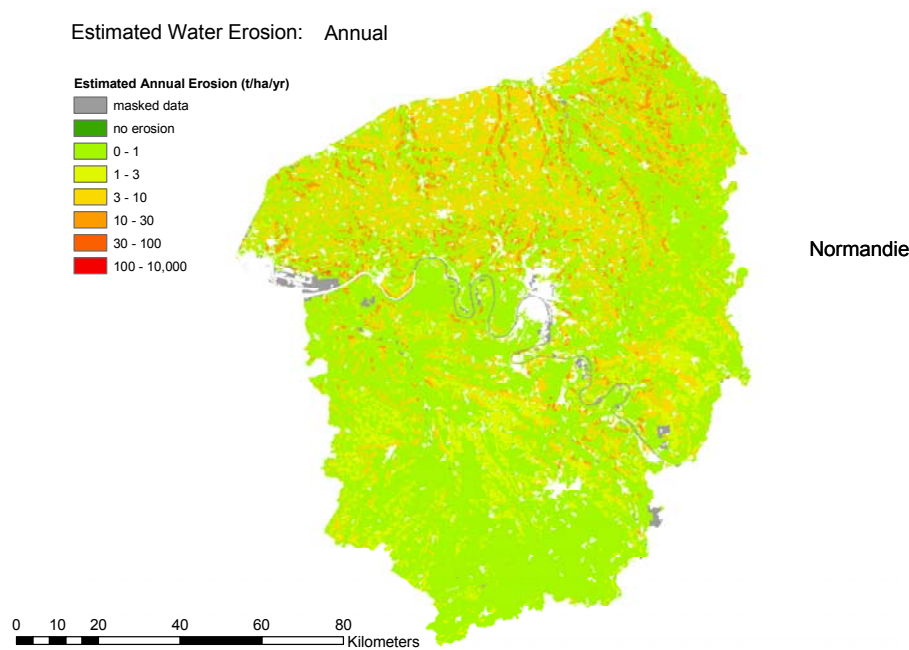


Figure 2.5: Estimated Annual Erosion, Normandie (50m grid resolution)

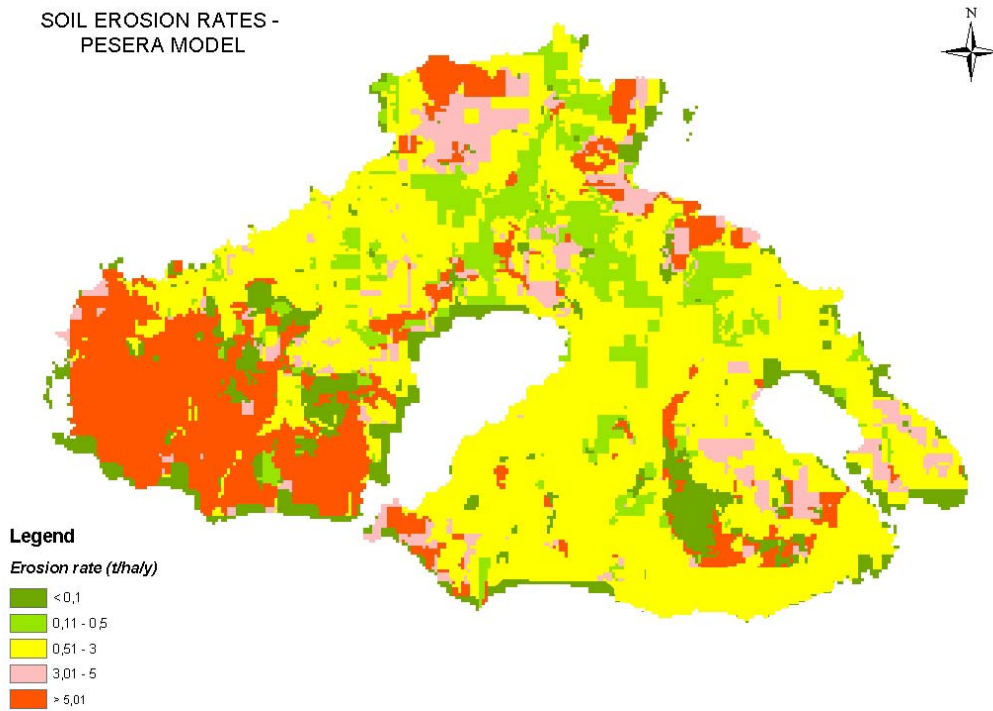


Figure.2.6: Estimated Annual Erosion, Lesvos (100m resolution) (courtesy of AU Athens)

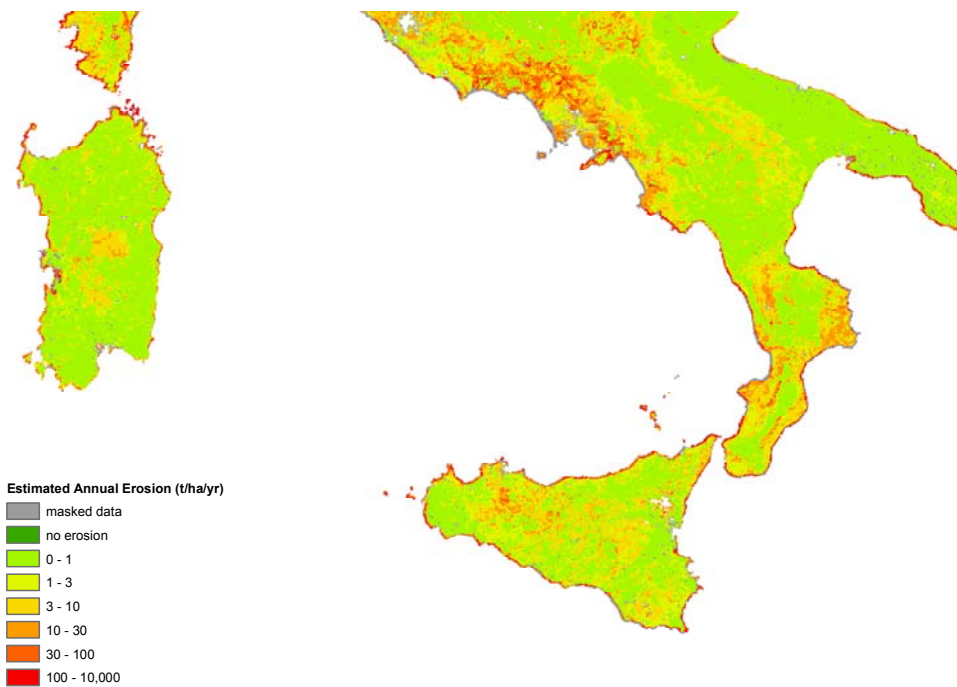


Figure 2.7: Estimated Annual Erosion, Southern Italy (250m resolution).

Further calibration erosion surfaces can be prepared with the data described in Table 2.3.

2.4.1. Data requirements and data format for the implementation of the PESERA model at 1km and higher resolution:

Data requirements and format for the execution of the PESERA model at 1km resolution are described. Possible sources of higher resolution data are highlighted. It is recognised that some available higher resolution data will require processing/editing to fit the model framework. Parameter descriptions and typical data values are given in Appendix 1.

The soil geographic database of Europe (SGDBE) provides a harmonised and spatial coverage of soil types and descriptions for European participating countries at a resolution of 1:500,000 (c. 1km x 1km). The database enables spatial data queries, data extraction and thematic mapping (European Soil Database: JRC, 2001). MARS agrometeorological data has been converted to the same projection system as the European Soil Database and corrected for temperature with respect to altitude (± 0.6 °C per 100 m altitude). Relief data, derived from Gtopo30 data, is converted to the same projection system.

Table 2.3: Input Parameters: Source data

	Input Parameter	Transfer Variable	Source Database (1km)	High Resolution Input: Source Data
Climate	Mean Monthly Rainfall (mm)		MARS	Local climate data: Rainfall: data extracted from extended record of daily rainfall data from gauges within and around the target areas. Similar for temperature & PET
	Mean monthly Rain/rainday (mm)			
	CV Rain/rainday	Rainfall		
	Mean monthly temperature			
	Mean monthly Temperature range			
	Mean Monthly PET			
Soil	SWSC	Soil Texture, Packing Density	SGDBE (TEXT)	Texture,
	Zm (drainage; TopModel)			
	Crusting	Advanced pedeo-transfer functions		
	Erodibility			
Land Use	Planting/harvest/WUE	Land-use/Crop	SGDBE (USE)	Land-use-classification
	Cover			
	Rootdepth			
	Rough0			
	Rough red			

Relief	Std_eudem2	Elevation	Gtopo30	30m dem supplied for Agri
--------	------------	-----------	---------	---------------------------

2.5. MODEL APPLICATION

Two options in model application remain available:

- Modular (free data)
- Windows Inter-face (fixed data)

The free-data version allows the required freedom when applying the model to personalised or non-stationary data on a grid basis. This version allows grids to be replaced and the model run. This will be of most value when considering land-use and climate scenarios.

Operation of the ‘modular’ version is highlighted in Figure 2.8. Model documentation is presented in Appendix 1. Through discussions with ISRIC the need for an integrated user interface became apparent.

Within the ‘Inter-face’ version areas of interest will be selected by co-ordinate input, by mouse. Climate scenarios may be varied prior to executing the PESERA programme but depend on a defined single value for the area of application. Final output may either be as arcGRIDS or finished maps.

2.5.1. Model Execution

The model runs successfully on a Windows platform: 1600MhZ, 512MB RAM

Although not released a UNIX version could be made available if required.

Hard disk space requirements for running the ‘Modular’ version of the model are highlighted in Table 2.4. The Windows Inter-face may prove to be more efficient in terms of memory demand.

Table 2.4: Disk Space Requirements when executing ‘Modular’ version

	GB	Memory Demand
Input Grids (93No’)	(3.5)	(3.5)
Extracting Ascii Data from Grid	6	9.5
Pre-processing (I)	12	21.5
Pre-processing (II)	12	33.5
Output	6	21.5

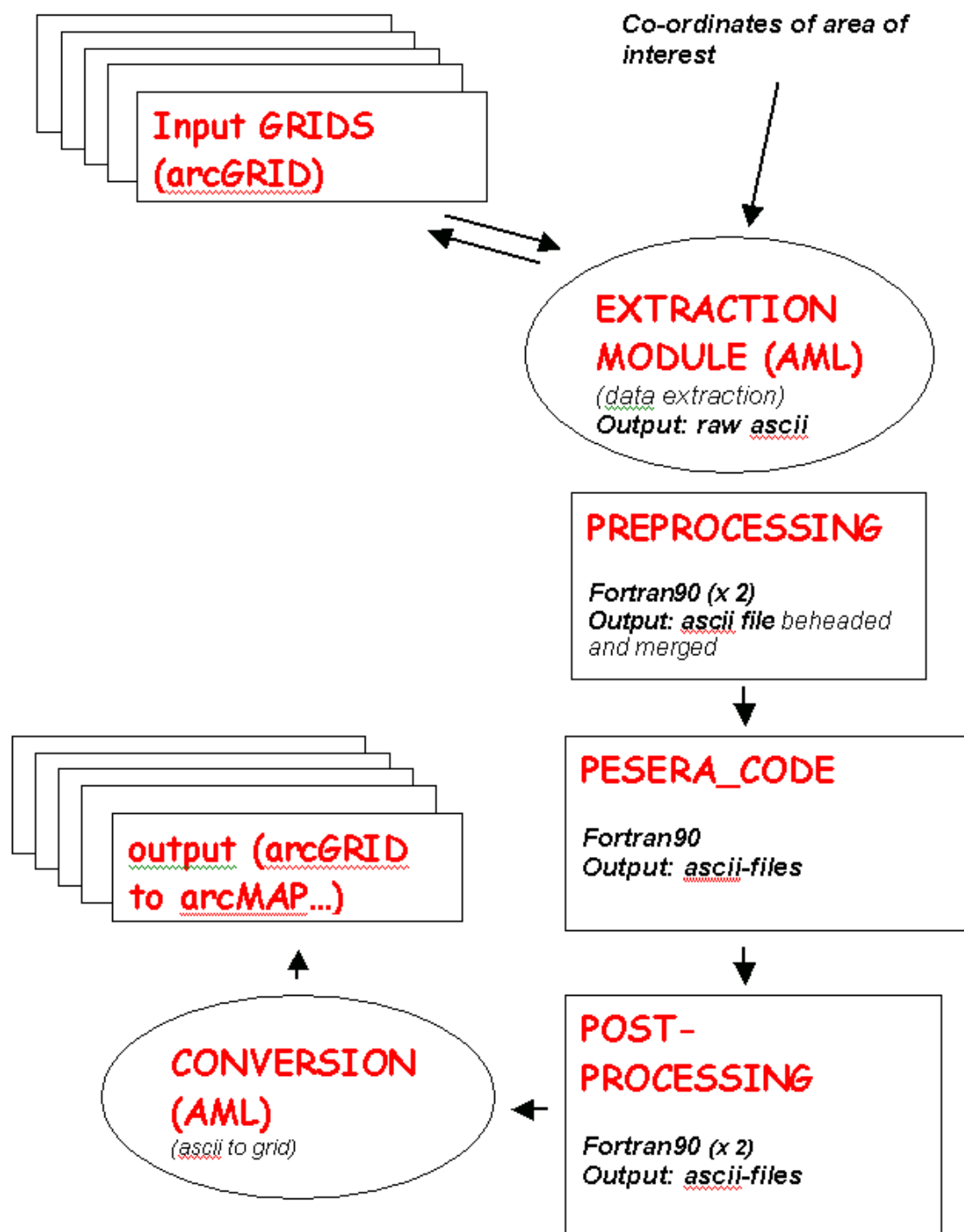


Figure 2.8: Modular components of PESERA-RDI_GRID

2.6. INTERNET APPLICATION

In collaboration with DesertLinks and Medaction a web-based facility is being developed. This will allow the user to identify an area of interest apply possible scenarios and execute/run the PESERA code over the web. The user will be subsequently notified when the operation is completed and results available. This work is being carried out at the Centre for Computational Geography at Leeds University. The web version allows open access to PESERA as only output data is provided to comply with data licensing.

Figures 2.9, 2.10 and 2.11 are screen shots from a prototype web-interface. The ‘windows’ interface is based on a similar applet.

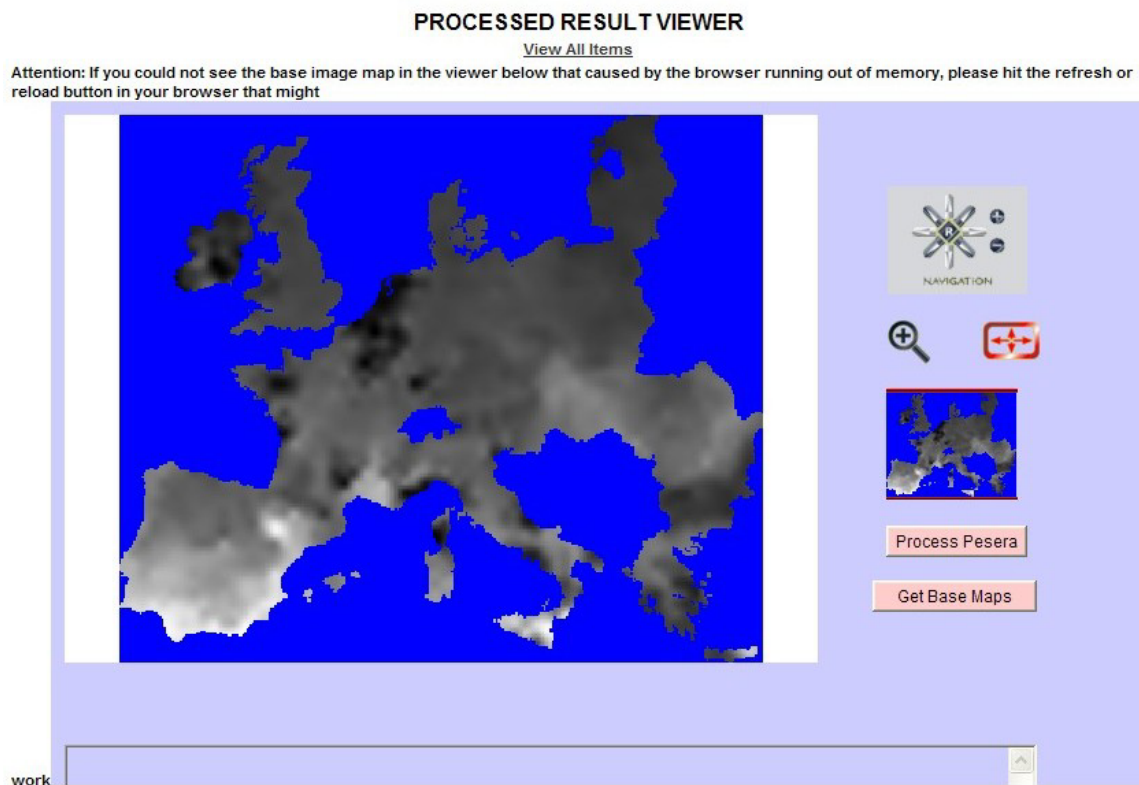


Figure 2.9: Prototype Web-Interface: Select area of interest and execute the PESERA model. (From this interface climatic variations can be applied).

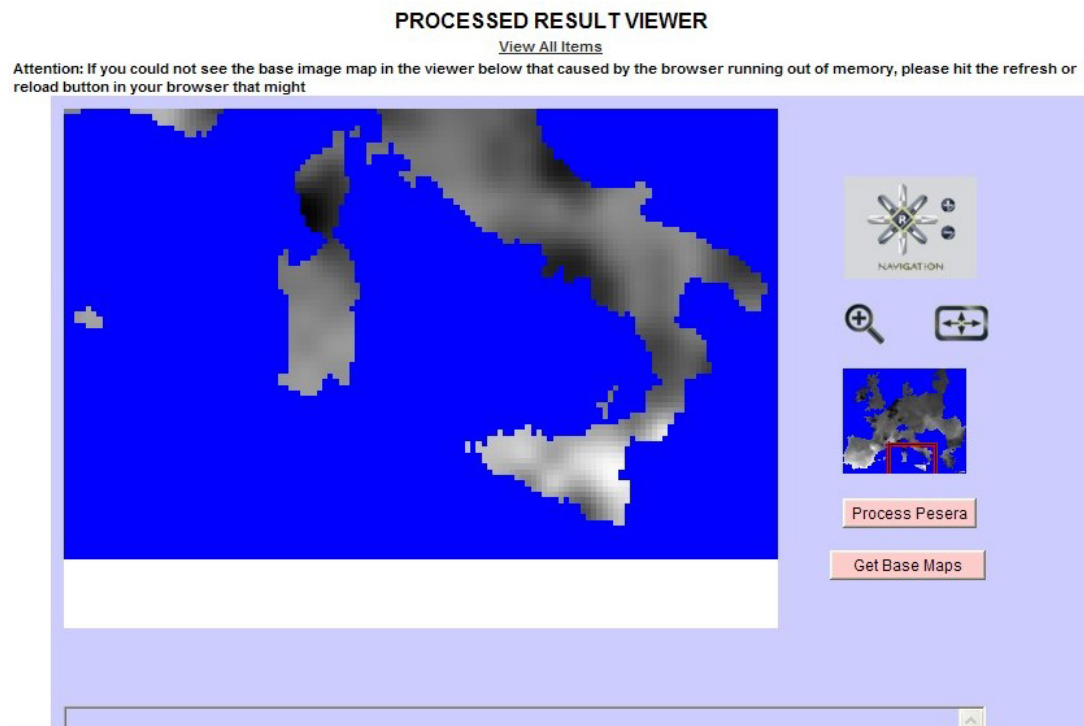


Figure 2.10: Selecting area: Prototype Web-Interface.

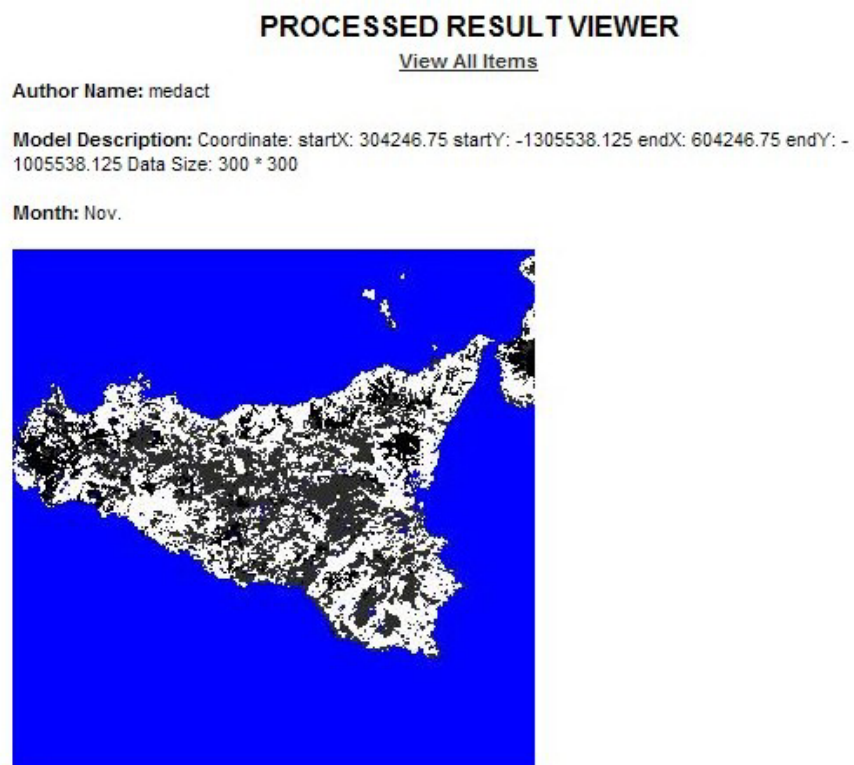


Figure 2.11: Model Output.

2.7. PESERA DOCUMENTATION

A user worksheet is available which describes setting input grids, pre-processing grids, running the Pesera_GRID and generating grid output, Appendix 1. This has enabled model investigations in Athens and Wageningen. Further to the direct application worksheet finalised documentation will include the following details.

Section	Contents
1	Description of model/Background: Model overview, Model Assumptions, Theory
2	Data requirements and format
3	Calibration Issues
4	Running the model
5	Potential Data sources

2.8. SUMMARY AND ISSUES TO BE ADDRESSED CONCLUSIONS

2.8.1. The PESERA model, Current Situation:

The PESERA-RDI_GRID model can be run by executing through a series of modules. Quantifying soil erosion risk from a series of harmonised data as described in Appendix 1. With this flexibility the PESERA_GRID methodology can be applied to areas outside the EU given the minimum required data sets are available.

PESERA_GRID methodology offers the flexibility to apply land-use and climatic scenarios to investigated potential erosion risk. Climatic scenarios can be determined from sources external to the project.

The interface module offers open web-access to the PESERA model as no direct access to source data is required to determine erosion surfaces.

Fuller assessment of intermediate model components is required, deficits/vegetation cover, to assess intermediate model performance. ‘Grown’ vegetation cover when incorporating planting dates can be compared with ‘observed’ vegetation cover.

Findings from temporal/spatial linkage, high and low resolution validation need to be included in the point and grid versions of the model.

Consideration has been given to applying ‘neural-networks’ to develop land-use change scenarios. The potential of ‘neural-networks’ to explore drivers in land use change has recently been discussed in DesertLinks.

High resolution local data is of significant value and would supersede the course 1km scale data where available. Significant improvements are envisaged with the incorporation off such data.

2.8.2. Key data requirements/considerations:

- local climate data
- Land-use: crop type if arable
- cultivation practice
- soil data: texture, bulk density, organic matter
- data attribute tables, essential to interpret data codes
- projection data
- data transfer formats

The reduced demand on RAM ensures the model operates on a greater number of machines allowing processing time to be split between available processors when considering the European scale. Split between three processors European grids can be processed ‘overnight’.

Uncertainty remains in how to best represent cover for the range of land-use categories given uncertainty in data availability.

Through the collation of available data sets it is now becoming possible to generate erosion maps and surfaces at a global scale. Initial estimates for North Africa and the Middle East are presented in Figure 2.12. However, it is considered that land cover is poorly defined and influencing erosion estimates in mountainous areas. Additional sources of ground cover estimates are being explored to enhance estimates and produce continuous surfaces.

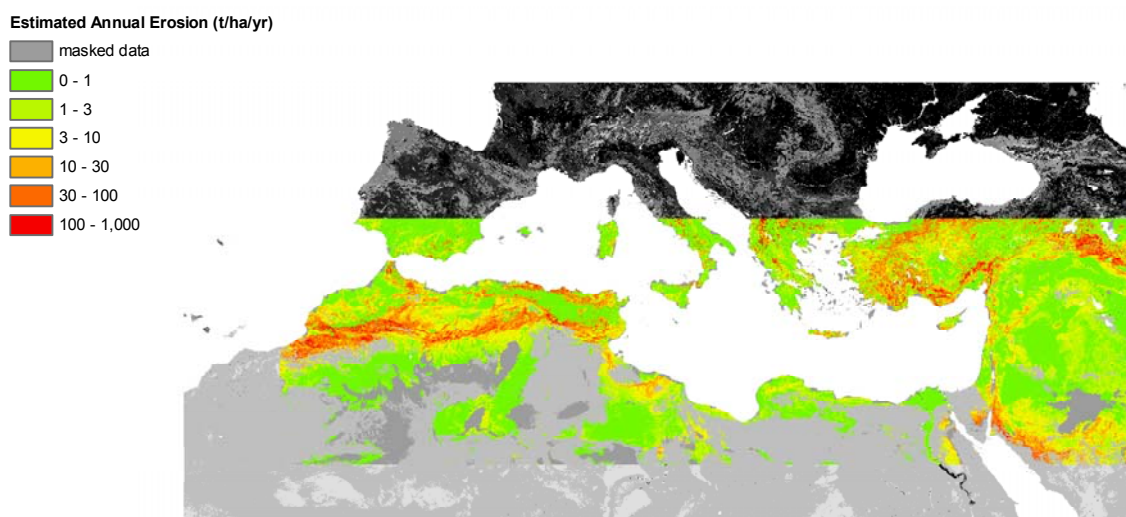


Figure 2.12: Preliminary Erosion Estimates for North Africa and Middle East at 5km Resolution

CHAPTER 3 ESTACION EXPERIMENTAL DE ZONAS ARIDAS (EEZA), CSIC

**Juan Puigdefabregas, Gabriel del Barrio, Matthias Boer, Sebastian Vidal
and Roberto Lazaro**

Estacion Experimental de Zonas Aridas (EEZA), Consejo Superior de Investigaciones Científicas (CSIC), General Segura 1, 04001 Almería – Spain

3.1. OBJECTIVES

CSIC (EEZA) contributes to WP 1 through research on the relationship between spatial vegetation patterns, and the redistribution of runoff and sediment on hillslopes; to WP 2 particularly by analysing the impact of changes in the spatial resolution of DEMs, terrain attributes, and vegetation properties on the model outputs; to WP 3 by comparing model outputs with field data from the Rambla Honda and El Cautivo field sites; to WP 4 by providing a comparison of PESERA model outputs on soil erosion risk with an assessment of actual land degradation status in SE-Spain. CSIC (EEZA) is taking the lead role for Work Package 2.

3.2. WP2: SYNERGETIC EFFECTS OF SPATIAL AND TEMPORAL VARIATION IN LAND ATTRIBUTES

This section details the work carried out on synergetic effects of spatial and temporal variation in land attributes on hillslope erosion rates and implications for the PESERA soil erosion model.

3.2.1. Work carried out during the reporting period

The objectives of the EEZA-CSIC contribution to WP1 and WP2 are, firstly to increase our understanding of synergetic effects of spatial and temporal variation in land attributes (i.e. vegetation cover, soil attributes, rainfall), as observed at a range of spatial and temporal resolutions, on hillslope runoff and erosion rates, and secondly to explore its implications for the PESERA soil erosion model.

In the second project year a simulation approach was already used to investigate effects of spatial patterns of vegetation cover and associated soil properties on hillslope erosion processes. A similar set-up was used in the current reporting period to investigate the interaction of spatial and temporal variability, and is also foreseen for the last months of the project to study effects of changes in model resolution.

The approach consists of using an existing, high-resolution, soil erosion model (LISEM) that was previously parameterised with field data from the Rambla Honda Field site in SE Spain on hypothetical hillslopes with simulated distributions of key vegetation and soil parameters and simulated storm profiles of known mean, variance and autocorrelation structures. By using the results for hillslopes with spatially uniform vegetation/soil properties and storms of constant rainfall intensity as a reference, the contribution of spatial and temporal variability to hillslope discharge and soil loss rates under dry Mediterranean conditions could be quantified.

To explore implications for the PESERA model sets of LISEM runs were used as populations of hypothetical field observations. Half of each data set was used for the parameterisation of the soil water storage and erodibility parameters of the PESERA model, whereas the other half was used to ‘validate’ the PESERA predictions.

3.2.2. Background and objectives

Low resolution soil erosion models, including the PESERA model, are designed to predict soil loss rates at daily to annual time steps for large land units at a time (e.g. 1-100 km²). The process knowledge on which these models are based, as well as the field information that is required to parameterise, calibrate and validate these models, was usually collected at much finer spatial (e.g. 1-100 m²) and/or temporal resolutions (e.g. minutes-hours). To cope with this scaling problem, input parameters to the soil erosion model, such as rainfall intensity or amount, soil erodibility, infiltration capacity, vegetation cover and slope angle, are often assumed to be invariant or to have a typical probability density function within a model grid cell or time step. These simplifying assumptions are likely to add uncertainty to soil erosion predictions by low resolution models. Though scale issues are actively researched in hydrology and geomorphology (e.g. (Blöschl & Sivaplan 1995; Beven 1995; Kirkby et al. 1996; Puigdefábregas et al. 1999), systematic analyses of the combined effect of spatial and temporal variability on uncertainty in soil erosion predictions have so far been rare.

Hillslope erosion by overland flow involves several thresholds, amongst others, for the generation of runoff, for the detachment of soil particles, and the transport of sediment (e.g. (Beven 2002; Govers 1990). Spatial and temporal variability in the landscape and its drivers, may cause these thresholds to be (temporally) exceeded in some areas, or fractions, of a large model grid cell, but not (yet) in others (Abrahams et al. 1991). The net soil loss from a hillslope or modelling unit depends on the connectivity of water and sediment fluxes among those dynamically responding areas (e.g. (Puigdefábregas et al. 1998); (Boer & Puigdefábregas 2003). Low resolution models in which spatial and temporal variation in system parameters and drivers is ignored can be envisaged to produce potentially unrealistic predictions when the hydrological and erosional response is highly localised in space and time.

This problem may be particularly important in semiarid landscapes where ‘patchy’ vegetation covers and highly variable rainfall cause water and sediment fluxes to be particularly difficult to predict for low resolution soil erosion models (Puigdefábregas & Sanchez 1996). The spatially structured vegetation patterns that characterise semiarid hillslopes tend to be mirrored by the spatial distribution of key soil and surface properties (e.g. (Cross & Schlesinger 1999; Aguiar & Sala 1999; Bolton et al. 1993). For example, soils

from vegetated patches often have, amongst others, greater porosity, higher organic matter content, higher infiltration and storage capacities, and are more strongly aggregated than those from adjacent bare patches (e.g. (Bergkamp 1996); (Bochet et al. 1999), (Wezel et al. 2000) (Virginia & Jarrell 1983). Consequently, runoff generation thresholds and critical overland flow velocities are more likely to be exceeded in bare areas than in vegetated patches ((Abrahams et al. 1995). The differential response of bare soil areas and vegetated patches favours the discontinuity of water and sediment fluxes across a hillslope as runoff generated in the clearings ('sources') may be intercepted by adjacent patches with high plant cover and greater infiltration capacity ('sinks') (e.g. (Kirkby et al. 1996);(Puigdefábregas et al. 1998; Kirkby et al. 1996). For a net loss from a hillslope those fluxes must reach the base of the slope. This can occur during storms of high intensity and/or long duration when all surface types become source areas (condition A), but also during storms of low intensity and/or short duration when runoff generation and sediment transport are localised in space and time and one or more source-sink systems connect to the base of the slope (condition B). In condition A, the spatial organisation of vegetated patches and bare soil areas has relatively little impact on the hillslope fluxes. In condition B, however, the spatial organisation of source and sink areas may be a key factor (Boer & Puigdefábregas 2003), whose importance can be envisaged to depend on the temporal correlation structure of rainfall intensity (Figure 3.1).

Figure 3.1 shows the variation in rainfall intensity recorded during a storm on 15 October 1994 at the Rambla Honda Field Site near Almería, SE Spain (Puigdefábregas et al. 1996). The mean intensity during the first 120 minutes of the event was only 11 mm.h⁻¹, which is less than the final infiltration capacity of most surface types in the area. At several stages of the storm, however, the rainfall rate was much greater than the mean value, exceeding 30 mm.h⁻¹ for six periods of several minutes. During those short rainfall pulses, the runoff generation thresholds of some surface types may have been exceeded. For runoff-producing areas to connect effectively, runoff must flow from one source area to another before rainfall intensities drop again below runoff generation thresholds. Hence, for a given hillslope, we may expect the frequency with, and distances over which, such hydrological connections are established to be affected by the spatial configuration of soil hydrologic and hydraulic properties on the one hand, and the temporal structure of the storm on the other hand.

The objectives of this study are:

- to explore and quantify synergetic effects of spatial patterns of key land attributes and temporal patterns of rainfall intensity on hillslope erosion rates for a typical dry Mediterranean environment,
- to quantify the effects of changes in spatial and temporal resolution on predicted erosion rates in those environments,
- to quantify the implications of these effects for the parameterisation and performance of the PESERA model.

During the current reporting period we have focused on objectives 1 and 3. Effects of changes in resolution will be studied in the next and last stage of the project.

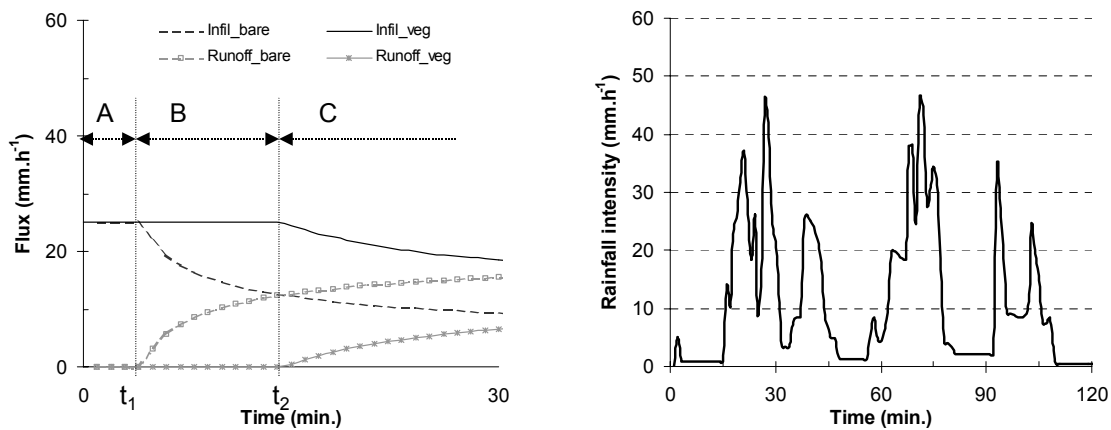


Figure 3.1: In dry Mediterranean environments the infiltration capacity of vegetated patches and bare soil areas may differ by a factor two or more. During a storm of constant rainfall intensity (left) differences in infiltration capacity will initially be unimportant (phase A), become apparent at $t=t_1$ as runoff starts to be generated in bare soil areas but not yet in vegetated patches (phase B), and then loose significance again at $t=t_2$ when both surface types generate runoff (phase C). During storms of variable intensity (right), phases A-B-C may occur in different order and be repeated more than once depending, amongst others, on the mean rainfall intensity and its temporal correlation structure.

3.2.3. Simulation study using LISEM

3.2.3.1. Approach and set-up

We use a simulation approach because the impact of spatial and/or temporal variability in vegetation, soil and rainfall attributes on hillslope erosion rates would be very difficult to separate from that of other factors, such as topography or land use, in field observations or in an experimental manner. An existing high-resolution soil erosion model, LISEM (De Roo et al. 1996a; De Roo et al. 1996b), was set-up as a simulation environment. The model was used to study the response of hypothetical hillslopes with simulated patterns of vegetation and soil properties to computer-generated storms of known mean rainfall intensity, variance and temporal correlation structure. Relevant features of LISEM and its parameterisation with field observations from Rambla Honda (Puigdefábregas et al. 1996) and other sites in southeast Spain were discussed in the second annual report of the PESERA project.

Table 3.1 lists the LISEM input parameters with their values as used in this study. As commonly observed in semiarid environments, the spatial distribution of several soil parameters - indicated by f(PER) in Table 3.1 - was assumed to vary in a systematic manner with the density of the vegetation cover. At the Rambla Honda field site vegetation cover fraction on the hillslopes lays in the range of 0.20-0.30. Hypothetical vegetation patterns with similar mean cover (i.e. 0.22-0.28) values but different structural properties were generated for a 100 m x 100 m area with gstat software (Pebesma 2001). Using unconditional gaussian simulation and a simple spherical semivariogram model with no nugget we created

vegetation patterns with autocorrelation lengths of 5 m, 10 m, 20 m, and 40 m (Figure 3.2). For every structured vegetation pattern, a spatially uniform pattern of the same mean cover fraction was created as a control.

Table 3.1: LISEM parameter values as used in the simulation experiments. The ‘range’ column refers to the value range recommended in the LISEM manual (Jetten 2002). Parameters indicated by ‘f(PER)’ in the ‘Applied value’ column are assumed to vary with vegetation cover fraction (PER) according to equation 1-9.

Parameter	Description	Unit	Range	Applied value
AREA	Mask for model area	-	1	-
ID	Area covered by rain gauges	-	1-n	-
LDD	Local drain direction	-	1-9	-
GRAD	Slope gradient (sine of slope angle)	-	>0, <=1.0	-
OUTLET	Location of outlet and suboutlets	-	1-3	-
PER	Soil fraction soil covered by vegetation	-		Simulated
LAI	Leaf area index	-		f(PER)
CH	Vegetation height	m	0-30	0.5
N	Manning’s n	-	0.001-10	f(PER)
RR	Random roughness	cm	0.05-20	f(PER)
STONEFR C	Soil fraction covered by stones	-	0-1	0.75
TP	Total porosity	-		f(PER)
KSAT1	Saturated hydraulic conductivity	mm.h ⁻¹	0-1000	f(PER)
THETAS1	Saturated volumetric soil moisture content	-	0-1	f(PER)
THETA11	Initial volumetric soil moisture content	-	0-1	0.05
PSI1	Soil water tension at wetting front	cm	0-1000	30
AGGRSTA B	Aggregate stability: number of drops required to destroy 50% of aggregates	-	0.00001-200	f(PER)
COH	Cohesion of bare soil	kPa	>=0.196	33.9
COHADD	Additional cohesion by roots	kPa	>=0.196	f(PER)
D50	Median of soil particles size distribution	µm	25-300	300

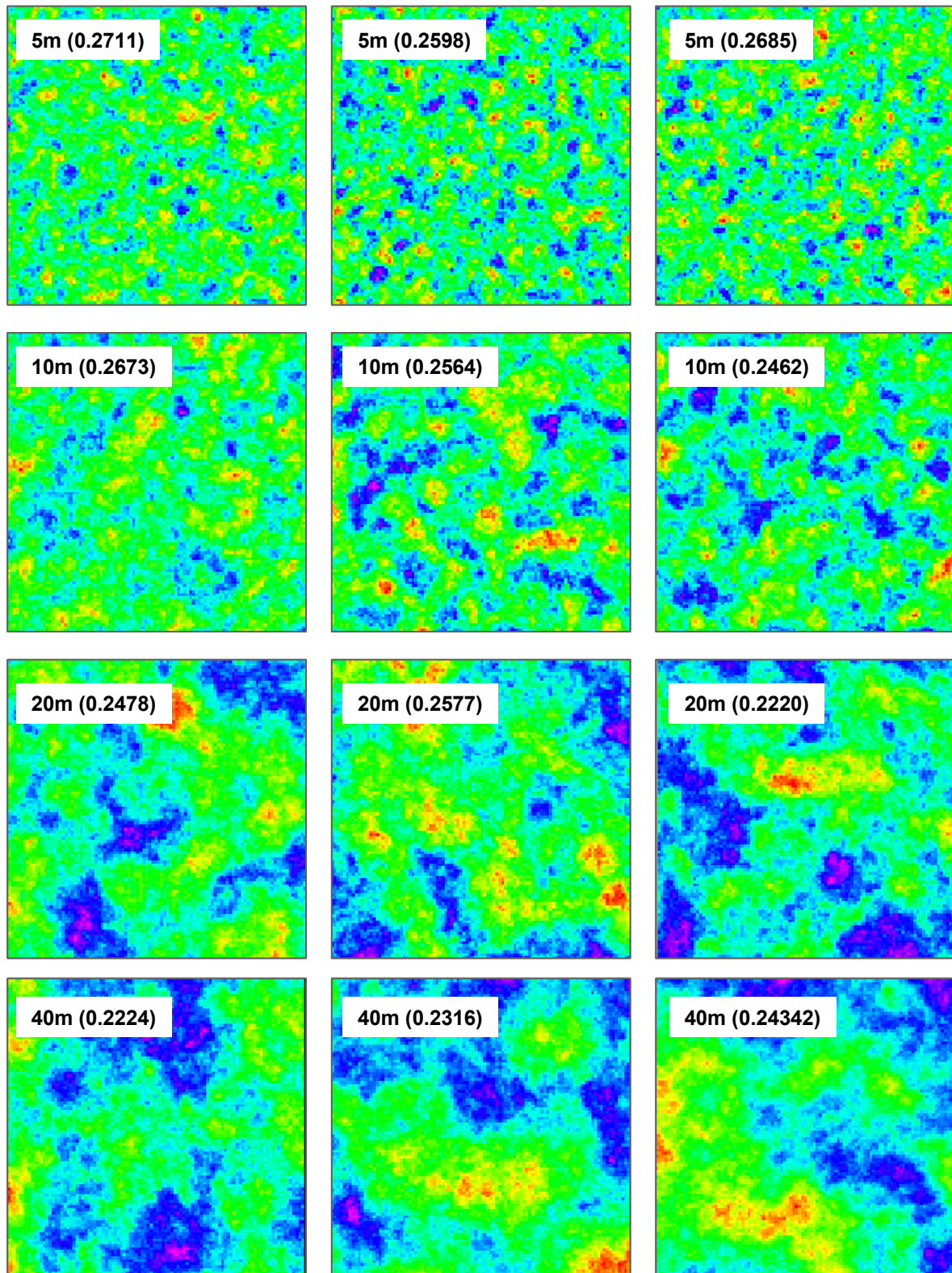


Figure 3.2: Simulated patterns of vegetation cover fraction at 1m spatial resolution. The autocorrelation lengths and mean vegetation cover fractions are shown in the right-hand corner of every map. The simulated area is 100 m x 100 m.

We used simple linear relationships to bring about a coupling of vegetation and soil patterns (see Table 3.1 for symbols, the 2nd Annual PESERA Report for details):

$$\begin{aligned} \text{NEWDEM} &= \text{DEM} + 0.1 * \text{PER} & [1] \\ \text{N} &= 0.15 + 0.25 * \text{PER} & [2] \\ \text{RR} &= 2.5 + 2.5 * \text{PER} & [3] \\ \text{KSAT1} &= 6.0 + 6.0 * \text{PER} & [4] \\ \text{TP} &= 0.20 + 0.05 * \text{PER} & [5] \\ \text{THETAS1} &= 0.93 * \text{TP} & [6] \\ \text{AGGRSTAB} &= 10 + 60 * \text{PER} & [7] \\ \text{COHADD} &= (38.2 - 33.9) * \text{PER} & [8] \end{aligned}$$

Leaf area index (LAI) was assumed to vary non-linearly with PER as:

$$\text{LAI} = \frac{\text{LAI}_{50}}{\left(\frac{1}{\text{PER}} - 1\right)} \quad [9]$$

where LAI50 is the LAI value coinciding with PER=0.5

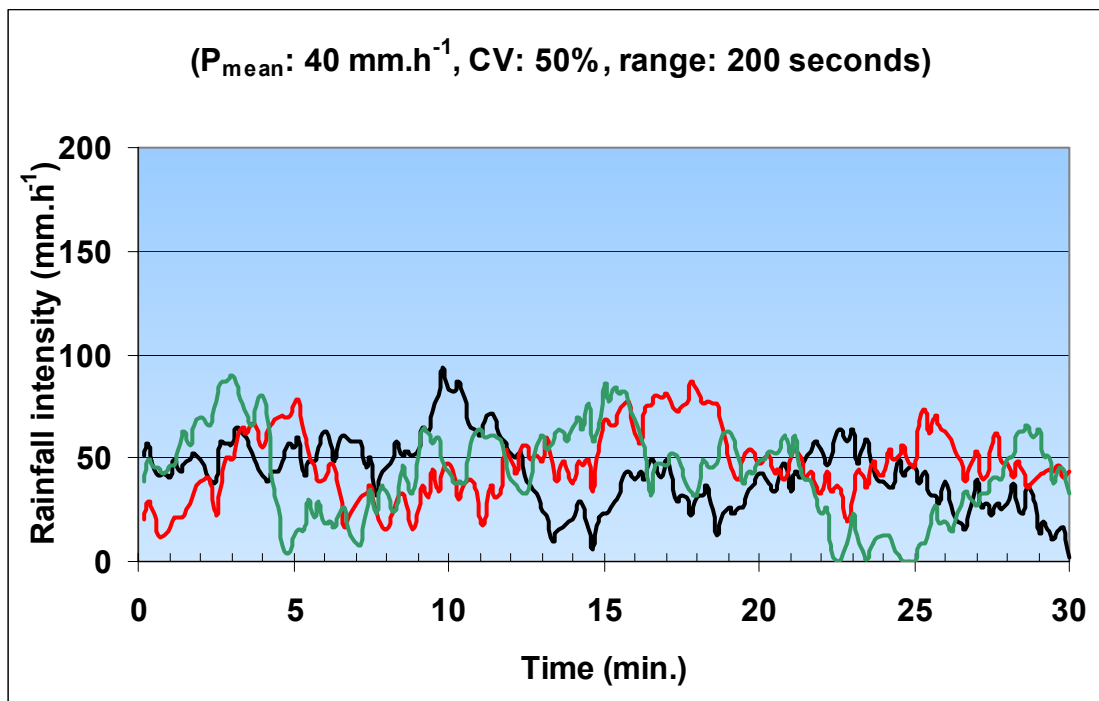


Figure 3.3: Example of simulated storms of ca. 40 mm.h-1 mean rainfall intensity and temporal autocorrelation length of 200 seconds.

A similar procedure was used to generate artificial storms of 30 minute duration and mean rainfall intensities of ca. 30-40 and 60-70 mm.h⁻¹, hereafter referred to as respectively ‘low intensity’ and ‘high-intensity’ events. Based on a spherical semivariogram model with no nugget and a coefficient of variation of 0.5 we used gstat to create multiple realisations (n=3) of storm profiles with autocorrelation lengths of 100, 200, and 300 seconds (Figure 3.3). Storms of constant rainfall intensities were created as input for the control runs. Basic statistics for the simulated storms are given in Table 3.2. All LISEM runs were over 60 minutes at time steps of 10 seconds. Antecedent soil moisture content was set at 0.05.

Table 3.2: Main characteristics of the simulated storms. All storms are of 30 minute duration. Storms 1-18 have variable rainfall intensities, whereas storms 19 and 20 are of constant intensity.

Storm	Mean Intensity (mm.h ⁻¹)	Autocorrelation length (min.)	Total Rainfall (mm)	I5 (mm.h ⁻¹)	Max. Intensity (mm.h ⁻¹)
1	39	1.7	19	31	104
2	37	1.7	18	37	98
3	40	1.7	19	30	89
4	39	3.3	21	42	93
5	44	3.3	23	43	87
6	39	3.3	21	35	90
7	36	5.0	17	39	90
8	40	5.0	17	50	100
9	31	5.0	15	38	88
10	68	1.7	34	53	183
11	64	1.7	32	65	171
12	70	1.7	33	53	155
13	69	3.3	37	73	163
14	77	3.3	40	76	153
15	68	3.3	36	62	158
16	63	5.0	29	68	157
17	71	5.0	30	88	175
18	55	5.0	26	67	154
19	37	-	19	37	37
20	65	-	32	65	65

The simulated patterns of vegetation cover and related soil attributes were overlain on digital elevation models (DEMs) of hypothetical straight slopes with gradients of 0.05, 0.10 and 0.20 to create simple landscapes to run LISEM on. While discussing the results we will refer to the gradients of 0.05 and 0.20 as respectively the ‘gentle’ and ‘steep’ slopes. The DEMs were modified to create a one grid cell wide ‘collection trough’ that led runoff water and sediment to a single outlet in the SE corner of the model area. LISEM was set up to record water and sediment at this outlet. As a measure against erosion in the collection trough, the corresponding grid cells were assigned a value of 1.0 for the ‘ROADWIDT’ parameter (Table 3.1), which causes the trough to function as a paved road.

Effects of spatial and/or temporal variability on hillslope runoff and erosion were quantified by computing deviations of predicted discharge and soil loss with those for the same amount of rainfall applied at constant intensity on a slope of the same gradient with spatially uniform vegetation cover of the same mean density.

3.2.3.2. Results

Storms of constant rainfall intensity

For storms of constant rainfall intensity, predicted discharge and soil loss rates from hillslopes with spatially structured vegetation and soil patterns are greater than from comparable hillslopes with spatially uniform vegetation and soil attributes. The effects of spatially structured vegetation and soil patterns are strongest just after exceeding runoff generation or sediment transport thresholds and then level off during the remainder of the storm. These maxima tend to decrease with rainfall intensity and to increase with slope gradient. The convergence of the hydrological responses of hillslopes with spatially structured and uniform vegetation patterns is more pronounced, and occurs sooner, for high-intensity storms on steep slopes than for low-intensity rainfall on gentle slopes (Figure 3.4). For the tested rainfall intensities and slope gradients, coarsely aggregated vegetation patterns (i.e. autocorrelation lengths of 20 m or 40 m) can be observed to affect hillslope discharge rates to a greater extent than finely aggregated vegetation patterns (i.e. autocorrelation lengths of 5 m or 10 m) (Figure 3.4).

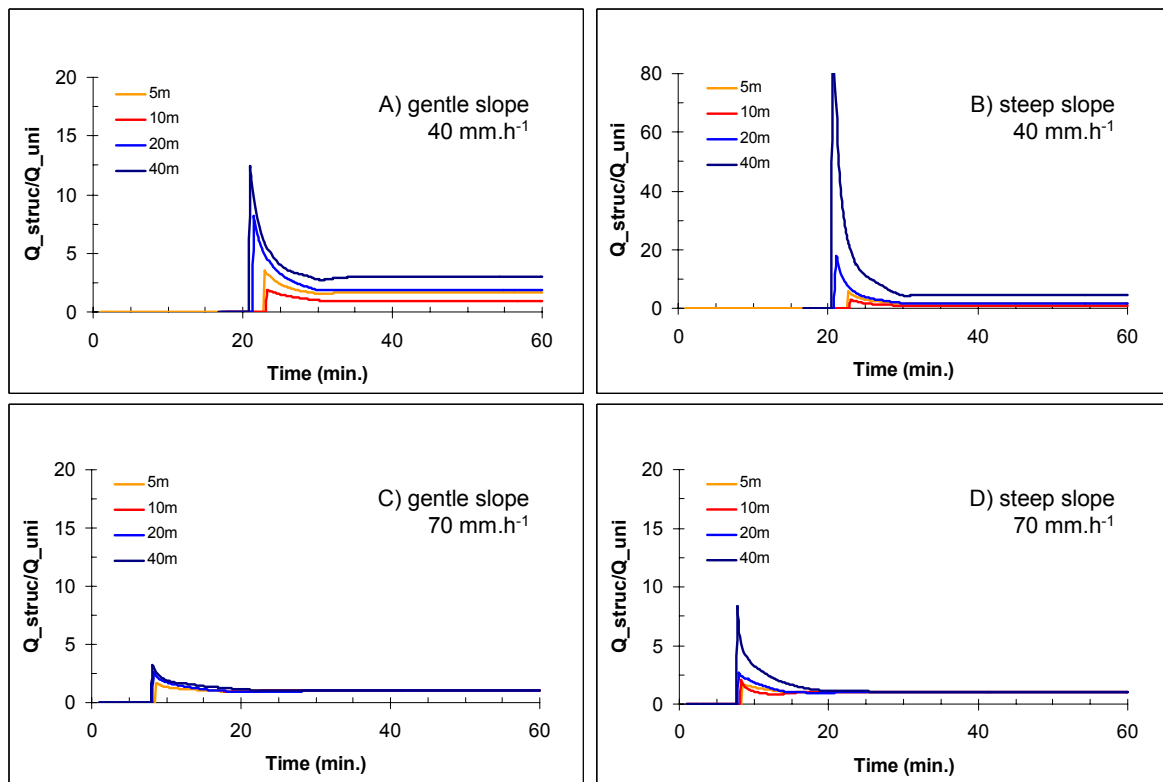


Figure 3.4: The predicted ratio of discharge rates from hillslopes with spatially structured and uniform vegetation covers during storms of 40 mm.h⁻¹ (upper graphs) and

70 mm.h⁻¹ (lower graphs). Results for gentle slopes are shown at left, and for steep slopes at right. Colours indicate spatial autocorrelation lengths of the vegetation patterns. Note different scale of Y-axis for graph b).

Similar to the effects on discharge rates, predicted net soil loss rates are most affected by the spatial structure of the vegetation cover shortly after the start of runoff generation and tend to decrease with additional rainfall. The length of this period of differentially responding bare soil areas and vegetated patches decreases with slope gradient and rainfall intensity. The effect of the spatial vegetation structure also changes with slope gradient (Figure 3.5). During storms at 60 and 70 mm.h⁻¹ on the gentle slope (i.e. gradient: 0.05) soil loss rates from the finely aggregated vegetation covers, with autocorrelation lengths of 5 m and 10 m, differ more from the spatially uniform controls, than those of the coarsely aggregated vegetation patterns, with autocorrelation lengths of 20 m and 40 m. At the same storm intensities on the steep slope (i.e. gradient: 0.20), however, only the soil loss rates from coarsely aggregated vegetation covers differ substantially from the spatially uniform controls, whereas the response of finely aggregated vegetation covers is very similar to those of spatially uniform covers. (Figure 3.5).

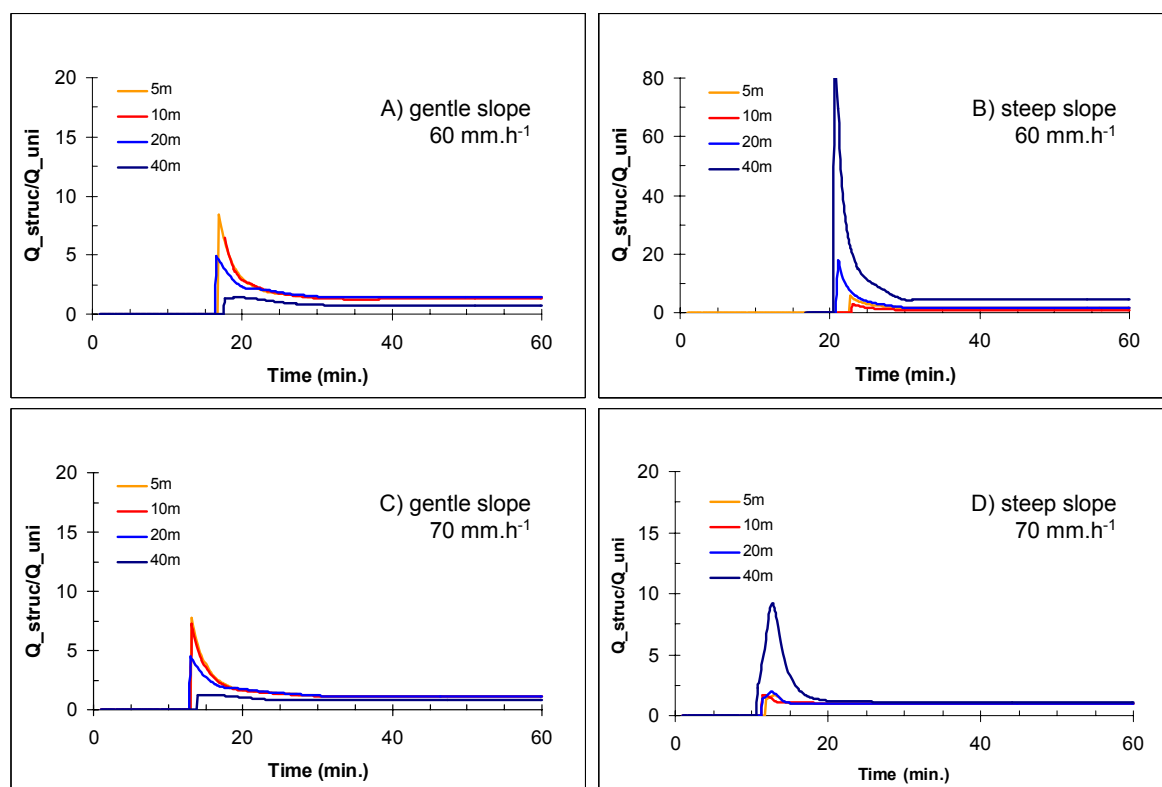


Figure 3.5: The predicted ratio of soil loss rates from hillslopes with spatially structured and uniform vegetation covers during storms at 60 mm.h⁻¹ (upper graphs) and 70 mm.h⁻¹ (lower graphs). Results for gentle slopes are shown at left, and for steep slopes at right. Colours indicate spatial autocorrelation lengths of the vegetation patterns.

Storms of variable rainfall intensity

As expected, temporal variation in rainfall intensity strongly affects the LISEM predictions of hillslope water and sediment yields. For a given amount of rainfall, predicted cumulative discharge and soil loss is nearly always greater for storms of variable intensity than for storms of constant intensity (Figures 6-10). These differences may temporarily reach several orders of magnitude. Effects of temporal variability in rainfall intensity are greatest just after the initiation of runoff or sediment transport and diminish with additional rainfall. Effects of temporal variation in rainfall intensity on cumulative discharge decrease with:

- the mean rainfall intensity (e.g. compare left- and right-hand panels in Figures. 3.6-9),
- slope gradient (e.g. compare Figures. 3.6 and 3.8 or Figures. 3.7 and 9)
- the temporal autocorrelation length of the variation in rainfall intensity (e.g. compare upper- and lower panels in Figures. 3.6-9),
- the spatial autocorrelation length of the vegetation and soil patterns, in particular at relatively low mean rainfall intensity (e.g. compare Figures 3.6a and 3.7a, or Figures 3.6b and 3.7b).

Effects of temporal and spatial variation on cumulative soil loss could only be analysed for storms of high mean intensity (ca. 70 mm.h⁻¹), since the low intensity events (ca. 40 mm.h⁻¹) did not generate a net soil loss for all slope/vegetation/storm combinations. For these high intensity storms, the spatial autocorrelation length of the vegetation and soil attribute patterns has relatively little effect on cumulative soil loss (e.g. compare left- and right-hand panels of Figures 3.10 and 3.11). Similar to the results obtained for cumulative discharge, effects of variation in rainfall intensity on cumulative soil loss strongly decrease with the temporal autocorrelation length of the variation in rainfall intensity (e.g. compare upper- and lower panels of Figs. 3.10 and 3.11) and with slope gradient (compare Figures 3.10 and 3.11).

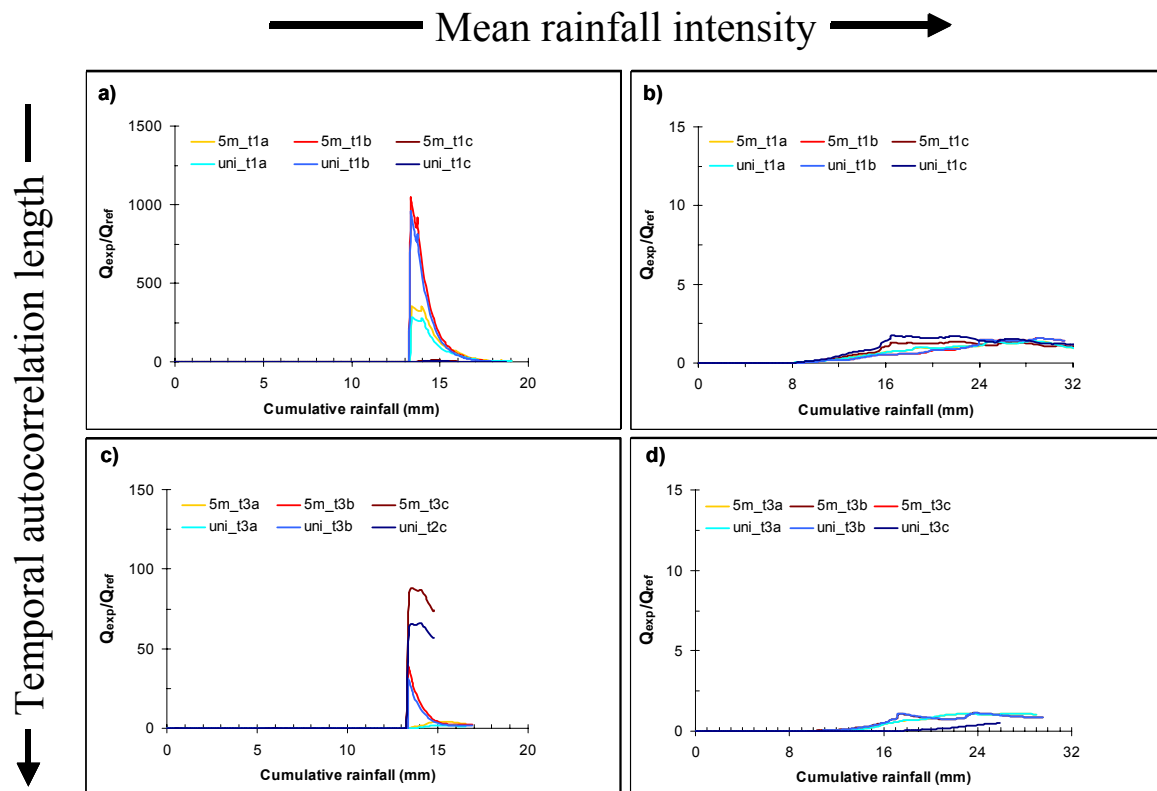


Figure 3.6: Predicted effects of finely aggregated vegetation and soil patterns on cumulative discharge from gentle slopes. Curves show ratios Q_{exp}/Q_{ref} for storms with variable rainfall intensity. Q_{ref} : response to storms of constant intensity by hillslope with spatially uniform vegetation and soil attributes; Q_{exp} : response to storms of variable rainfall intensity by hillslopes with spatially uniform vegetation and soil ('uni_ curves') or spatially structured vegetation and soil patterns ('5m_ curves'). Low intensity storms with variation of short (i.e. 1.7 min.) or long autocorrelation length (i.e. 5.0 min.) are shown, respectively, in graphs a) and c). High intensity storms with variation of short (i.e. 1.7 min.) or long autocorrelation length (i.e. 5.0 min.) are shown, respectively, in graphs b) and d). Note differences in the scale of the y-axes.

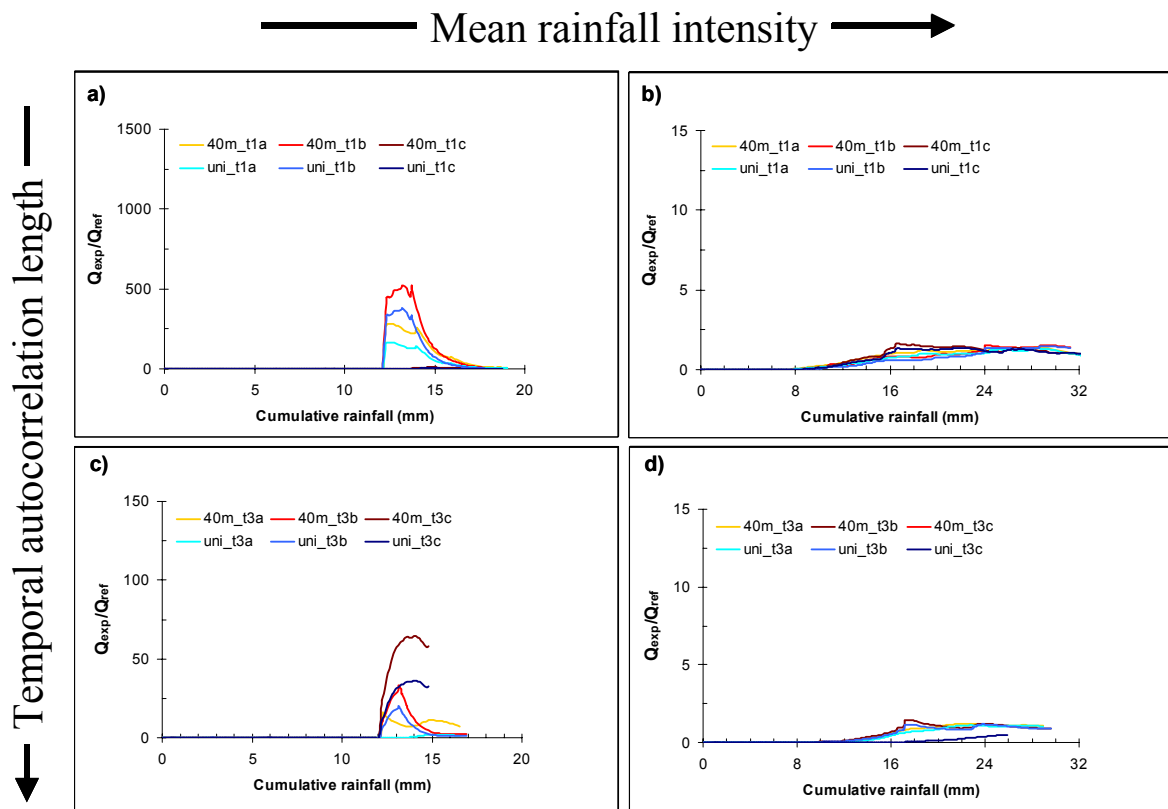


Figure 3.7: Predicted effects of coarsely aggregated vegetation and soil patterns on cumulative discharge from gentle slopes. Symbols and storms as in Figure 3.6.

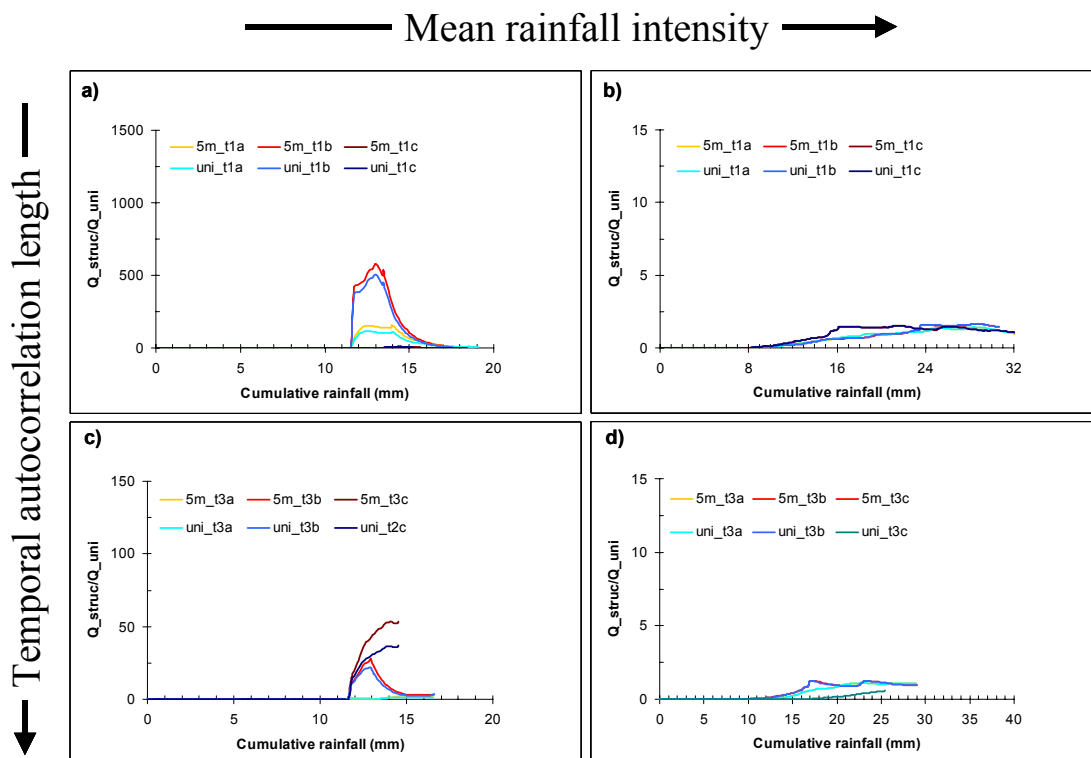


Figure 3.8: Predicted effects of finely aggregated vegetation and soil patterns on cumulative discharge for a steep slope. Symbols and storms as in Figure 3.6.

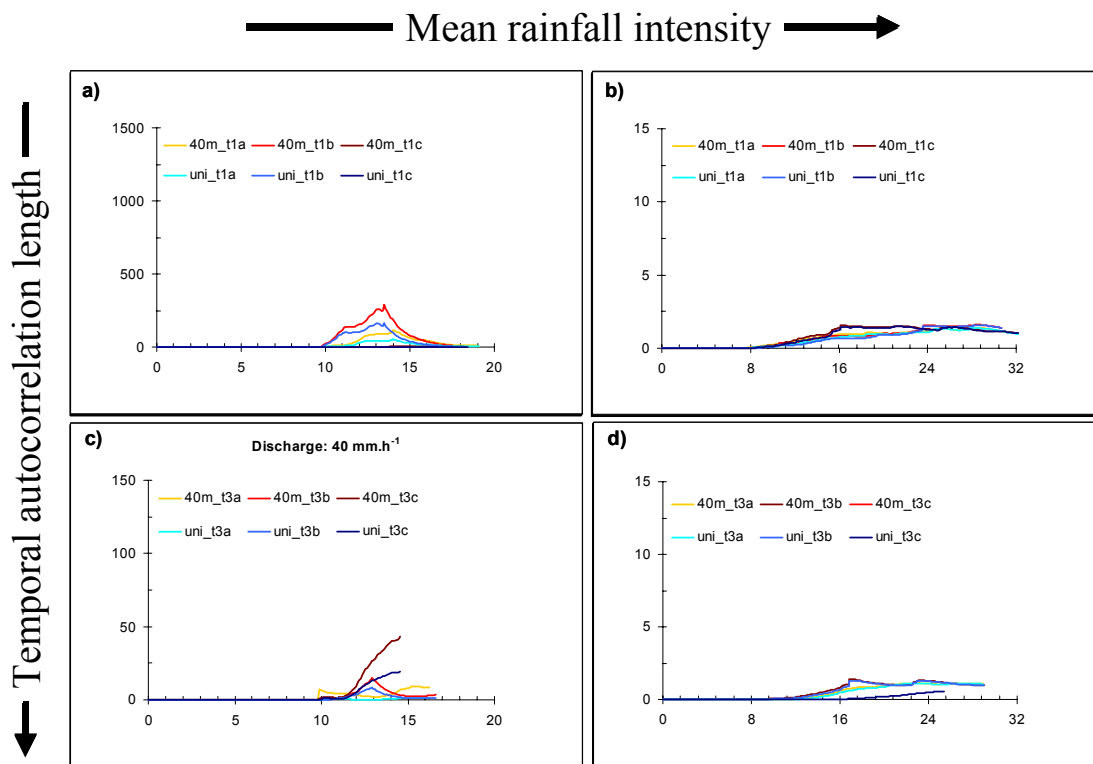


Figure 3.9: Predicted effects of coarsely aggregated vegetation and soil patterns on cumulative discharge for a steep slope. Symbols and storms as in Figure 3.6.

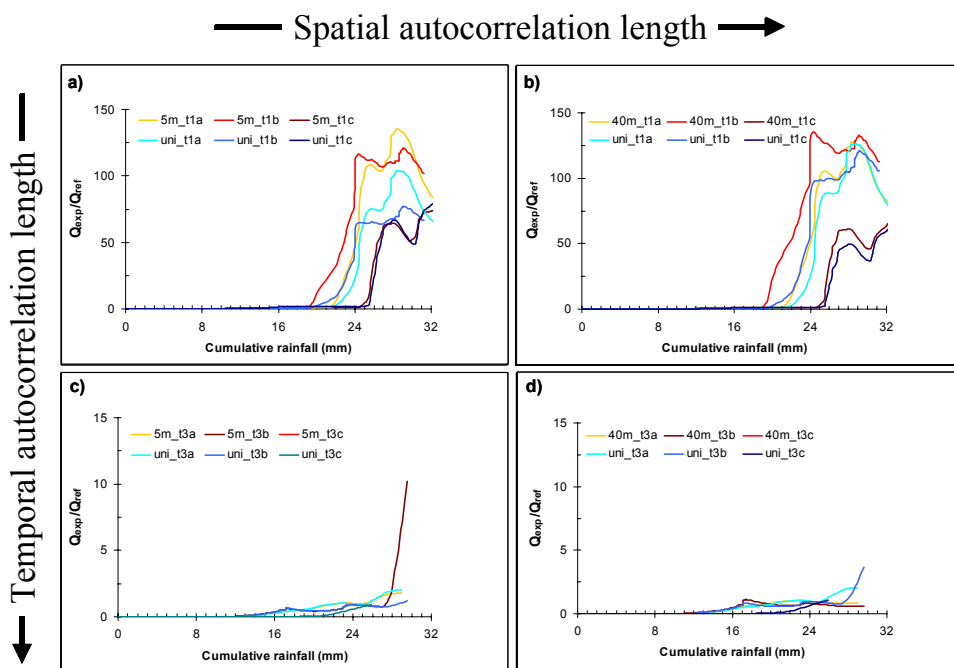


Figure 3.10: Predicted effects of finely (left) and coarsely (right) aggregated vegetation and soil patterns on cumulative soil loss for a gentle slope. Results for storms with

rainfall intensity variation of short and long autocorrelation length are shown in, respectively, the upper and lower graphs. Other symbols as in Figure 3.6.

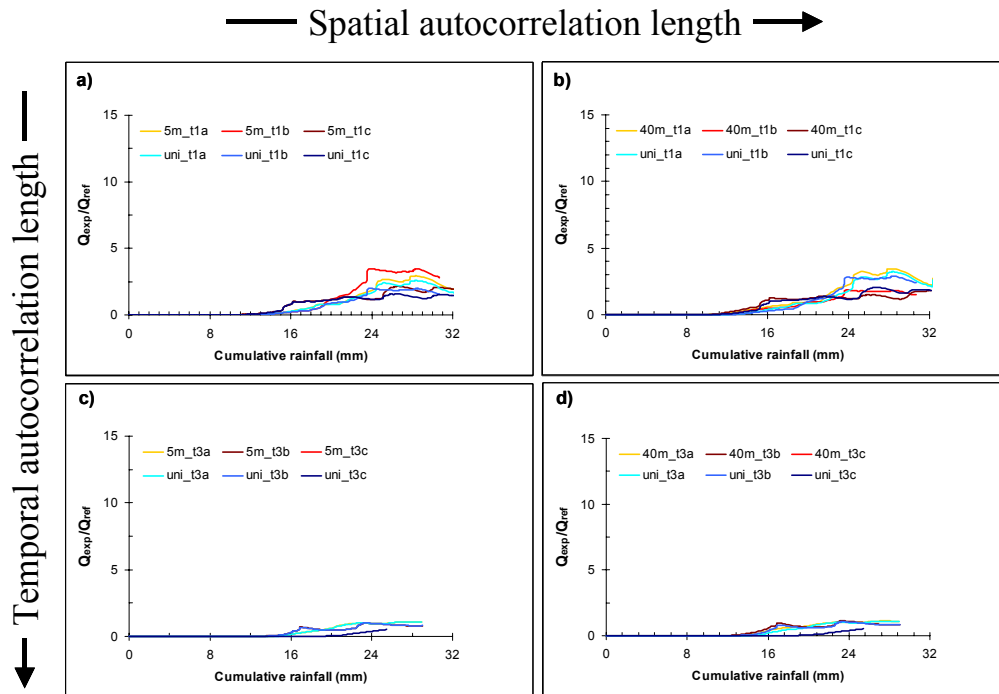


Figure 3.11: Predicted effects of finely (left) and coarsely (right) aggregated vegetation and soil patterns on cumulative soil loss for a steep slope. Results for storms with rainfall intensity variation of short and long autocorrelation length are shown in, respectively, the upper and lower graphs. Other symbols as in Figure 3.6.

3.2.3.3. Discussion

The simulation results are compatible with our qualitative understanding of these hillslope systems. We have compared responses of systems with temporally and spatially localised runoff/soil loss with those of reference systems that have spatially and temporally continuous runoff/soil loss. The net difference between the two systems at a given moment within a storm is a function of the connectivity (in time and space) of runoff/sediment producing grid cells. When we increase the mean rainfall intensity on a hillslope with spatially structured vegetation and soil attribute patterns we increase the fraction of grid cells in which runoff generation or sediment transport thresholds are exceeded, that is we increase spatial connectivity, which causes the response to converge with that of the reference situation. Increasing the temporal autocorrelation length of variation in rainfall intensity will cause runoff generation and sediment transport to be increasingly continuous in time, whereas increasing spatial autocorrelation of vegetation and soil attribute patterns causes runoff and sediment transport to be increasingly continuous in space. Slope gradient affects the connectivity of runoff and soil loss in both space and time.

A remarkable finding is that temporal variability in rainfall intensity affects the predicted hillslope water and sediment yields to a much greater extent than spatial variability in vegetation cover and related soil attributes. This can be explained from the fact that the

differences in runoff and soil loss rates for given locations between spells of low and high rainfall intensity tend to exceed the differences in runoff and soil loss rates for a given moment between bare soil areas and vegetated patches. Soil hydrological and erosional responses of bare soil areas and vegetated patches may differ by orders of magnitude but these differences are usually short-lived (e.g. Figs. 4-5) and have relatively little effect on the event-based results. On the other hand, a given site will continue throughout the storm to respond very differently to peaks and lows in rainfall intensity, which involved a range of over 70 mm.h⁻¹ and 120 mm.h⁻¹, respectively, for the storms of low and high mean intensity (see Figure 3.3). This result suggests that for these environments within-storm variability in rainfall intensity contributes more to uncertainty in soil erosion predictions by low-resolution models than spatial variability in vegetation and soil properties within the grid cells.

3.2.4. Implications for the PESERA model

3.2.4.1. Approach and set-up

Under the assumption that LISEM reproduces at least part of the synergetic effects of spatial and temporal variation in land attributes on hillslope erosion rates, we used the LISEM runs as virtual sets of field observations. Four sets of LISEM simulations allowed us to assess the impact of different factors on PESERA model performance:

- Set A: Spatially uniform vegetation/soil attributes – storms of constant rainfall rate (n=104)
- Set B: Spatially uniform vegetation/soil attributes – storms of variable rainfall rate (n=144)
- Set C: Spatially variable vegetation/soil attributes – storms of constant rainfall rate (n=104)
- Set B: Spatially variable vegetation/soil attributes – storms of variable rainfall rate (n=144)

Half of the LISEM runs of each set was used to ‘parameterise’ the PESERA model by deriving values for the soil water storage and soil erodibility parameters. The other halves were used to ‘validate’ the PESERA model predictions. For set A, deviations of PESERA predictions from LISEM results are indicative of the inherent differences between the two models. Deviations between the predictions of the two models for the other sets are assumed to indicate what the impact of temporal variability in rainfall rate and/or spatial variability in vegetation and soil attributes may be on PESERA model performance.

3.2.4.2. Discussion of results

Soil water storage and erodibility parameters

Two main equations of the PESERA model are:

$$q = \sum_{r>h} p(r - h) \quad [1]$$

$$S = k \cdot q^n \cdot \Lambda \quad [2]$$

where

- k: soil erodibility (m⁻²)
- S: sediment transport per unit contour length (m²)
- q: storm discharge per unit contour length (m²)
- L: slope gradient (m.m⁻¹)
- r: rainfall (m)
- p(r-h): proportion of rainfall exceeding storage capacity becoming runoff
- h: soil storage capacity (m)
- n: constant

Values for h and p can be obtained by plotting storm runoff (q) against storm rainfall (r) (Figure 3.12a-d). The soil erodibility parameter (k) is obtained by plotting event-based soil loss (S) against the product of squared storm runoff (q) and slope (L) (Figure 3.13a-d). Table 3.3 lists the obtained parameter values. Here we use a value of 2 for n.

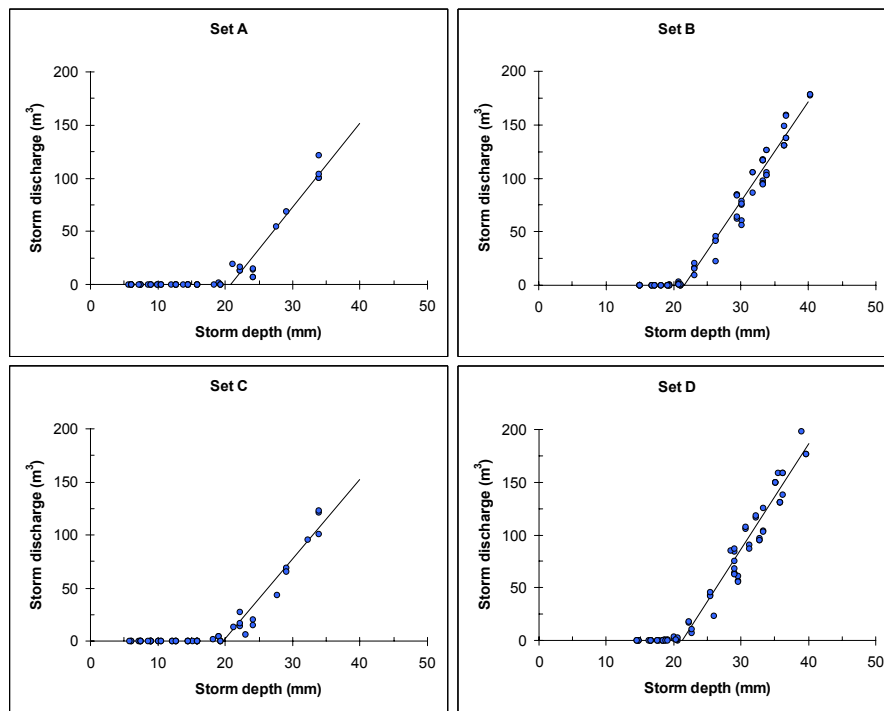


Figure 3.12: Storm discharge as a function of storm rainfall predicted by the LISEM model. The curves are fitted through all data points for which storm discharge is greater than 1 m³. See text for description of data sets A-D.

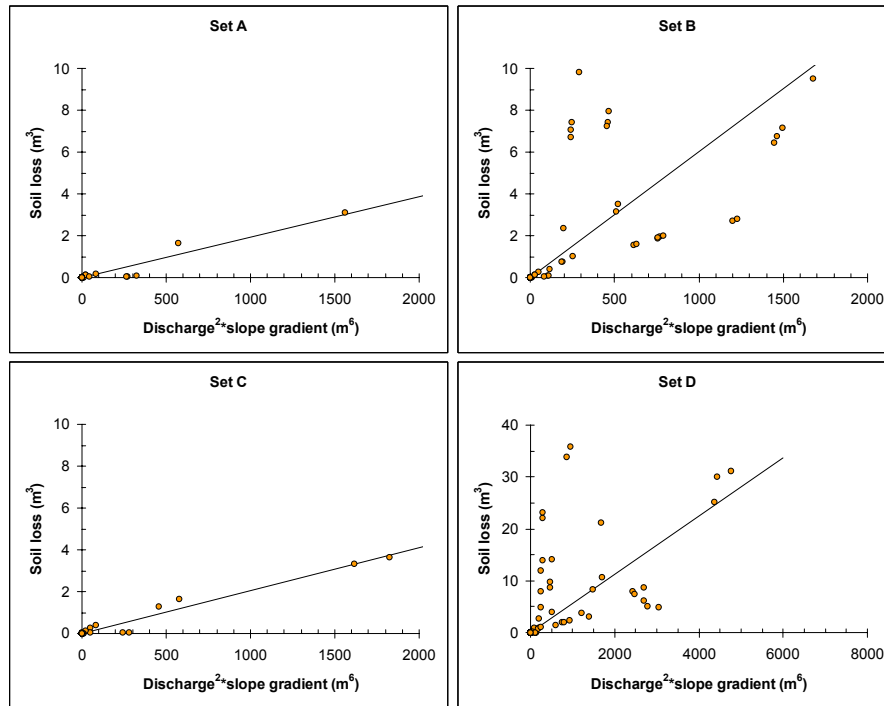


Figure 3.13: Soil loss as a function of storm discharge and slope gradient predicted by the LISEM model. See text for description of data sets A-D.

Table 3.3: PESERA parameter values obtained for the four sets of LISEM runs

Parameter	Set A	Set B	Set C	Set D
h (mm)	20.8	21.5	19.8	21.3
p (m ⁶)	7.9	9.3	7.5	10.0
k (m ⁻³)	0.0019	0.0060	0.0021	0.5470

Obtained values for the soil water storage parameters, h and p, vary relatively little, whereas those obtained for the soil erodibility parameter, k, vary strongly among the four sets of LISEM runs. Temporal variability in rainfall rate can be seen to affect the k-value to a much greater extent than spatial variability of vegetation and soil attributes (i.e. compare set A-B and set A-C). Combination of both temporal and spatial variability appeared to have a rather dramatic effect on the obtained value for the soil erodibility parameter (i.e. compare set A-D) and the goodness-of-fit of the corresponding curve (Figure 3.13).

PESERA model predictions

Using the parameter values from Table 3.3, equations 1 and 2 were applied to predict storm runoff and soil loss for the second half of the slope-storm combinations within each set of LISEM runs (Figure 3.14-15). A summary of the results is given in Table 3.4.

Storm discharge predictions by the PESERA model are relatively unaffected by temporal variability in rainfall rate and/or spatial variability in vegetation and soil attributes. The standard errors of the discharge predictions for sets A to D vary little: 0.77, 0.78, 0.79 and

0.67 m³/ha respectively. As for event-based soil erosion, spatial variation in vegetation and soil attributes alone does not really affect the accuracy of the PESERA predictions, since the predicted soil loss rates and corresponding standard errors for set A and C are similar. Temporal variation in rainfall rate, however, does lead to an eight-fold increase of the standard error of the soil loss predictions for individual events (i.e. 0.79 T.ha⁻¹), even in absence of spatial variation in vegetation and soil attributes. Adding that spatial variation causes the standard error of event-based soil loss predictions to increase with a very small amount (i.e. 0.80 T.ha⁻¹).

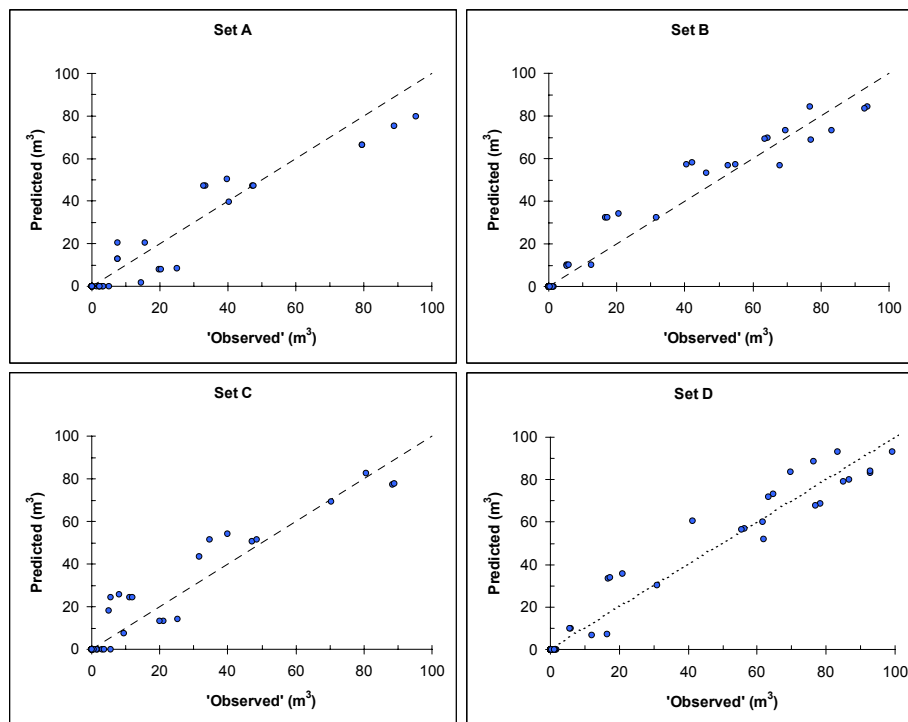


Figure 3.14: Storm discharge predicted by the PESERA model against ‘observed’ values (i.e. LISEM predictions). See text for description of data sets A-D.

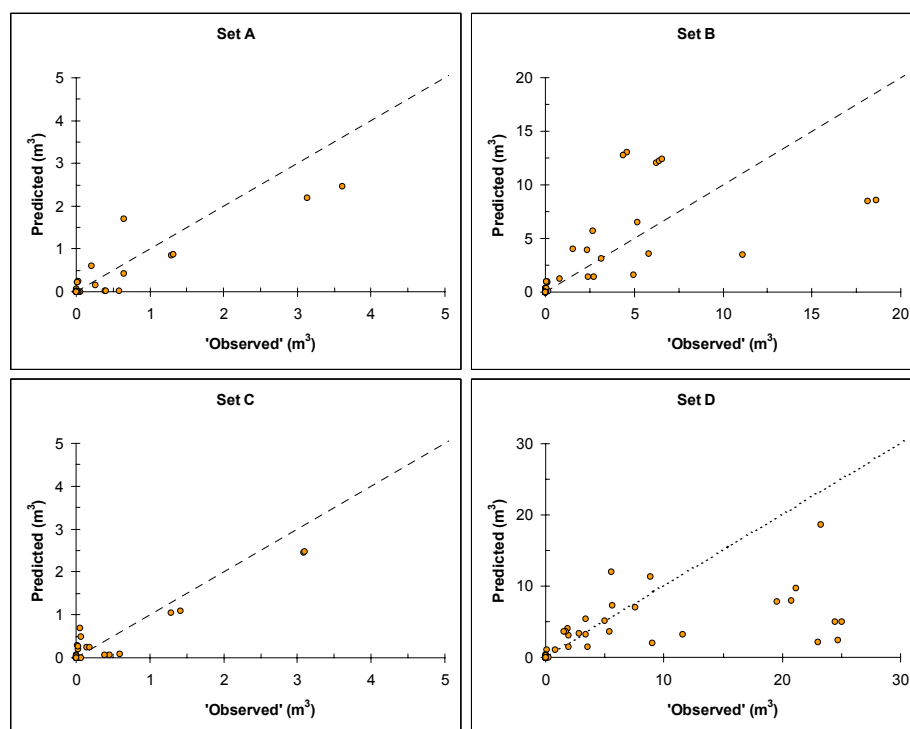


Figure 3.15: Soil loss predicted by the PESERA model against 'observed' values (i.e. LISEM predictions). See text for description of data sets A-D.

Table 3.4: Summary of results obtained with the PESERA model for water and soil losses from the hypothetical hillslopes and storms simulated with LISEM.

Set	Vegetation/soil	Rainfall rate	Total rainfall (mm)	Discharge			Soil loss		
				Obs overall runoff coefficient	Pred. overall runoff coefficient	Standard error (m ³ /ha)	Obs. erosion (T/ha/m)	Pred. Erosion (T/ha/m)	Standard error (T/ha)
A	uniform	constant	944	0.08	0.07	0.77	0.021	0.017	0.10
B	uniform	structured variation	1719	0.15	0.15	0.78	0.230	0.194	0.79
C	structured variation	constant	926	0.07	0.08	0.79	0.019	0.017	0.04
D	structured variation	structured variation	1650	0.15	0.15	0.67	0.255	0.139	0.80

The PESERA model was designed for the assessment of the long-term soil erosion risks rather than for event-based predictions of discharge and soil loss. A comparison of the average soil loss rates over multiple storms may therefore provide a more realistic indication

of what the ignorance of spatio-temporal variation in land attributes may mean for its performance in dry Mediterranean landscapes. In the most realistic set-up of hillslopes with spatially structured vegetation cover and soil attributes, and temporally variable rainfall rates, the average soil loss rates per mm of rainfall predicted by the PESERA model are very similar to those resulting from the high-resolution simulations with the LISEM model. At long timescales under- and over-predictions of soil loss rates happen to cancel out. The cancelling out of over- and under-predictions could be (partly) due to the linear relationships between vegetation cover fraction and several soil parameters (eqn. 2-9) assumed for this simulation study, but this could not be quantified in further detail.

3.2.5. Conclusions

The main conclusions that can be drawn from this simulation study are:

- During an individual storm, effects of spatial and temporal variability of land attributes on hillslope discharge and soil loss rates are most pronounced just after runoff generation and sediment transport thresholds are exceeded in areas of particular surface types (e.g. bare soil), but not (yet) in others. Within the simulated environment, effects of temporal variability in rainfall intensity were much greater than those of spatial variation in vegetation and soil attributes.
- During an individual storm the magnitude of the effects of spatial and/or temporal variability decreases with mean rainfall intensity, with the autocorrelation length of variation in rainfall intensity and with slope gradient. For discharge rates, the magnitude of effects also decreases with the autocorrelation length of spatial variability in vegetation and soil attributes.
- At the event scale, effects of spatio-temporal variation in land attributes decrease with the amount and intensity of the rainfall, and with slope gradient.
- Ignoring spatial variation of vegetation/soil attributes within grid cells and temporal variation of rainfall intensity within a storm has relatively little effect on PESERA model predictions of storm discharge, but may be the cause of substantial uncertainty in predictions of event-based erosion rates.
- Average results for a large population of event-based predictions are relatively unaffected by spatio-temporal variation in land attributes as over- and under-predictions tend to cancel out. In environments with strongly non-linear relationships between vegetation cover fraction and soil hydrological/erosional properties this may, however, not be the case.

3.2.6. Work to be done by the end of the project

An IKONOS image providing panchromatic (1m) and multispectral (4m) information has been purchased for an area of 3km x 3km that includes the Rambla Honda filed site. The image was taken the 28/04/03 and it has been subsequently processed. An ancillary field campaign was carried out in order to obtain ground information about plant biomass and LAI.

An analysis of spatial patterns observed on this image, and of the temporal pattern in the quasi-continuous rainfall records from Rambla Honda, SE Spain, are two tasks planned for

the last part of the project, with the objective of placing the results of the simulation experiments in a regional context.

3.3. WP3: CALIBRATION AND VALIDATION AT RAMBLA HONDA FIELD SITE

3.3.1. Work carried out during the reporting period

As a contribution to work package 3 we have evaluated the performance of the PESERA model (spreadsheet version) at the plot and hillslope scales by comparing model predictions with field measurements from the Rambla Honda field site in Almería Province (SE Spain). Plot data have also been used to estimate values for the soil water storage and soil erodibility parameters of the PESERA model.

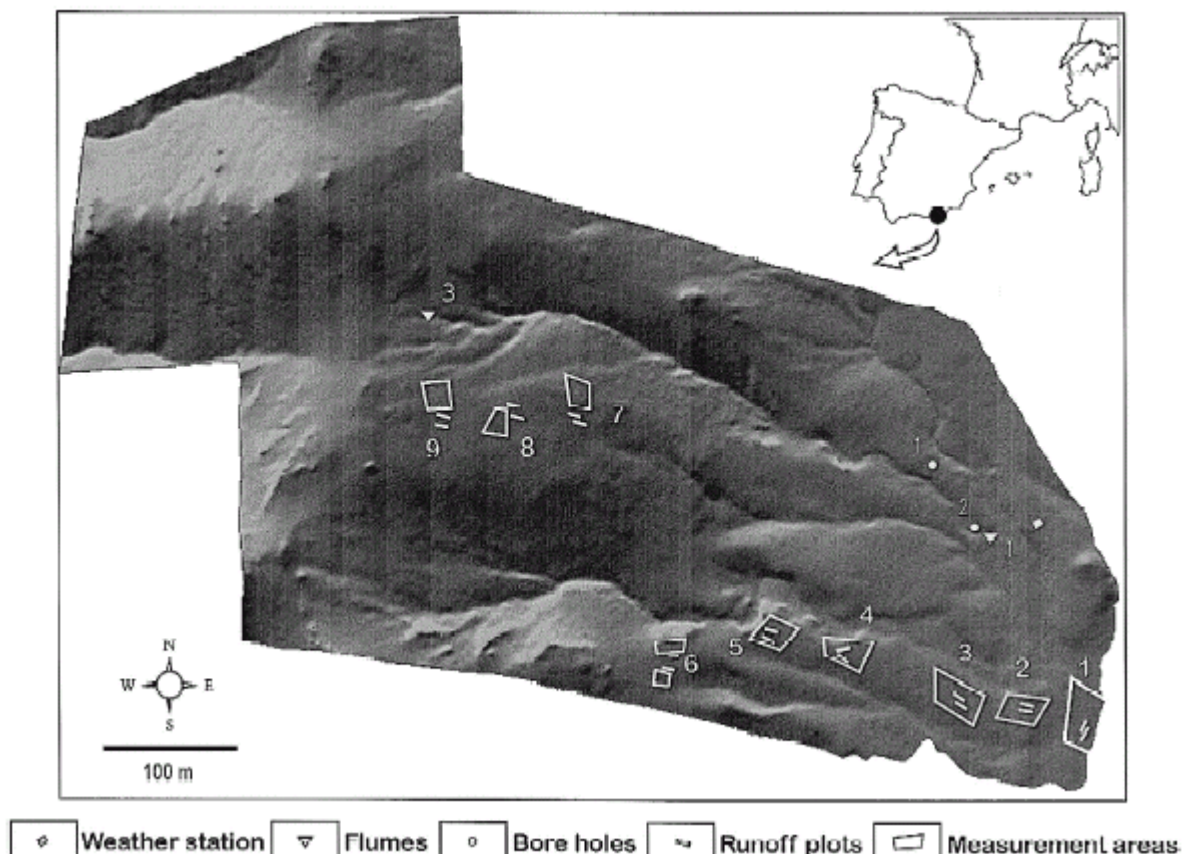


Figure 3.16: Location and lay-out of the Rambla Honda field site. Source: Puigdefábregas et al., 1998.

3.3.2. Evaluation of PESERA model performance

3.3.2.1. Rambla Honda field site

The field site at Rambla Honda, near Tabernas, Almería, Spain (37° 8’N, 2° 22’W, 630 m.a.s.l.) represents a non-agricultural landscape under semi-arid mediterranean climate conditions with a mean annual temperature of 16°C and mean annual rainfall of 279 mm (see (Puigdefábregas et al. 1996; Nicolau et al. 1996) for details). The site consists of a 18 ha hillslope section stretching from the dry bed of an ephemeral river (‘Rambla Honda’), at 630 m altitude to the water divide at 800 m. The area is characterised by a catena of soils and associated vegetation types. In the upper hillslope Typic Torriorthent soils and *Stipa tenacissima* L. tussocks occur on micaschist bedrock, while Typic Torrifluent soils with *Anthyllis cytisoides* L. and *Retama sphaerocarpa* (L.) Boiss. shrubs are dominant, respectively, in the upper and lower parts of the alluvial fan sectors. *Retama* is also abundant in the dry stream bed. In the upper hillslopes, *Stipa tenacissima* used to be harvested for cellulose, while the footslope sedimentary fill was used for the rainfed cultivation of cereals. Both types of land use ceased about 35 years ago. The site was instrumented with a meteorological station, runoff plots, three H-type flumes, moisture sensors and other equipment in the late 1980s and early 1990s as part of the LUCDEME and MEDALUS research projects.

Table 3.5: Basic characteristics of the Field plots at Rambla Honda, Se Spain.

Site ID	Dominant species	vegetation	type-	Vegetation cover fraction	Slope gradient (m.m ⁻¹)	Slope length (m)	Open/close d plot
MA4a	Drought <i>Anthyllis</i>	deciduous	shrubs-	0.48	0.12	10	closed
MA4b	Drought <i>Anthyllis</i>	deciduous	shrubs-	0.24	0.16	10	closed
MA5a/b	Drought <i>Anthyllis</i>	deciduous	shrubs-	0.36	0.21	10	closed
MA5a	Drought <i>Anthyllis</i>	deciduous	shrubs-	0.36	0.21	10	closed
MA5b	Drought <i>Anthyllis</i>	deciduous	shrubs-	0.22	0.21	10	closed
MA6a	Drought <i>Anthyllis</i>	deciduous	shrubs-	0.48	0.36	10	closed
MA6b	Drought <i>Anthyllis</i>	deciduous	shrubs-	0.15	0.40	10	closed
MA7a	Tussock grass- <i>Stipa</i>			0.40	0.45	10	closed
MA7b	Tussock grass- <i>Stipa</i>			0.23	0.42	10	closed
MA8a	Tussock grass- <i>Stipa</i>			0.44	0.38	10	closed
MA8b	Tussock grass- <i>Stipa</i>			0.30	0.32	10	closed
MA9a	Tussock grass- <i>Stipa</i>			0.32	0.38	10	closed
MA9b	Tussock grass- <i>Stipa</i>			0.29	0.42	10	closed

NA	Tussock grass- <i>Stipa</i>	0.40	0.16	17	open
NB	Tussock grass- <i>Stipa</i>	0.50	0.18	60	open
SA	Tussock grass- <i>Stipa</i>	0.25	0.21	23	open
SB	Tussock grass- <i>Stipa</i>	0.33	0.23	49	open

In this validation exercise we used field records of event-based runoff and soil loss from 12 closed runoff plots of 2 m x 10 m and from 4 open plots representing hillslope sections of 17-60 m. The closed plots are representative of the *Stipa* and *Anthyllis* communities. The ones used in this analysis have been operational since September 1991. The open plots are dominated by *Stipa* and have only been operational for two hydrological years (i.e. Oct.1990-Nov.1992) (see (Sanchez 1995) for details). Basic characteristics of the plots are shown in Table 3.5.

3.3.2.2. PESERA model set-up

The spreadsheet-version of the PESERA model (i.e. eros111b.xls, d.d. 21/02/02) was set up for a 'natural degraded' land cover, 'medium' soil texture, straight slopes (i.e. 0% convexity) and mean monthly climate parameters calculated from the meteorological station at Rambla Honda (1989-2001). A calibrated version of the Hargreaves and Samani formula (Hargreaves & Samani 1982; Boer 1999) was used to estimate mean monthly potential evapotranspiration rates. Climate parameters are shown in Table 3.6. The PESERA model was run in two modes:

- With plot-specific relief parameters (gradient and slope length) and the standard cover table for 'natural degraded land';
- With plot-specific relief parameters (gradient and slope length) and a plot-specific cover table (Table 3.5).

In mode 1 the vegetation cover fraction is assumed to vary substantially at a monthly timescale (i.e. 10-25%), whereas in mode 2 the vegetation cover fraction of the plots is supposed to be constant in time (see Table 3.5).

Table 3.6: Climate parameters for the Rambla Honda Field site. PET: potential evapotranspiration

Month	Rainfall	Mean	CV of mean	Mean	Mean	daily
Unit	mm	rainfall/rainda	rainfall/rainda	temperature	temperature	PET
		y	y	°C	°C	mm
January	19.4	2.2	0.80	7.8	10.5	71
February	26.6	6.5	0.89	9.5	10.3	86
March	20.7	3.6	0.42	11.3	10.3	103
April	26.0	3.8	0.67	13.2	11.7	126
May	21.5	4.0	0.24	17.6	11.9	149

June	19.3	6.7	0.51	21.2	12.6	169
July	7.1	6.0	0.30	25.3	12.9	188
August	10.3	6.8	0.23	25.6	12.7	186
September	45.8	8.2	0.69	21.3	11.6	151
October	47.8	8.9	1.06	15.9	10.0	109
November	37.2	7.3	0.69	12.5	9.9	85
December	44.2	5.7	0.39	9.6	9.1	69
Annual	326	5.81	0.57	15.89	11.12	1492

3.3.2.3. Discussion of results

In all runs the model took 16-22 years to reach an equilibrated vegetation cover and water balance. The output consists of mean monthly and annual predictions for the main components of the water balance, plant biomass, and soil loss. We compared the predicted mean annual runoff coefficients and soil loss rates for individual plots with the observed values (Table 3.7). Predicted long term runoff coefficients (RC) are in the range of 0.017-0.024 (m.m⁻¹) when the standard cover table is used and 0.001-0.045 (m.m⁻¹) when the plot specific cover tables are used. With the standard cover table the model does not reproduce observed RC values of individual plots, but does provide a reasonable estimate of average long-term RC values on these dry Mediterranean hillslopes (Figure 3.17a). In mode 2, with the plot-specific cover-tables, the model under-estimates the RC for both the closed and the open plots (Figs. 17b, 18).

Table 3.7: Observed and predicted runoff coefficients and soil loss rates for the plots.

Site ID	Mode 1		Mode 2		Mode 1		Mode 2	
	Obs. RC (m.m ⁻¹)	Pred. RC (m.m ⁻¹)	Pred. RC (m.m ⁻¹)	Obs. Soil loss (T.Ha ⁻¹ .y ⁻¹)	Pred. Soil loss (T.Ha ⁻¹ .y ⁻¹)	Pred. Soil loss (T.Ha ⁻¹ .y ⁻¹)	Pred. Soil loss (T.Ha ⁻¹ .y ⁻¹)	
MA4a	0.018	0.017	0.001	0.027	0.018	0.001		
MA4b	0.051	0.019	0.014	0.122	0.027	0.019		
MA5a/b	0.040	0.019	0.008	0.045	0.035	0.014		
MA5a	0.048			0.058				
MA5b	0.032			0.031				
MA6a	0.038	0.023	0.002	0.035	0.076	0.004		
MA6b	0.043	0.023	0.045	0.058	0.087	0.183		
MA7a	0.039	0.024	0.004	0.133	0.101	0.013		
MA7b	0.038	0.024	0.019	0.051	0.093	0.073		
MA8a	0.027	0.023	0.003	0.096	0.082	0.007		
MA8b	0.063	0.022	0.009	0.071	0.066	0.024		
MA9a	0.042	0.023	0.008	0.122	0.083	0.024		
MA9b	0.050	0.024	0.011	0.062	0.093	0.037		
NA	0.034		0.003	0.113		0.006		
NB	0.024		0.001	0.094		0.005		
SA	0.033		0.009	0.639		0.035		

SB	0.009	0.003	0.557	0.023
----	-------	-------	-------	-------

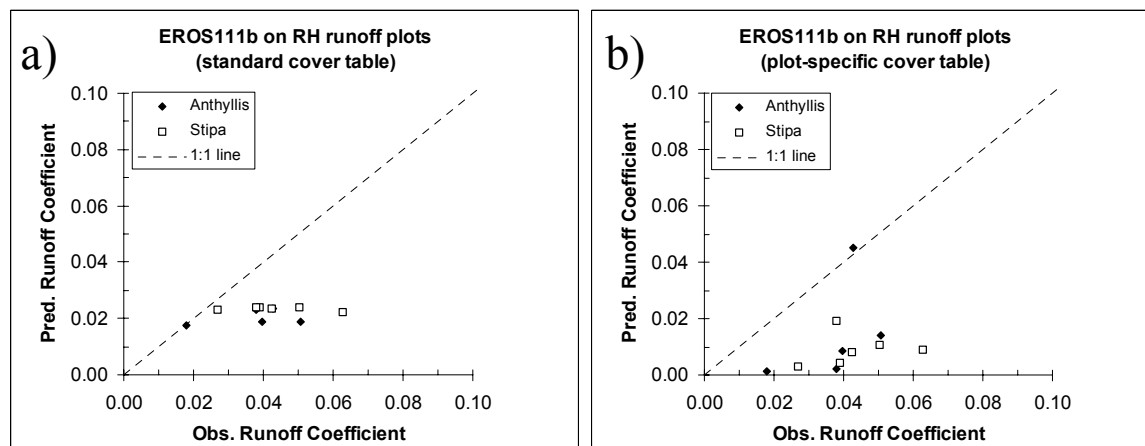


Figure 3.17: Observed (10 year record) and predicted runoff coefficients for closed runoff plots, using the standard cover table (a) or plot-specific cover tables (b).

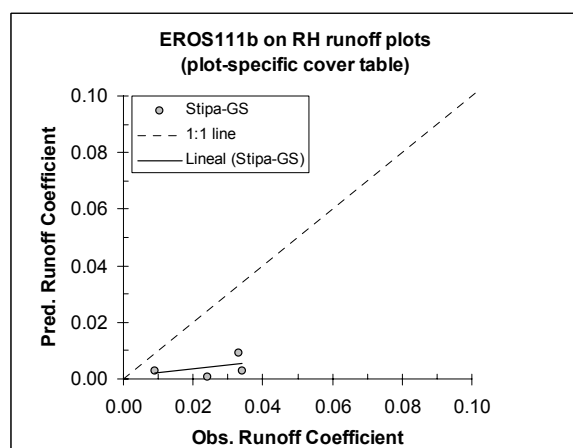


Figure 3.18: Observed (2 year record) and predicted runoff coefficient for open plots with variable cover of Stipa.

Predicted mean annual soil loss rates are in the range of 0.01-0.10 T.Ha-1.y-1, whereas observed values are 0.03-0.64 T.Ha-1.y-1. When the model is run with the standard cover table for 'natural degraded land' (mode 1) the predicted soil loss rates are of the same order of magnitude as the observed values (Figure 3.19a). Using only plot-specific relief parameters and potential evapotranspiration data the model can, however, not reproduce the observed differences in erosion rates among the closed runoff plots. When we add a plot-specific cover table (mode 2) results do not improve (Figure 3.19b).

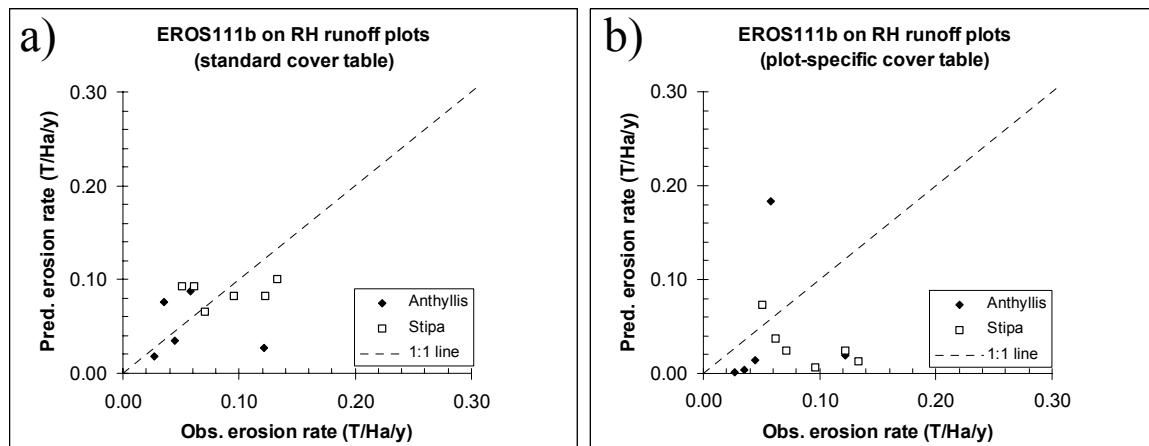


Figure 3.19: Predicted mean annual soil loss rates against observed values for closed runoff plots at Rambla Honda, using the standard cover table (a) and a plot-specific cover table (b).

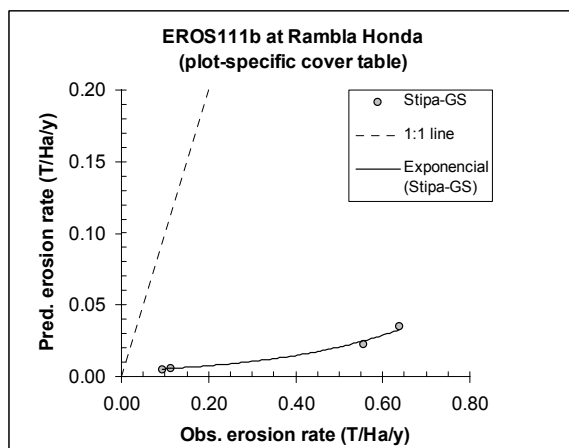


Figure 3.20: Predicted against observed mean annual soil loss rates for open plots in Stipa vegetation.

Interesting results were obtained for the open plots (Figure 3.20). Although the model under-predicts the erosion rates quite strongly it does seem to respond consistently to subtle variation in vegetation cover and slope gradient. The systematic under-estimation could result from the different observation periods for the rainfall record and the erosion rates, being 1989-2002 and Oct.1990-Nov.1992 respectively. During the two years of the erosion measurements (Sanchez 1995) the number of rain-days per month were similar to the 10 year mean value at Rambla Honda (Figure 3.21), but the amount of rain per rain day was greater in eight months of the year (Figure 3.22). The maximum 5 minute intensities also indicate that storms have been particularly intense during the 1990-1992 measurement period.

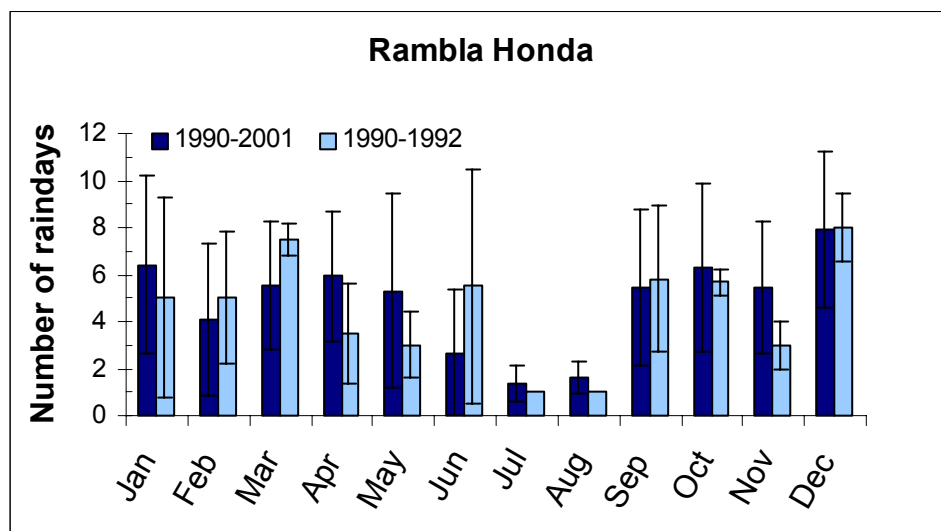


Figure 3.21: Number of raindays per month at Rambla Honda for the total observation period at Rambla Honda (1990-2001) and the measurement period for the open plots (1990-1992).

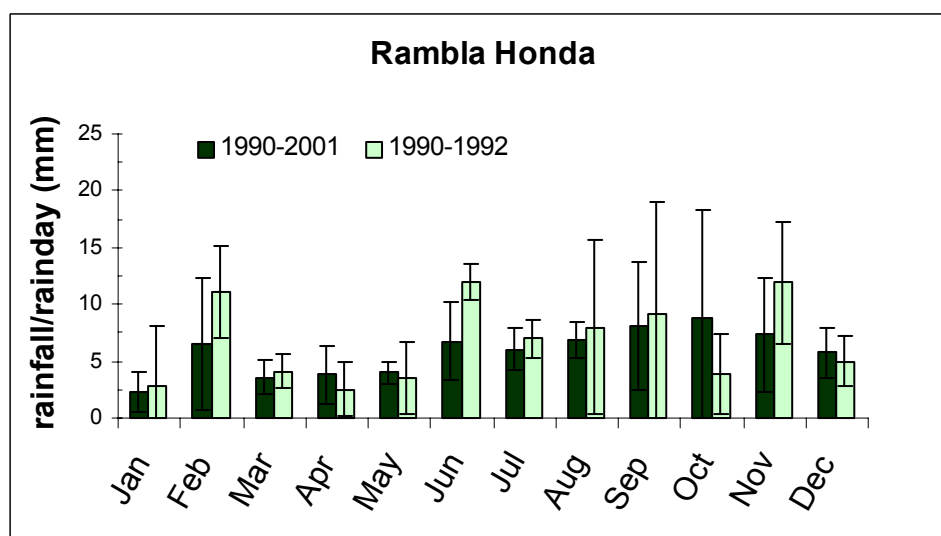


Figure 3.22: Mean rainfall per rainday at Rambla Honda for the total observation period at Rambla Honda (1990-2001) and the measurement period for the open plots (1990-1992).

In this validation exercise we (deliberately) forced the PESERA model to make predictions at a scale it was not intended for. The model was obviously not designed to predict relatively subtle variation in runoff coefficients and soil loss rates among highly similar plots. At the 1.0 km resolution, and the associated scales of the model input parameters, all the tested plots would fall in a single cell and have the same land cover class, relief index and climate parameter values. A fairer test of its performance would therefore be a comparison of the observed and predicted mean RC and soil loss rate for all plots, as if they were samples from a 1 km grid cell. At this scale, the model prediction for mean annual

runoff and soil loss agrees reasonably well with the observed values when we use the standard cover table, but less so when we use a plot-specific cover table (Table 3.8).

Table 3.8: Predicted and observed mean runoff coefficients and soil loss rates for all plots at Rambla Honda.

	Mode 1	Mode 2		mode 1	mode 2	
	Obs. RC (m.m ⁻¹)	Pred. RC (m.m ⁻¹)	Pred. RC (m.m ⁻¹)	Obs. Soil loss (T.Ha ⁻¹ .y ⁻¹)	Pred. Soil loss (T.Ha ⁻¹ .y ⁻¹)	Pred. Soil loss (T.Ha ⁻¹ .y ⁻¹)
Mean	0.037	0.022	0.009	0.136	0.069	0.031
SD	0.013	0.002	0.011	0.178	0.029	0.046

A possible explanation for the difference in accuracy between the two prediction modes could be that the model gives too much weight to the vegetation cover fraction. Most of the field plots actually have a denser vegetation cover than assumed in the standard cover table for ‘natural degraded’ land covers (mode 1). The model, however, is more accurate when the standard cover table (i.e. too low cover fraction) is used, than when the actual vegetation cover fraction is used. Figure 3.23 illustrates this point: observed long-term runoff coefficients decrease with vegetation cover fraction but at a smaller rate than the predicted runoff coefficients.

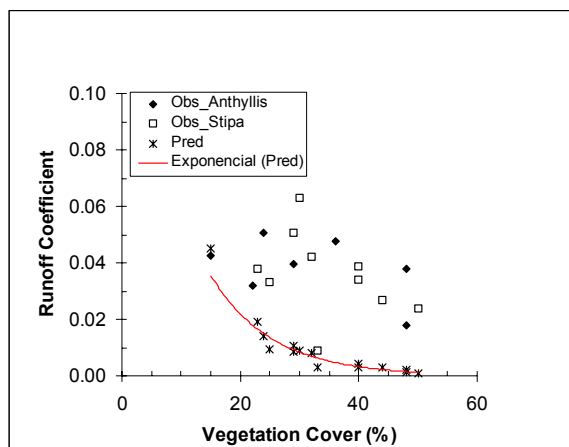


Figure 3.23: Observed and predicted trends of the runoff coefficients with vegetation cover.

3.3.3. Pesera parameter estimation

The field records from the closed plots have also been analysed for the estimation of four PESERA model parameters: the soil water storage capacity (h and p), the exponent (n) used on runoff, and the soil erodibility (k). Parameter values (Table 3.9) were calculated separately for each of the three main vegetation types at Rambla Honda by fitting linear functions to plots of:

- discharge (q , in m^3) against rainfall (r , in mm) @ soil water storage capacity (h , in mm), and proportion (p) of rainfall becoming runoff for $r > h$ (Figure 3.24-26)
- soil loss over slope (S/L) against discharge (q), log-log scale @ exponent (n),
- soil loss (S , in m^3) against discharge (q , in m^3) to the power of n times slope (qnL) @ soil erodibility (k) (Figure 3.27-29)

Table 3.9: PESERA parameter values obtained from runoff and soil loss measurements in closed plots at Rambla Honda.

parameter	Retama plots		Anthyllis plots		Stipa plots	
	value (SD)	R^2 (p)	value (SD)	R^2 (p)	value (SD)	R^2 (p)
h (mm)	4.1	0.21 (<0.000)	9.3	0.57 (<0.000)	14.5	0.72 (<0.000)
p (-)	0.001		0.002		0.004	
n (-)	0.56	0.31 (<0.00)	0.23	0.08 (<0.00)	0.34	0.14 (<0.00)
k (*)	0.0012 (0.0009)	0.06-0.45 (<0.000)	0.0002 (0.0002)	0.09-0.24 (<0.000)	0.0003 (0.0001)	0.18-0.41 (<0.000)

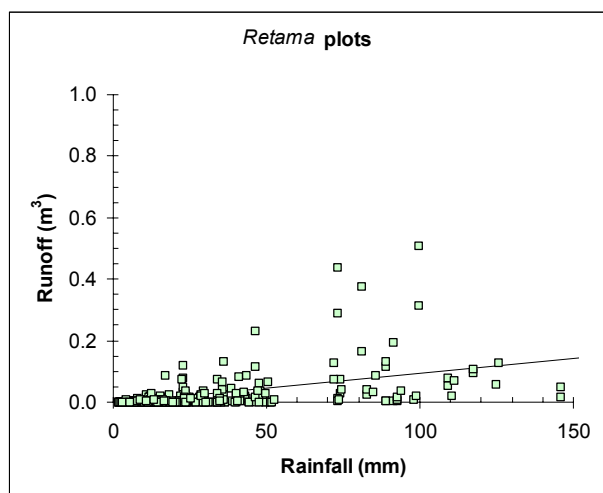


Figure 3.24: Observed relationship of plot runoff as a function of rainfall depth for six plots dominated by Retama spp. at Rambla Honda.

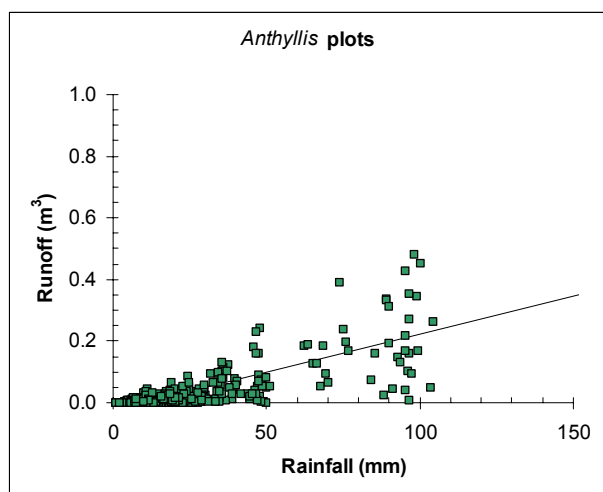


Figure 3.25: Observed relationship of plot runoff as a function of rainfall depth for six plots dominated by Anthyllis spp. at Rambla Honda.

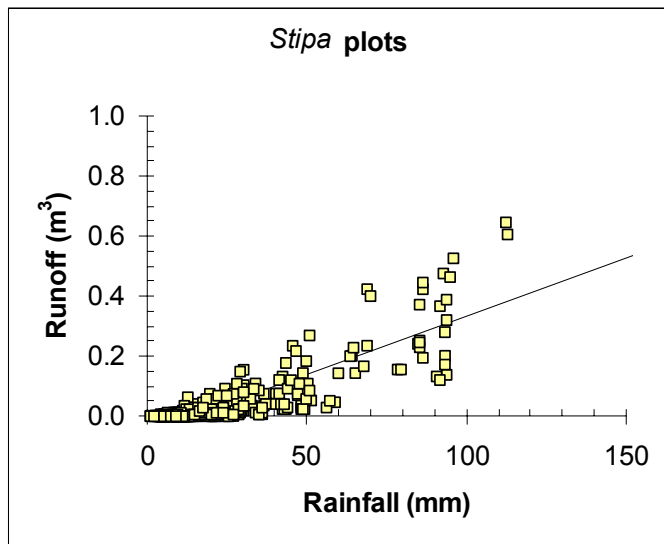


Figure 3.26: Observed relationship of plot runoff as a function of rainfall depth for six plots dominated by Stipa spp. at Rambla Honda.

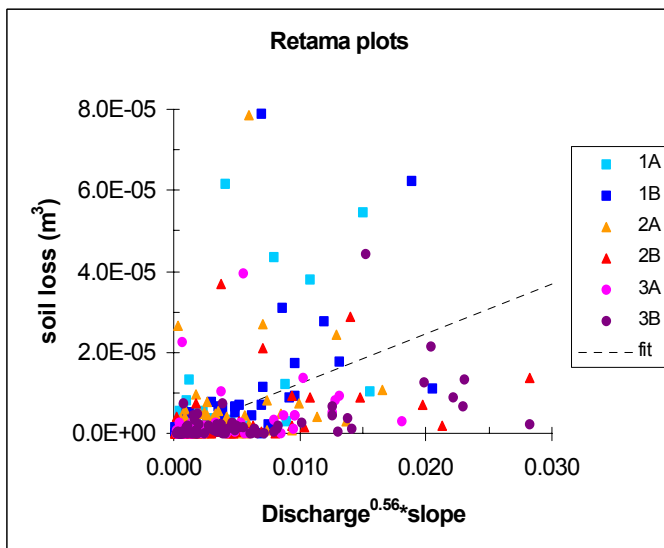


Figure 3.27: Event-based soil loss as a function of discharge and slope observed in closed plots dominated by Retama spp. at Rambla Honda.

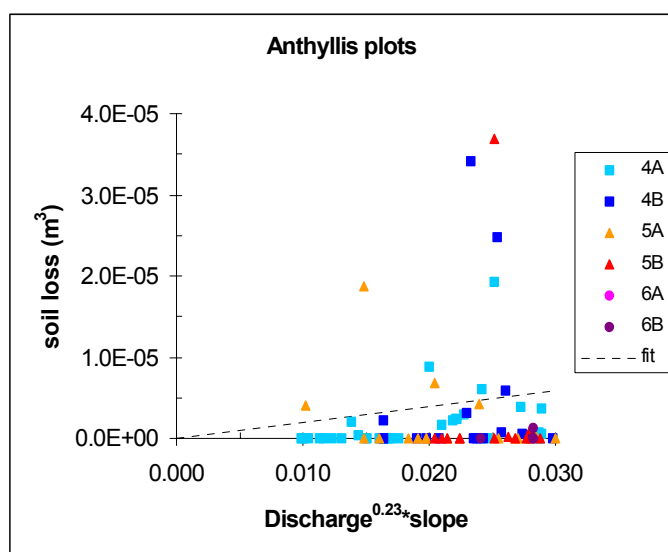


Figure 3.28: Event-based soil loss as a function of discharge and slope observed in closed plots dominated by *Anthyllis* spp. at Rambla Honda.

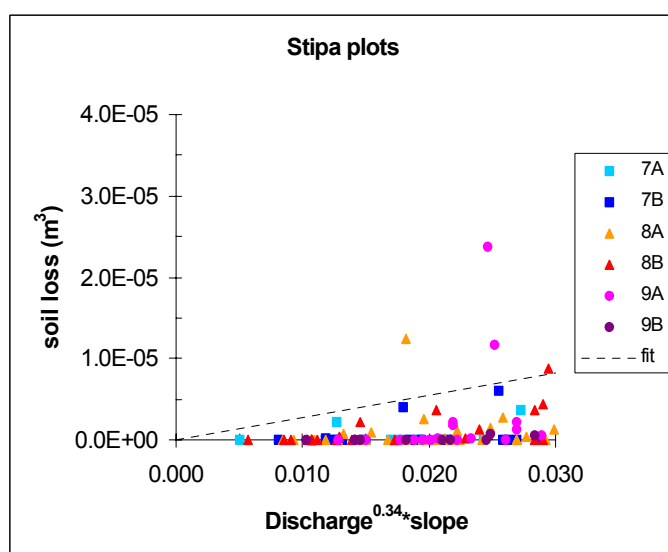


Figure 3.29: Event-based soil loss as a function of discharge and slope observed in closed plots dominated by *Stipa* spp. at Rambla Honda.

In general, the scattergrams from which the parameter values were estimated show substantial dispersion of observations. Consequently the obtained parameter values are not very precise and should be used as such. The parameter values do reflect known differences between the hydrological and erosional functioning of the three landscape units (Nicolau et al. 1996; Puigdefábregas et al. 1998). The Retama-dominated footslopes may produce some runoff for small rainfall amounts, but runoff coefficients remain small even for large storms due to the relatively high infiltration capacity of the deep sandy soil. On the alluvial fans and abandoned terraces (*Anthyllis* plots), and rocky upperslopes (*Stipa* plots) soils tend to be more structured and shallower than in the Retama area, which translates into greater initial

soil water storage capacity but also into greater runoff coefficients for storms that exceed that storage capacity. The different values obtained for the exponent n and the soil erodibility parameter, k , though not very precise, also seem to make sense. The Retama area is characterised by large patches of bare sandy soils with little coherence, causing both n and k to be greater than in the Anthyllis and Stipa areas where vegetation cover is denser, bare soil patches are smaller, soils are more coherent, and soil surfaces are rough and stony.

3.4. WP4: VALIDATION AT SE SPAIN AND COMPARISON WITH CSIC-EEZA APPROACH

Now that Pesera model applications at the regional scale start to be available, during the extended project time it is planned to compare its results in South-East Spain with a previously land degradation assessment, carried out by EEZA-CSIC, in a test area of intermediate size (900 km²) located in the Guadalentin basin.

CHAPTER 4 KATHOLIEKE UNIVERSITEIT LEUVEN

Anne Gobin, Olivier Cerdan and Gerard Govers

Laboratory for Experimental Geomorphology, Katholieke Universiteit Leuven
Redingenstraat 16, 3000 Leuven

4.1. ROLE AND CONTRIBUTION

The Katholieke Universiteit Leuven is the overall Project Co-ordinator. Major tasks undertaken during the past year included compiling and writing financial and progress reports, minutes of meetings and technical reports following research meetings.

A plant growth model, consisting of three sub-models was sent to Leeds for incorporation in the grid-version of the model. However, it was decided that the number of input grids would increase substantially and make the PESERA model too complex and difficult to run.

A major effort was undertaken to simplify the inputs for vegetation growth to the minimum input feasible but still enabling meaningful scenario analysis to be undertaken. This involved the interpolation of planting dates for different crop groups across Europe, and construct average monthly crop covers calculated from cropping calendars.

Agricultural land use was spatialised through the coupling of the Farm Structure Survey Census data per harmonised NUTS region and CORINE Land Cover. A series of programmes was developed to determine the arable land uses in order of importance and their corresponding area per harmonised NUTS region, and subsequently spatialised with CORINE Land Cover.

The long-term high-resolution database was used to test the underlying equations to simulate runoff and sediment transport in the PESERA model. This investigation has led to calibration results for k and h values.

The 1 km² PESERA map was validated using a database of measurements and observations across Europe. The comparison between measured and observed erosion rates was performed in a visual, numerical and categorical way.

Co-operations at the European level with the European Environment Agency and the ENRISK concerted Action have been further elaborated. Meaningful links with Syngenta and the SOWAP Project have also been maintained.

4.2. WP1: LAND USE AND VEGETATION GROWTH

4.2.1. The plant growth model

The plant growth model is developed so that it explicitly links to the regional and continental scale, and so that it can replace the vegetation module present in some of the older PESERA point-model versions. The vegetation module in the older PESERA point-model versions does not incorporate some of the current methods in plant growth modelling, e.g. calculation of biomass should be based on radiation and not on evapotranspiration.

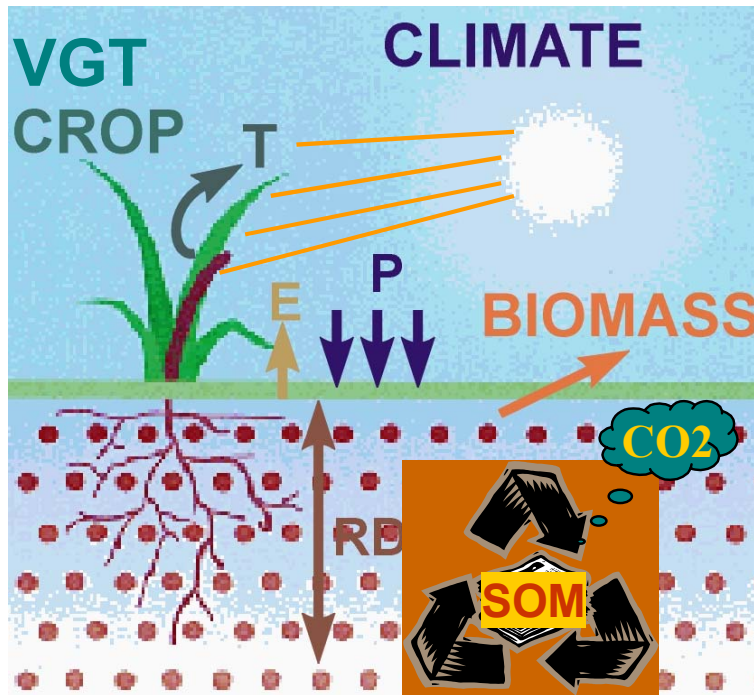


Figure 4.1 Major components of the plant growth model

The plant growth model consists of three major modules: water balance, biomass generation and plant litter decomposition. The model has the potential to be used for all types of annual and perennial vegetation. The link with the erosion model happens at multiple stages. It is used to determine water consumption from the root zone, determine the amount of biomass production and vegetation cover, establish evapotranspiration from the bare and covered fractions of vegetation and calculate soil organic matter. The plant growth model is primarily designed to run in a forecasting mode and to link explicitly to methodologies used in remote sensing to calculate biomass. In a monitoring mode, the biomass module could then be replaced by data obtained from optical remote sensing, using the FPAR. The methodology of using the remotely sensed variable FPAR and an example for Flanders were elaborated in the first progress report and the first annual report.

The model code was finalised and sent to Leeds early June 2002. At the meeting in Ispra, it was decided to use only a number of components of the plant growth model in the forecasting mode of the PESERA grid-model. The reasons are that the introduction of the full plant growth model would increase the number of input grids and the run-time of the model in regional applications. The components that were decided to be included were planting

dates from the plant growth parameters database, for different crop groups and interpolated across Europe. In Wageningen, it was decided to refine the look-up table for plant cover.

4.2.2. Plant growth parameters database

A comprehensive spatial plant growth parameter database was developed. The data originally collected by Ground for GIS (GfG) at the Katholieke Universiteit Leuven (Van Orshoven et al., 1999) were used as a starting point and expanded upon. The original data describe planting dates, phenological stages linked to cumulative temperature days and crop coefficients linked to phenological stages for calculating the crop actual evapotranspiration parameters. The original data were collected from agricultural research stations across Europe and contain data for certain cereals, oilseeds and root crops.

The GfG-KULeuven database was expanded to include additional crop data for other crop groups considered. Also included were data for areas where no information was previously available, but where the specific crops were grown, e.g. for wheat in some of the Scandinavian countries and the UK. Crops were aggregated into similar crop groups; maize was kept as a separate data layer. The major crop groups in the plant growth parameters database are: maize, spring cereal, winter cereal, pulses, rootcrops, oilseed, vegetables and flowers, forage and other arable crops. These crop groups relate directly to the classes used in the Farm Structure Survey Census Data by Eurostat. The resulting plant growth parameters database includes parameters for major arable crop groups across Europe.

Plant parameters in the database were calculated in relation to the growth characteristics for each of the major crops and crop groups. Arable crops are grown from planting to harvest dates or until the accumulated temperature days equal the potential cumulative temperature days for the plant, whichever information was available. For the majority of plants, the plant parameters and growth stages were expressed in thermal days. For winter-sown crops this also provides a way of establishing the dormancy period.

In order to comply with the temporal structure of the PESERA model, the temporal linkages of the plant parameters had to be assigned to Julian days and aggregated to monthly values where appropriate. Cumulative temperature days marking the boundaries of the different plant growth stages were converted to Julian days of the year using plant specific base and optimum temperature values, which in turn form the boundaries of phenological plant activity.

For the major crop groups, the data were interpolated on the basis of meteorological stations and related to the 50 x 50 km grid covering Pan-Europe, Turkey and the Maghreb countries. The planting dates were converted to Julian days and interpolated using a Delauney-base TIN with water bodies as hard breaklines. Figure 4.2 shows spatially interpolated planting dates for spring sown grain maize, whereas Figure 4.3 shows spatially interpolated planting dates for winter sown cereals.

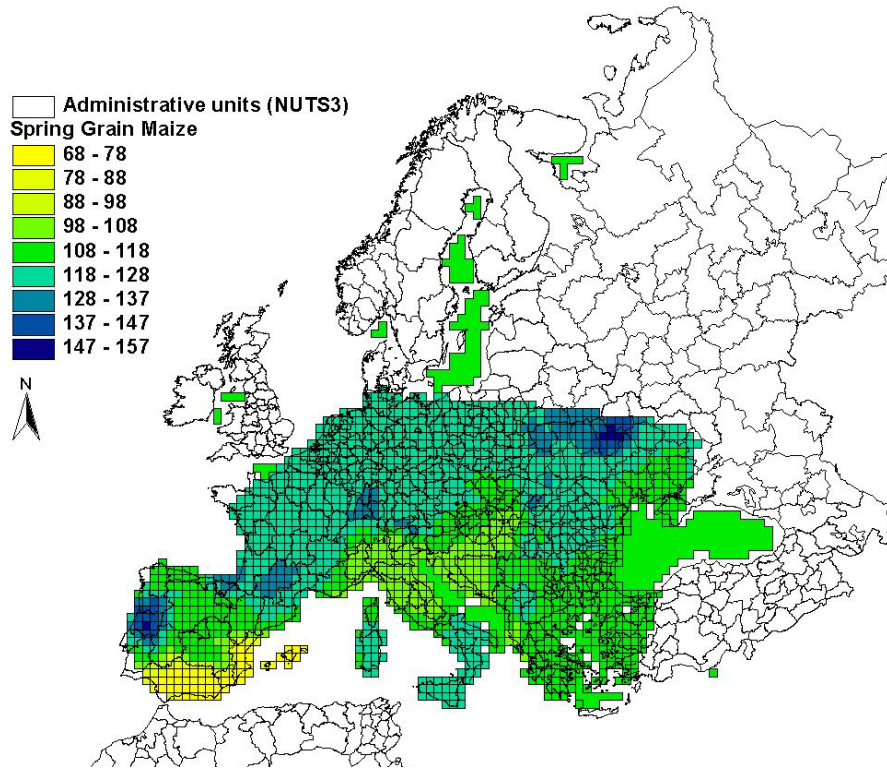


Figure 4.2: Spatially interpolated planting dates for spring sown grain maize (in JD).

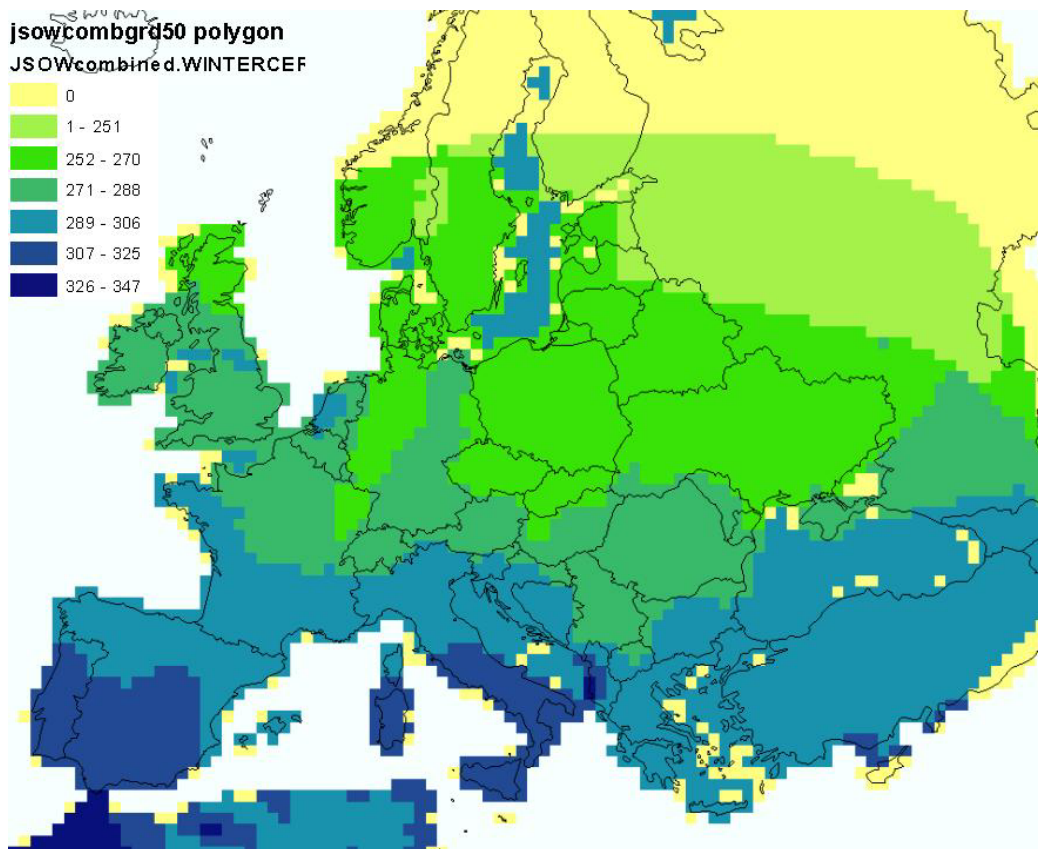


Figure 4.3: Spatially interpolated planting dates for winter sown cereals (in JD).

The ratio between actual and potential evapotranspiration is an important plant characteristic to calculate the water balance. As an example, Figure 4.4 shows the variation of this ratio during the different growth stages of maize for the climate of Iowa. The plant parameter database contains values of the ratio for different growth stages and for different crops across Europe, expressed in thermal degree days. For the majority of plants the ratio varies considerably during the growth season with the absolute maximum ratio being reached during the flowering period. For drought tolerant plants and crop cultivars, actual evapotranspiration may not reach the potential evapotranspiration (as is the case for maize in Iowa in Figure 4.4). Mid-season ratios are typically reaching between 1.0 and 1.2 for most arable crops.

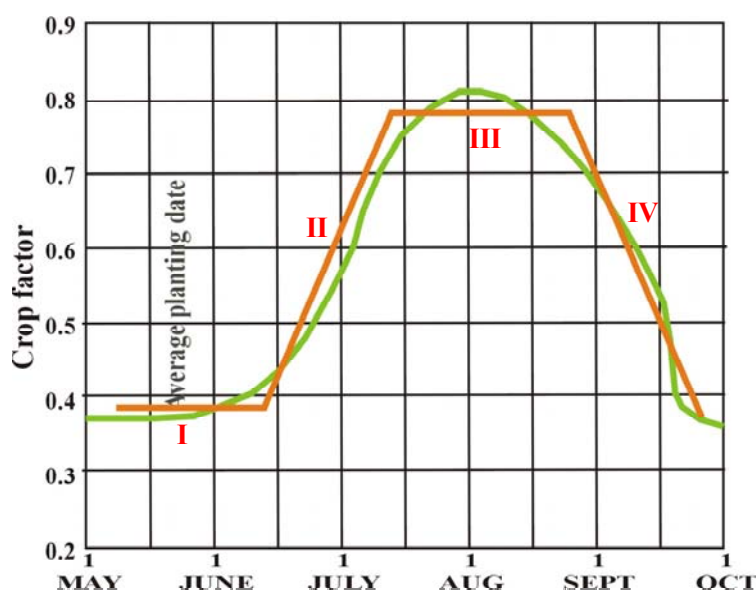


Figure 4.4: Variation of maize factor during the growing season (green) and simplified plant characteristic curve according to the different growth stages (initial stage: I / crop development: II / mid-season: III / late season: IV), expressed in actual days of year for Iowa, USA.

The same procedure as described above was followed for interpolating the data across Europe. Figure 4.5 presents spatially interpolated ratios for the initial development stage (I, according to Figure 4.4) of winter wheat. The interpolated surface is linked to thermal degree days and has not been converted to Julian days. Note that the initial development stage is taking place at different times of year for the different agro-environments of Europe.

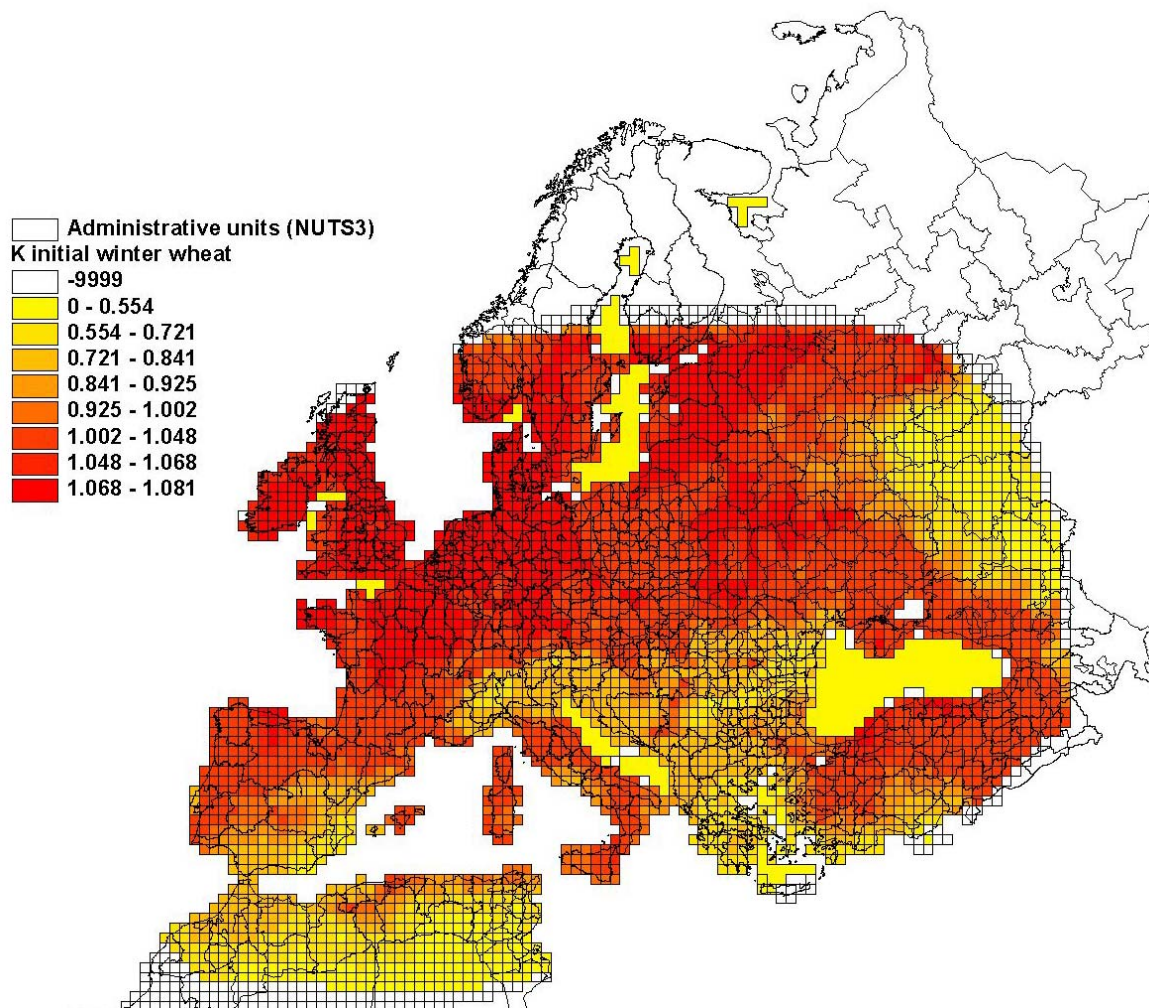


Figure 4.5: Spatially interpolated ratios for the initial development stage of winter sown wheat.

4.2.3. Plant cover for arable crop groups

In order to reconstruct crop cover, a vegetation growth model would be needed not least to incorporate effects of temperature and precipitation. However, it was decided not to incorporate a vegetation growth model but use a cover look-up table in order to save on memory and model run-times. The original look-up table contains cover data for a number of land uses, including arable land (see Appendix 1).

We proposed a refinement to incorporate plant cover for different arable crop groups. Linked to plant characteristic curve are other crop characteristics such as crop cover (Figure 4.6). An average arable crop is reaching its maximum coverage around the flowering period. This allows a reconstruction of the crop cover, provided that the crop does not experience any stress. Growth stress can be related to climate, nutrient supply or pests and diseases, and results in retarded development.

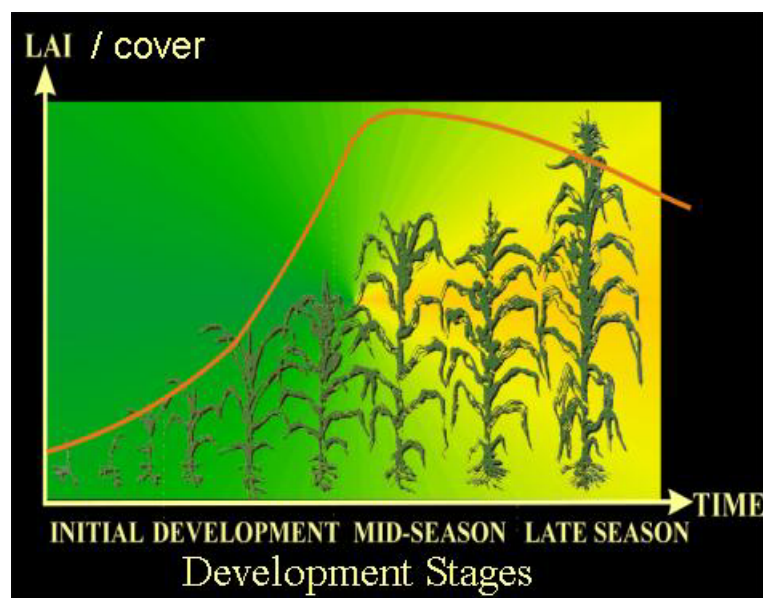


Figure 4.6: Leaf area index and crop cover development at different growth stages.

The sigmoidal growth curve (Figure 4.6) was reconstructed for each group of crops. Per crop group, the growth stage boundaries were converted to Julian Days. It was assumed that a maximum crop cover was reached during the flowering period. The model was run for an average growth calendar for each average crop group. The resulting table (Table 4.1) provides monthly average cover percentages, relative to the planting date. This enables the calculation of cover with changing planting dates and relating it to actual months. The crop group relates directly to the FSS nomenclature and the respective grids.

Table 4.1: Canopy Cover in percentages for different arable crop groups.

CropGroup	Month1	Month2	Month3	Month4	Month5	Month6	Month7	Month8	Month9	Month10
Maize	17	61	94	94	43					
SpringCereal	9	46	88	94	37					
WinterCereal	8	27	47	67	78	87	96	98	86	32
Pulses	19	66	98	72						
RootCrops	11	68	99	94	86	36				
Oilseeds	13	68	95	94	45					
Veg&Flowers	18	64	98	91	45					
Forage	10	67	69	72	77	81	70	54		

4.2.4. Spatialising agricultural land use and dominant arable crops

The CORINE Land Cover (CLC) map was reclassified for PESERA purposes and aggregated to a 1 km² resolution keeping the dominant land use (Figure 4.7, see Appendix 2). According to this map, agricultural areas cover about 60% of the total land cover of Europe, and include arable land, pastures and grassland, permanent crops (olive groves, fruit tree and berry plantations, vineyards) and heterogeneous agricultural areas.

The CLC class ‘arable land’ covers a vast proportion of Europe (31% of total, and 54% of agricultural land), where a wide variety of arable crops are grown: cereals, root crops, industrial crops, vegetables, fruits, flowers and forage crops. The majority of the class heterogeneous agricultural land, which accounts for 13.1% of the total area is, provided the distribution between different land use classes (Table 4.2), most likely also under arable crop production. The contribution of arable land to the overall land use across Europe and the fact that the majority of soil erosion happens on agricultural land, are compelling reasons for taking this land use class explicitly into account when modelling soil erosion.

Table 4.2: Contribution of land use to total area (reclassified according to PESERA needs).

Land Use	Percentage
Artificial land	3.08
Arable land	31.12
Vineyards	1.01
Fruit tree and berry plantations	0.55
Olive groves	1.02
Pastures and grassland	12.83
Heterogeneous agricultural land	13.13
Forest	28.49
Scrub	5.24
Bare land	0.68
Degraded natural land	0.80
Water surfaces and wetland	2.05

In order to refine the class ‘arable land use’, information is needed on arable crops grown in different regions of the Europe. The Farm Structure Survey (FSS), conducted by each member state and compiled at Eurostat, provides 10-yearly census data on crop types, cropping areas and yields but the information made public is aggregated to administrative units. The nomenclature of territorial units for statistics (NUTS) serves as a base map of regional boundaries covering the entire EU territory. The nomenclature subdivides the EU economic territory into 6 administrative levels, from country (level 0), through regional (level 1,2,3) to local (level 4,5) level. At present, 3 versions (V5, V6 and V7) for three scale ranges (1M, 3M and 10M) are maintained at GISCO- Eurostat. Available to the wider scientific community on a paid service are the NUTS 2 and NUTS 3 aggregated data (Figure 4.9).

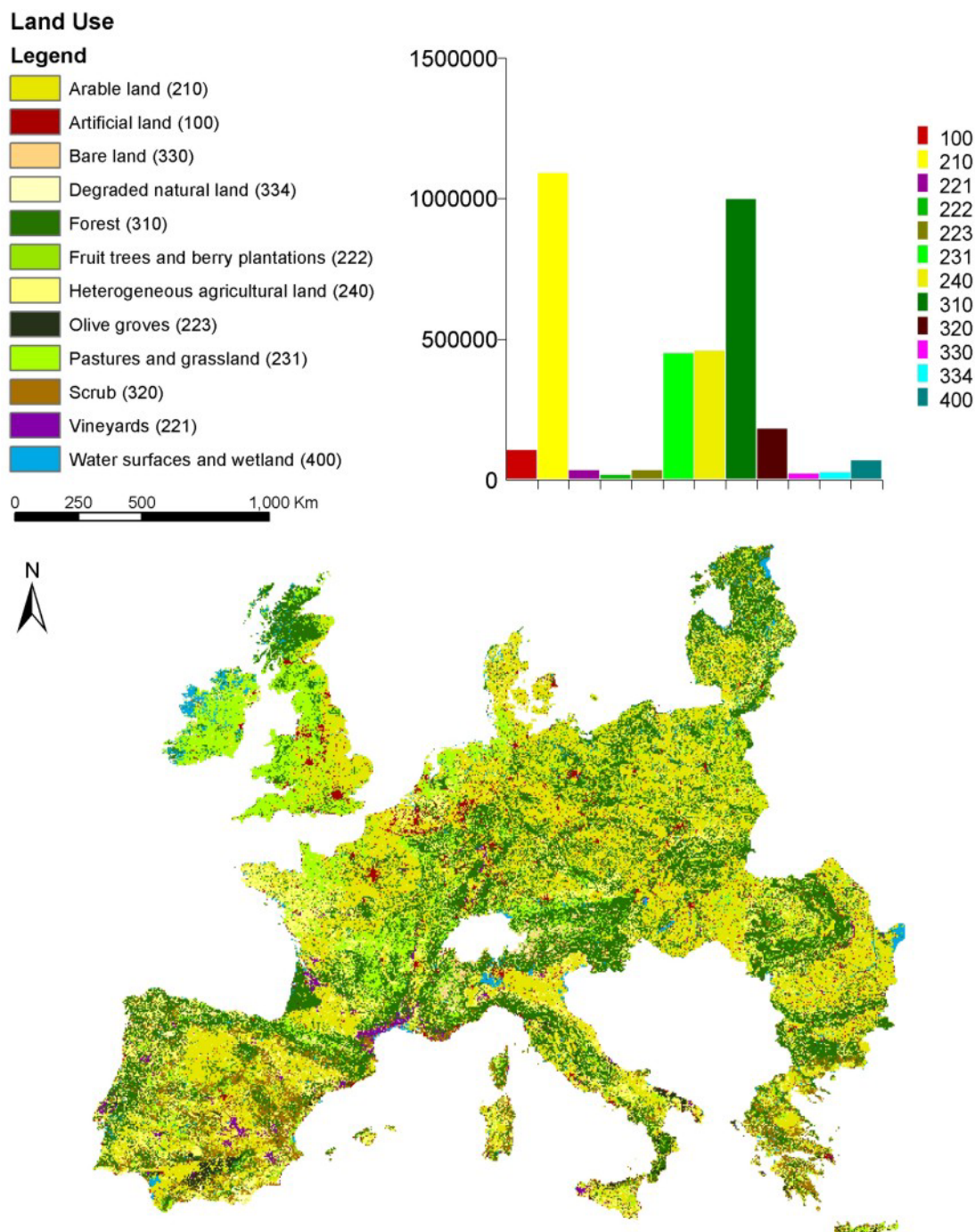


Figure 4.7: The importance of arable land across Europe according to Corine Land Cover.

A major challenge was the spatialisation of the crop information through coupling the FSS data to CLC. Three levels of differences exist between FSS and CLC: spatial referencing, classification differences and time of data acquisition. Crop area is part of FSS census data and is aggregated to administrative units, whereas CLC provides direct spatial referencing with a minimum mapping unit of 25 ha. The classification differences relate to the purpose of data collection: FSS presents agricultural holding data, whereas CLC focuses on land use/cover classification. Temporal differences relate to image acquisition (CLC) and survey

administration (FSS). Both CLC data and census FSS data are available at approximately the same year for NUTS2&3 every 10 years. At present, the only matching datasets available are for 1990 for Europe of 12. Despite the differences between the two datasets, it is useful to combine them for environmental modelling purposes. Moreover, yearly sampled data enable statistical trend analysis that can be related to spatialised agricultural land use.

Although the analysis can only be carried out on 1990 datasets since these are the only matching pair available between CLC and FSS datasets at present, the question arises whether 1990 datasets are still relevant now. An analysis of some of the available data on major land uses according to the FSS sample data were carried out for a period between 1990 and 2000 across the European countries available in the datasets. A general downwards trend of agricultural area can be observed (7.9% when comparing 2000 with 1990 data; Figure 4.8). A comparison between 1993 and 2000 data shows a downward trend of 6% for agricultural land use, 4.5% for arable land, 7.6% for grassland, 9.1% for permanent crops, 1% for olive stands and 18.7% for vineyards. An analysis on a country basis (not shown here) confirms this overall European trend. As a result of the mid-term CAP review it is expected that more agricultural land will be taken out of production. The results of a 10 year analysis of FSS data (Figure 4.8) shows that it makes more sense to relate the 2000 FSS census dataset to the yet to be released CORINE Land cover 2000 dataset.

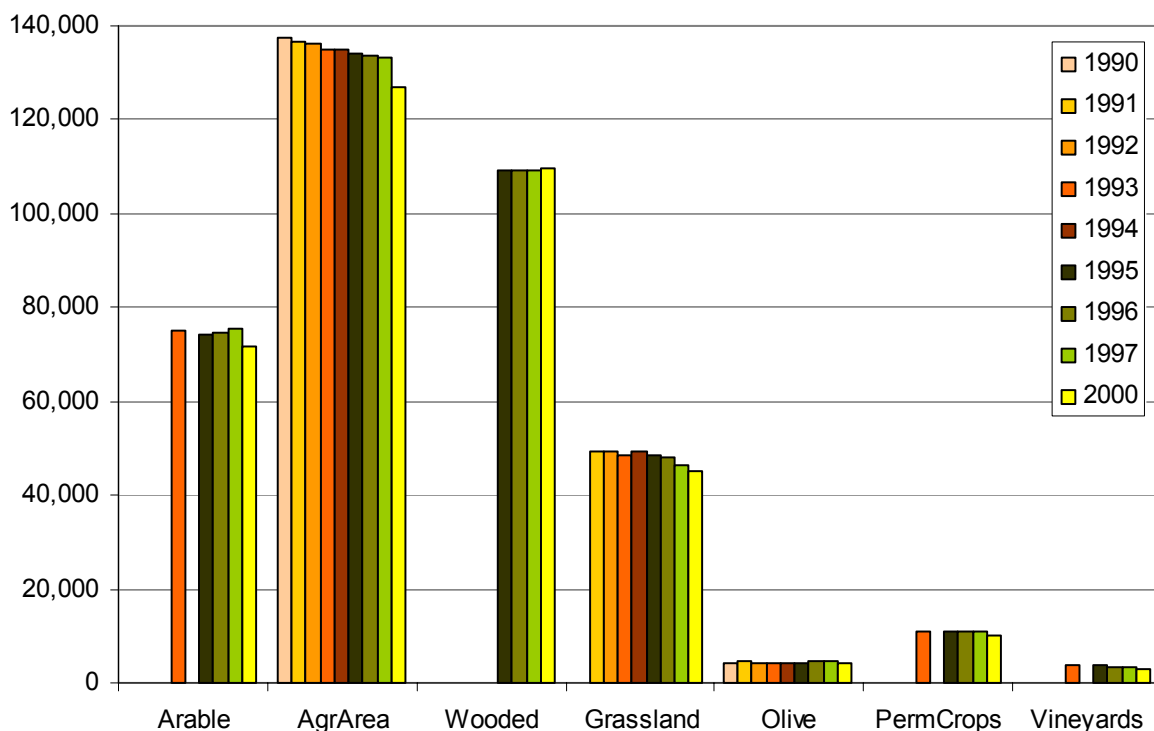


Figure 4.8: Trends in agricultural land use area across Europe (in thousands of ha).

A next compelling question was the comparison between the FSS and CLC classification and its implications in areal terms. The FSS data structure and classification is briefly discussed in Appendix 3, whereas the CLC land cover and its reclassification for PESERA purposes is presented in Appendix 2.

Table 4.3: Relationship between FSS and CLC data (for CLC, the PESERA reclassification was used).

Classification (PESERA-CLC)	CLC class	FSS class
Arable	211+212	D+G5-I5-D7
Vineyards	221	G4
Fruit tree and berry plantations	222	G1+G2
Olive Groves	223	G3
Pasture and Grassland	231	F
Heterogeneous agricultural land	241+244	I5

See Appendix 2 for CLC class and Appendix 3 for FSS class.

In a first step of spatialising FSS data, the regional differences in area were harmonised (Figure 4.9). In practice, the FSS data of the BENELUX area, Germany and the UK were taken for NUTS2, the data of the remaining countries were for NUTS3. For reasons of identification between the different databases, version 6 was used for Ireland and the UK and version 7 for all other countries. All the analysis listed below was carried out for the resulting four databases, which were merged into one layer afterwards.

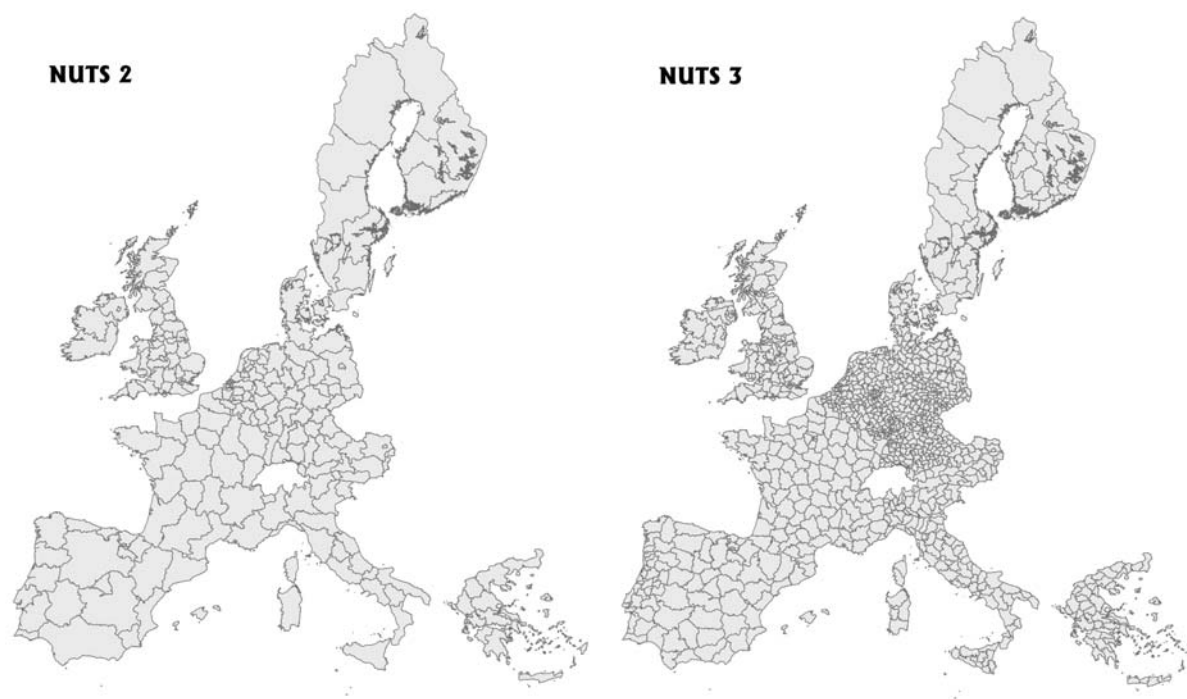


Figure 4.9: Areal differences between different levels of administrative regions (NUTS) across Europe.

Coupling FSS to CLC data was done through matching agricultural land use classes as provided in Table 4.3 and subsequent redistribution. The result is a redistribution of agricultural land use across the 12 European countries where both datasets are available for (Figure 4.9).

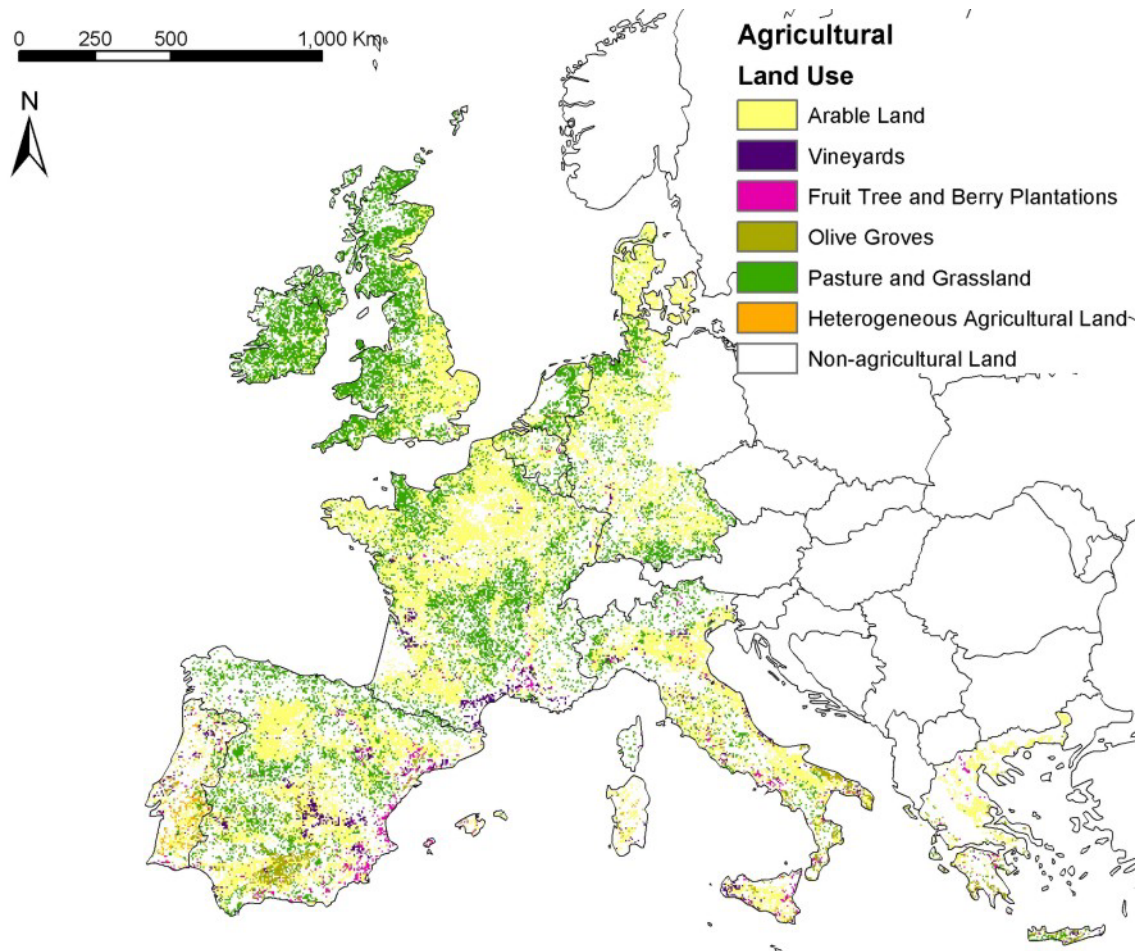


Figure 4.10: Spatialising agricultural land use: coupling FSS data to CLC data

Within the FSS database, a number of programs were set up in order to identify the order of importance of each arable land use class, the percentage that each class represents within the total of arable land within that specific region, and to link the information to the correct NUTS region. Table 4.4 presents an overview of the arable land use classes within the FSS database. The dominant arable crop was identified per harmonised NUTS region and linked to the appropriate NUTS layer. The four resulting NUTS layers were merged and spatialised using Corine Land Cover. Figure 4.11 presents the results for the most dominant arable crop.

Table 4.4: Arable land use classes within the Farm Structure Survey database from Eurostat.

FSS Class	Crop Group
D1 to D8	Cereals
D9	Pulses
D10 to D12	Root crops
D13	Industrial Plants &
D14 to D17	Oilseeds
D18	Vegetables & Flowers

D19 to D20	Forage
D21	Other Arable
	Non-subsidised Fallow

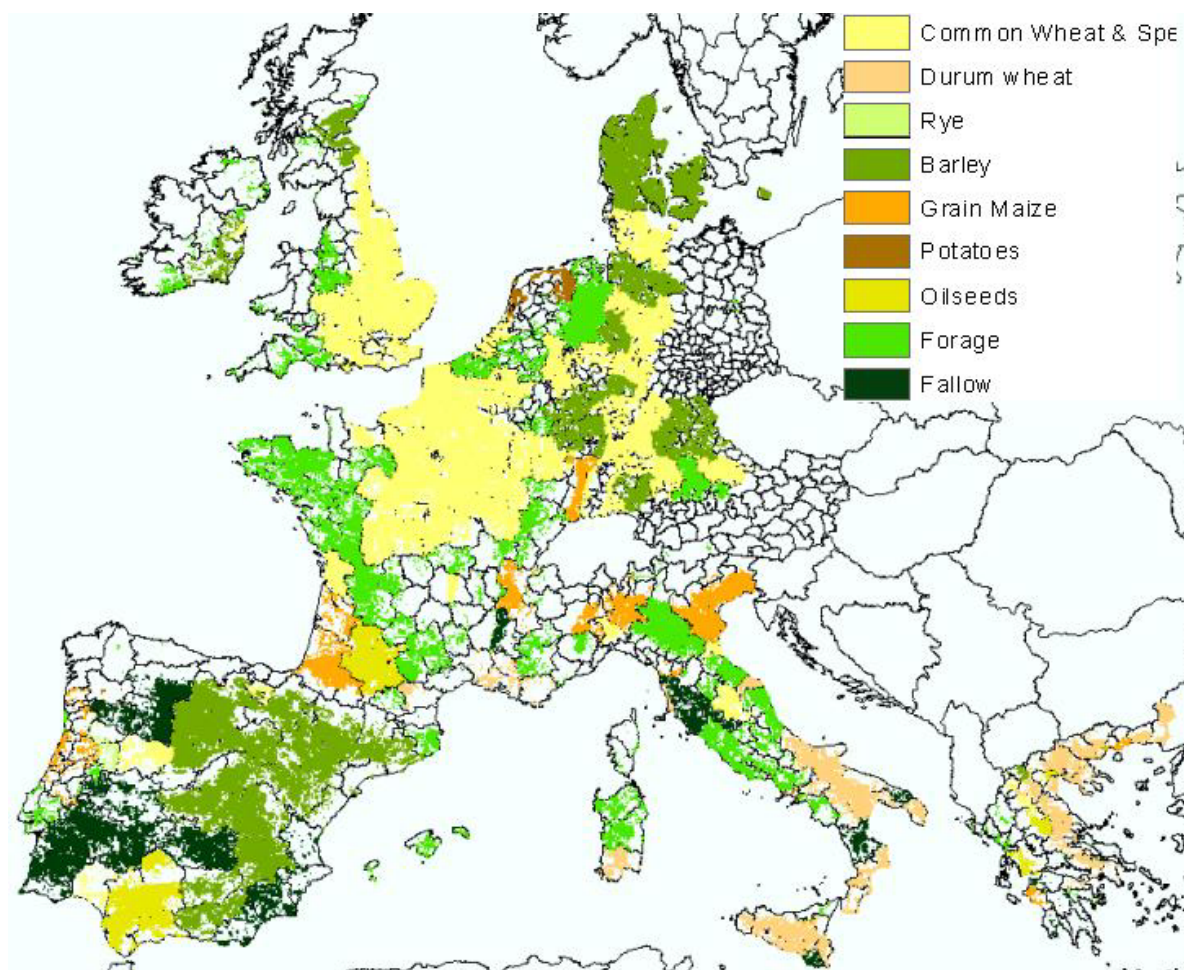


Figure 4.11: Dominant Arable Crop per Harmonised NUTS region, spatialised using CORINE LAND Cover.

4.2.5. Land use scenarios

Considering the difficulties that other Fifth Framework Projects encountered while defining land use scenarios across Europe, the following three land use scenarios were suggested during the meeting in Wageningen:

1. Dominant Arable Crop (Actual PESERA runs):
Spatialised FSS layer (Dominant) (Figure 4.10)

- Planting Dates Database
- 2. Worst case scenario: Maize
 - CLC Arable assigned as only Maize
 - Planting Dates for Maize
- 3. Scenarios of Changing Land Use:
 - Spatialised FSS layer (2nd Dominant Arable Crop)
 - Planting Dates Database

These land use layers may not reflect actual land use changes but will clearly demonstrate the effects of arable land use changes that may take place because of policy implementation. The necessary data layers have been distributed to the partners concerned and are to be combined with climate change scenarios.

4.3. WP3: CALIBRATING AND VALIDATING THE PESERA MODEL WITH HIGH RESOLUTION MEASUREMENTS

4.3.1. Testing the PESERA approach with long-term soil erosion plot data

The PESERA model is a process-based erosion model, which has been developed to investigate the land's sensitivity to erosion at a Pan-European scale. On the basis of a long-term dataset of soil erosion measurements at the plot scale, the objective of this study is to evaluate to what extent the basic concepts of the model can be considered valid in various agro-ecological environments and to assess how the basic model parameters (runoff threshold, soil erodibility) vary according to different soil textures, land uses or to seasonal variation in rainfall regimes.

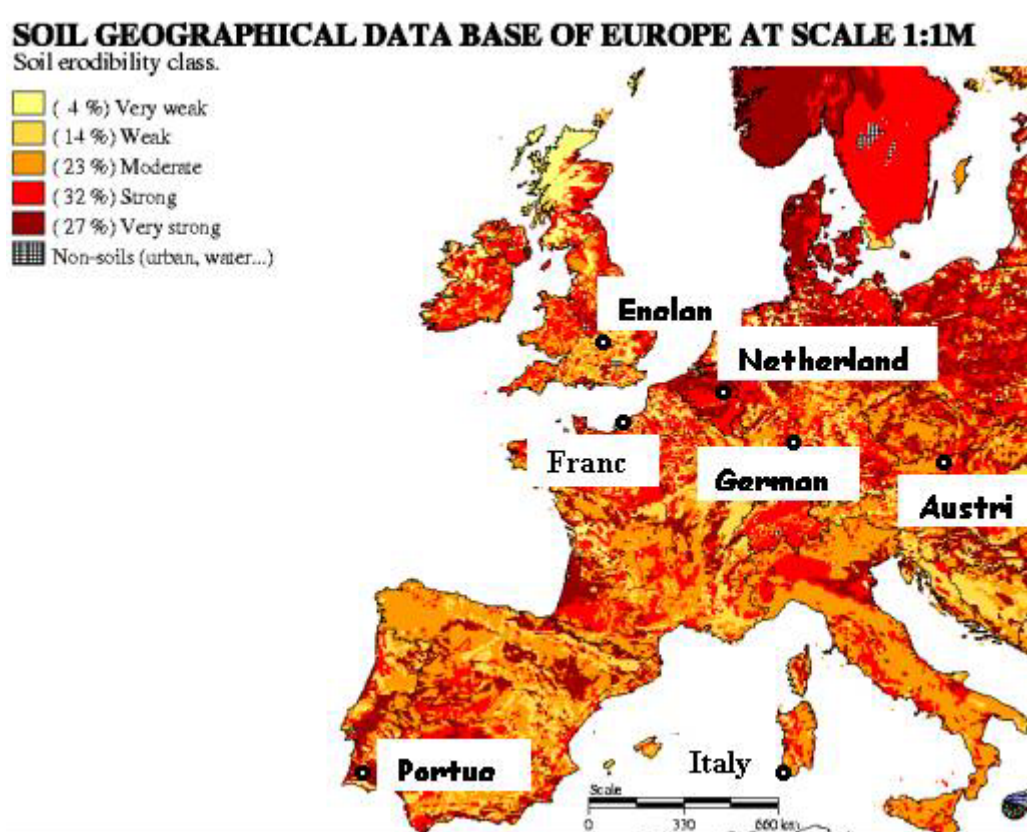


Figure 4.12: Location of the experimental sites.

The evaluation database is composed of runoff and erosion measurements from England, Netherlands, France, Germany, Austria, Portugal and Italy (Figure 4.12).

All the data have been aggregated into monthly values. The factors present in the database are: rainfall, mean rainfall per rain day, potential evapotranspiration, land use, slope length and gradient, soil texture, runoff height and erosion rate (Table 4.5).

Table 4.5: Description of the long-term soil erosion database.

Location	Soil texture	Date	Number of plots	Length (m)	Area (m ²)	Slope (%)	Land use
England	Coarse	07/89-10/93	8	35	765 - 955	7.6 - 12.8	Potatoes, Cereals*, sugar beat, bare, ploughed
		11/79-08/80	1	165	330	11.4	Cereals
Germany	Medium-fine	10/79-10/81	2	40 - 60	80 - 120	17.6, 21.3	Maize, Sugar beat, Cereals
	Medium-fine	05/79-04/82	11	1 - 20	2 - 40	22.2 - 31.1	Grass, Conifers, Bare
	Medium-fine	06/86-03/90	12	22	39.6	6	Cereals, Maze, bare, ploughed

Austria	Medium & Medium-Fine	05/94-09/00	9	15	45 - 60	5 - 15.2	Maize, Sunflower, ploughed	Cereals, Sugar beet,
Portugal	Medium	09/61-05/94	9	20	80 - 167	10 - 18	Cereals, Ploughed	Grass, Cistus,
France	Medium	10/93-04/98	11	10-54	20 - 480	1.6 - 4	Cereals, Mustard, Flax, Bare, Grass	Pea, Ploughed,
Italy	Medium	03/92-02/98	18	10	20	12 - 47	Cistus, Eucalyptus	Burnt macchia,

The PESERA model can be disaggregated into a runoff generation and a sediment transport component. The runoff threshold and runoff fraction are simplifications of cumulative infiltration and runoff curves. The runoff threshold is calculated from the vegetation cover, soil organic matter and soil texture. Runoff and erosion rates are calculated with a monthly time step.

The overland flow runoff (per unit area) is estimated as:

$$J = p(r-h)$$

where r is the rainfall amount, h is a runoff threshold and p the proportion of runoff above the threshold.

Sediment transport is calculated as:

$$S = kq^2G$$

where k is the soil erodibility, q is the overland flow discharge per unit width and G is local slope gradient.

Principal component analysis shows that, overall, the monthly aggregated values present in this database do not explain the variability of the erosion response (Figure 4.13). Runoff variability is partly explained by rainfall amounts ($r^2 = 0.34$, $n = 2260$). h appears to be strongly related to rainfall amounts ($r^2 = 0.92$).

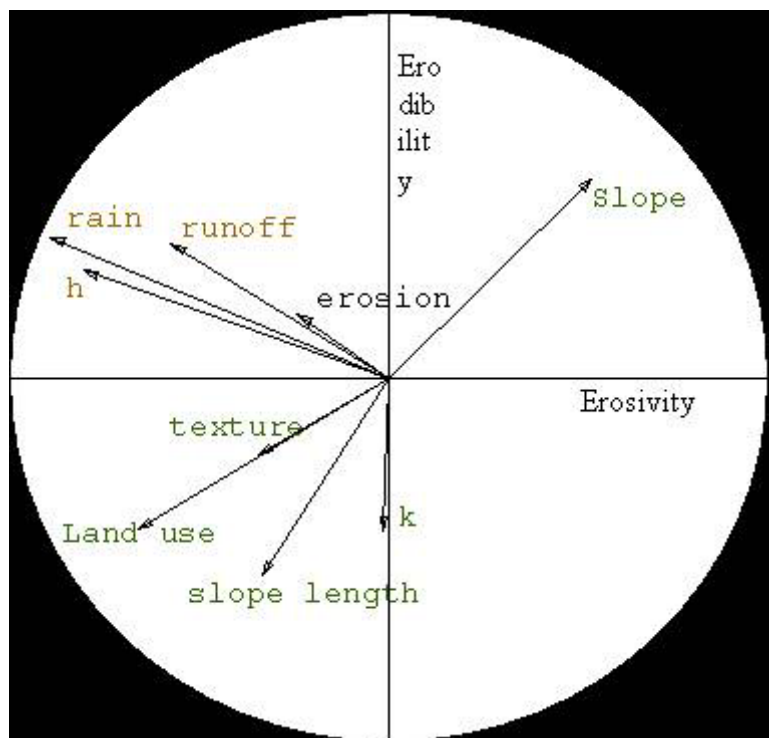
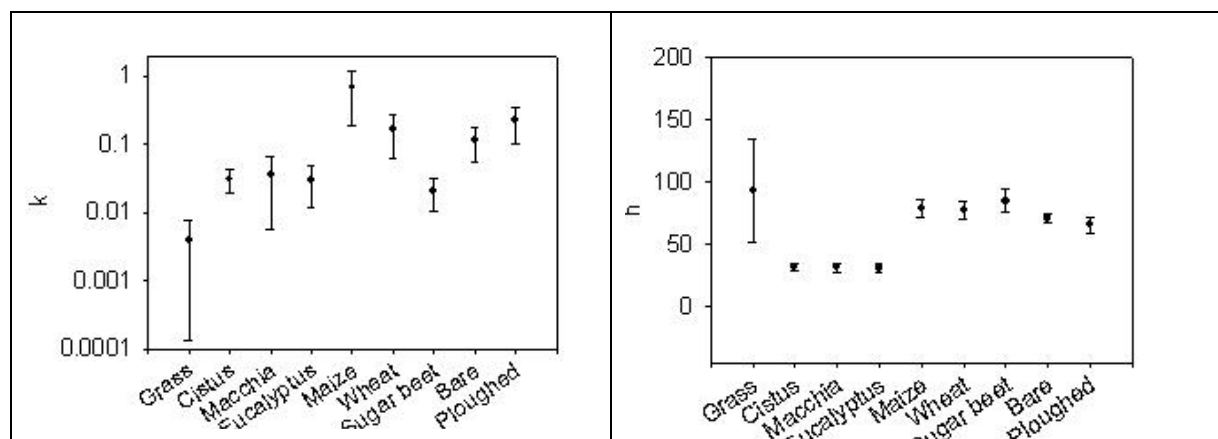


Figure 4.13: Principal component analysis (first and second component).

The mean k and h values are significantly different (ANOVA, $p < 0.0001$) for the different land use and soil texture classes present in the dataset (Figure 4.14, Table 4.6).

k varies over several order of magnitude (0.0001 to 0.1), with lower values for land uses with a permanent cover (the higher value being for maize) and for coarser textures (Figure 4.14, Table 4.6).

Some variations of h are more difficult to interpret. This is probably due to the use of monthly aggregated values that cannot fully characterise processes of runoff generation occurring at the rainfall event scale.



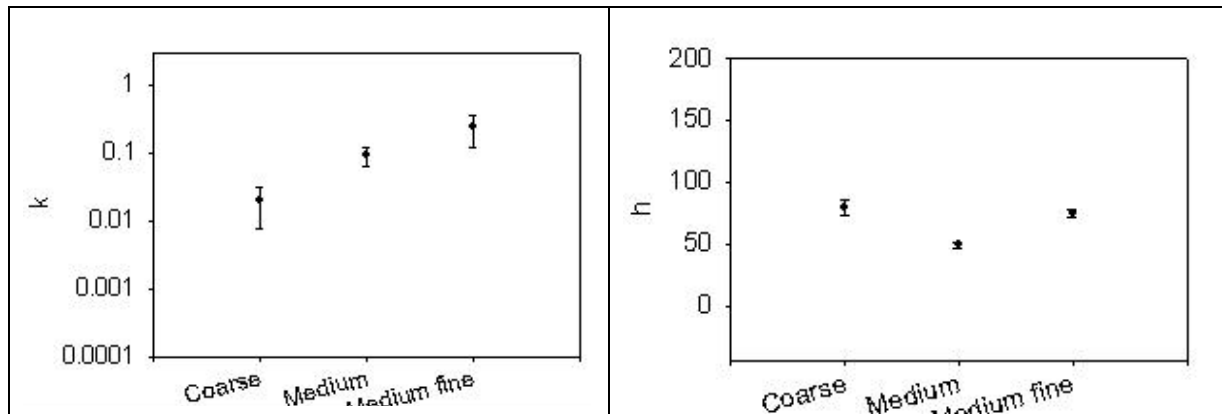


Figure 4.14: Histograms of the group means with 95% confidence intervals

Table 4.6: Average and standard deviation of h and k according to the different land uses and texture classes.

	Land use								
	Grass	Cistus	Macchia	Eucalyptus	Maize	o.Cereal	S. beet	Bare	Ploughed
Count	19	309	300	305	105	306	50	549	260
Mean h	92.72	31.38	31.16	30.92	79.10	77.91	84.79	70.94	65.38
StdD of h	83.77	29.03	27.72	27.85	37.07	62.51	31.73	47.60	49.13
Mean k	0.004	0.031	0.036	0.030	0.679	0.165	0.021	0.116	0.225
StdD of k	0.01	0.11	0.26	0.16	2.51	0.92	0.04	0.72	1.01
	Texture								
	Coarse			Medium			M. fine		
Count	95			1667			500		
Mean h	78.91			48.70			74.45		
StdD of h	30.68			48.16			42.97		
Mean k	0.019			0.093			0.239		
StdD of k	0.06			0.60			1.38		

This study represents a first evaluation step using an extensive database of runoff and erosion measurements from western and central Europe. It confirms the difficulty to model complex system processes at a regional scale, especially regarding the input data resolution. The erodibility parameter shows very high variations that, to a certain extent, can be related to changes in land use and soil texture.

Final validation of the model performance will be carried out at the regional scale, by comparing the model results with results from other regional risk assessment methods carried out by local experts and alternative methodologies.

4.3.2. Validating the PESERA map with high resolution observations

More than 100 literature references to soil erosion rates were screened for their use to validate the 1 km² PESERA output map. Measurements and observations at 42 locations

across Europe were retained (Figure 4.15). Records based on a concatenation of single events or rainfall simulation were discarded. Also excluded were observations based on less than 2 years of investigation or where contacted authors could not give a precise location for.

A database was set up to contain the following fields of information: geographic location; region; min, mean and max erosion rate in $\text{t}\cdot\text{ha}^{-1}\cdot\text{yr}^{-1}$; area of investigation (number and size of plots, fields, micro-catchments); period of investigation; general land use; crop rotation where applicable; references.

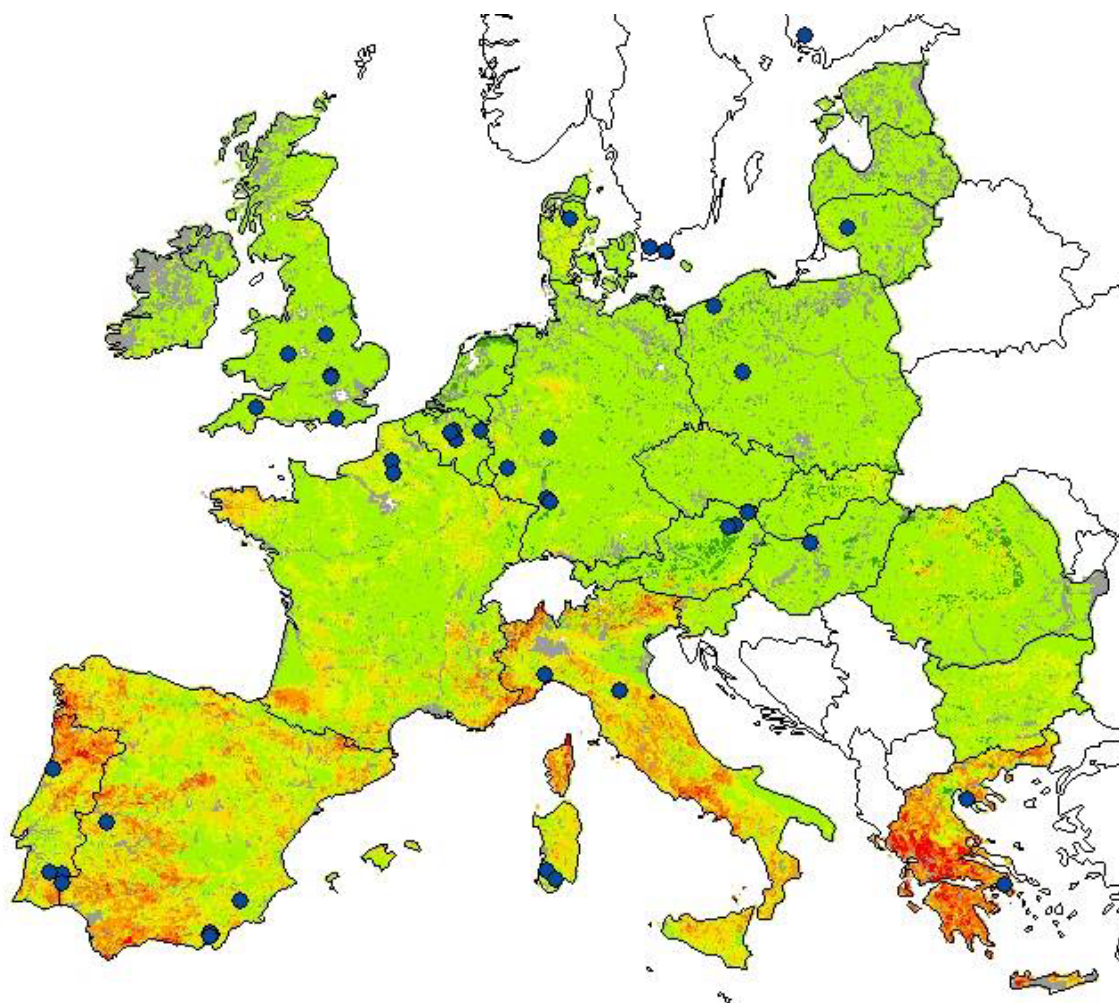


Figure 4.15: Location of observed erosion rates projected against the PESERA output map.

For purposes of comparison, the following data layers were compiled: the PESERA 1 km² map with masked data being removed, and the mean, minimum and maximum of a 5 x 5 moving window applied across the PESERA 1 km² map. The application of a moving window was justified on the basis of a landscape scale analysis and of the explicit incorporation of a hillslope component in the model.

A comparison between observed rates and predicted rates using the PESERA model was performed at three different levels: (1) visual comparison, (2) numerical comparison and (3) categorical comparison.

Visual comparison shows the occurrence of low to medium erosion rates in Northern Europe, high rates in Central and Eastern Europe, and either low or high rates in Southern Europe. The frequency distribution indicates a better spread of values across the different classes for the mean erosion layer than the 1 km² PESERA map as compared to the observed erosion rate classes (Figure 4.16). A numerical comparison gives a Pearson correlation of 0.253 with the 1 km² PESERA map and 0.409 with the mean erosion map (based on a 5 x 5 moving window). There is an overall underestimation of the PESERA model for observed erosion rates more than 1 t.ha⁻¹.yr⁻¹ (Figure 4.17). There is a -43% difference compared to the mean erosion map and a -52% difference compared to the 1 km² PESERA map. An overestimation was observed for rates less than 1 t.ha⁻¹.yr⁻¹ (Figure 4.17). There is a 347% difference compared to the mean erosion map and a 69% difference compared to the 1 km² PESERA map. This general pattern is visualised in a cross-tabulation for categorical comparison (Figure 4.18).

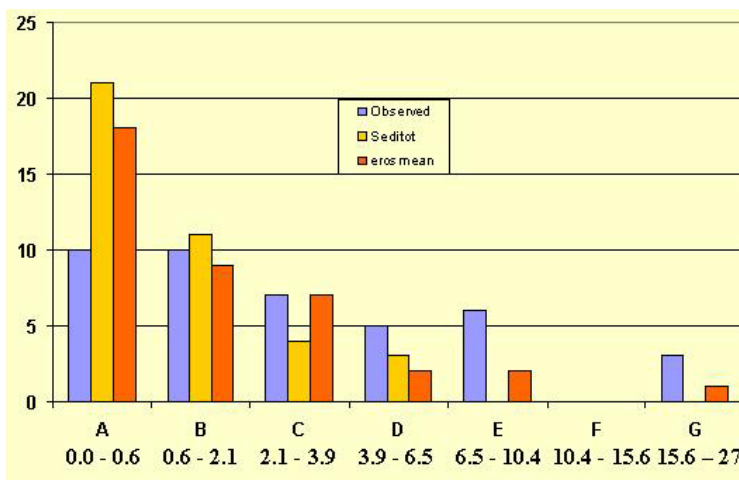


Figure 4.16: Frequency distribution of sample points per class, where observed refers to the database of observed rates, seditot refers to the 1 km² PESERA map and erosmean refers to the mean of the moving window across the PESERA map.

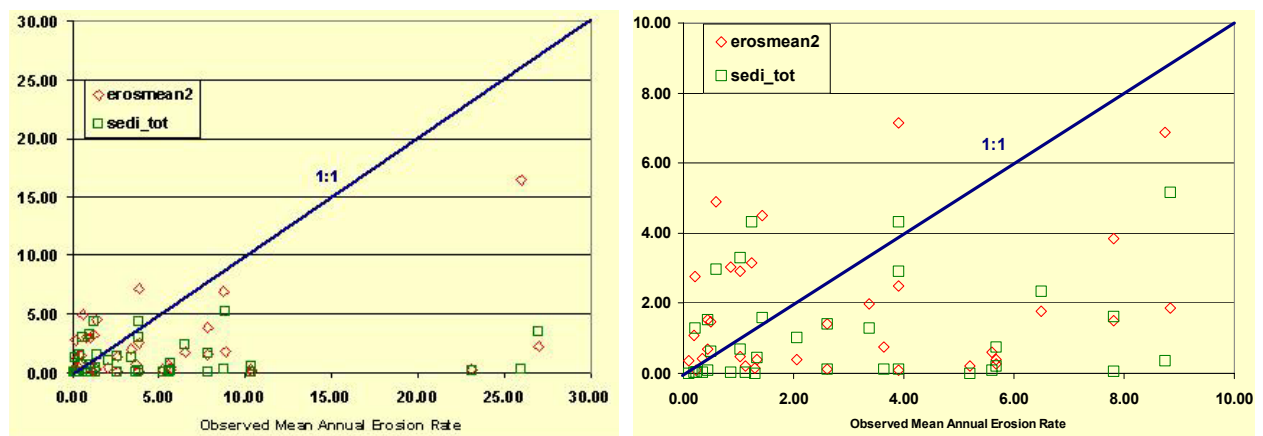


Figure 4.17: Results of a numerical comparison between observed erosion rates and the PESERA 1 km² map and the mean erosion surface for a 5 x 5 window.

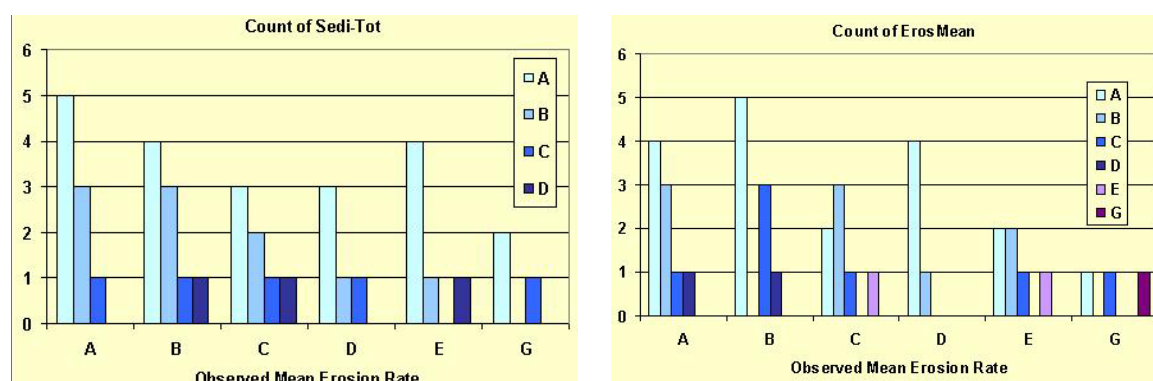


Figure 4.18: Results of a categorical comparison between observed erosion rates and the PESERA 1 km² map (seditot) and the mean erosion surface for a 5 x 5 window (erosmean).

The observed erosion rate database provides a good basis for comparison with predicted erosion rates. The comparison favourably improved after applying a 5 x 5 moving window across the 1 km² PESERA map. However, substantial differences remain between observed and predicted erosion rates. These may be attributed to the patchiness of erosion process in both temporal and spatial terms, differences in measurement and observation techniques so that comparison between observed rates becomes less meaningful, and representativeness of the observation or measurement for that area (e.g. location).

4.4. END-USER INVOLVEMENT

4.4.1. The European Environment Agency

Contact is maintained on a regular basis with the Project Manager on soils at the European Environment Agency. Advice is also given on some of the issues involved in developing sound indicators to estimate soil erosion.

Effective monitoring of and reporting on soil erosion can only take place when the underlying biophysical and socio-economic factors that influence (accelerated) soil erosion, are taken into account. Based on previous work undertaken for the European Environment Agency, the DPSIR (Driving Force-Pressure-State-Impact-Response) framework, applied to soil erosion, was reviewed and suggestions for improvements were proposed. An integrated approach is advocated and should incorporate a set of soil erosion indicators that can be objectively calculated, validated against measurements and evaluated by experts. The proposed soil erosion indicators are discussed in relation to Pan-European data availability, policy requirements and analytical soundness. This should be valuable input to the development of indicator factsheets at the Environment Agency.

4.4.2. The ENRISK Project

ENRISK, Environmental Risk Assessment for European Agriculture, is an EU Concerted Action that identifies environmental risk zones by testing agri-environmental indicators and their application for environmental risk assessment throughout Europe. The European Centre for Nature Conservation is coordinating this concerted action. The role of the PESERA team within this concerted action is to provide expertise on regional soil erosion risk assessment in the form of risk indicators and mapping as a tool for policy implementation. A Pan-European estimation of average annual soil loss due to water erosion will be calculated on the basis of the PESERA methodology and incorporated in a wider strategy for testing and implementing agri-environmental indicators for sustainable agriculture.

4.4.3. The SOWAP Project

The SOWAP (Soil and Surface Water Protection using conservation tillage in Northern and Central Europe) Project seeks to address some of the current environmental, social and economic concerns of practising conventional arable crop production in northern and central Europe. Present arable cropping systems rely on intensive mechanical cultivation. The agronomic benefits of this system are however counterbalanced by the environmental consequences of such intensive soil management: the potential for soil erosion, reduced soil biodiversity, lack of opportunity for sequestering carbon and damage to aquatic ecosystems from transported sediments. SOWAP aims to assess the viability of a more “Conservation Agriculture” approach, where fewer tillage practices replace the numerous cultivations carried out under more “conventional” arable farming systems. The use of appropriate herbicides is tested, and their potential for off-site contamination assessed.

The PESERA team and Syngenta’s Environmental Safety Assessments Unit have mutually benefited from interactions at Project meetings. Mike Lane from Syngenta, the Project Manager of the SOWAP Project, has attended all the PESERA plenary meetings. Current understandings in soil erosion modelling will play a vital part in the SOWAP Project.

CHAPTER 5 INRA-ORLÉANS

Yves Le-Bissonnais, Joel Daroussin and Dominique King

Unité de Science du Sol
BP 20619 Domaine de Limère, 45166 Olivet Cedex, FRANCE

5.1. ROLE AND CONTRIBUTION

INRA co-ordinates the validation of the PESERA model at low resolutions and the comparison of the PESERA model output with other regional models or expert methods to assess erosion risk at the regional scale (WP4). Together with JRC, INRA is responsible for database management and application of the PESERA model at European level (WP5). INRA also contribute to model development, particularly to developing transfer rules for linking data sets to model parameters.

5.2. ORIGINAL OBJECTIVE OF WP 4 AND WP5

The objective of WP4 is to validate the PESERA model, developed under WP1, for large territories which are chosen as pilot areas. The PESERA model output is compared to expert systems, notably those developed within the CORINE project and those developed by Le Bissonnais et al. (1998), which was designed specifically for the French territory. The model is also compared to the predictions derived from existing models such as USLE for larger areas. It will also be investigated how the available information will be incorporated into the PESERA model structure. Transfer functions or rules will have to be developed for deriving model parameters from regionally available information.

The objective of WP 5 is to compile comprehensive databases for all input variables in both raw and pre-processed form, i.e. after applying the necessary transfer rules and equations. It is essential that a standard database format be used throughout the project.

5.3. RESEARCH ACTIVITIES DURING THE THIRD REPORTING PERIOD

5.3.1. WP5: Database development at European level

During the period the final European wide data sets was completed with the last version of all available parameters. It has been distributed to all PESERA teams in a set of four CD's. It includes (see appendix 2):

- meteorological data layers
- soil data layers derived from the European Soil Geographical Database using pedotransfer rules
- Relief parameters
- Land cover parameters

5.3.2. Regional approach for validation at low resolutions (WP4)

5.3.2.1. Method for PESERA validation at regional level

The PESERA model and the French expert erosion model have been both run at the European level with data that are used for the “standard” PESERA output, and at the level of Normandy region with high quality data and a resolution of 50 m cells. The French expert erosion model with high-resolution data has been validated by several local and catchment scale runoff and erosion measurements and monitoring. Therefore, it can itself be considered as a regional validation data set, or at least as the best available regional data set, and the comparison with PESERA model can be performed as a validation exercise. However, because both the spatial resolution and data quality for a given resolution play an important role in the modelling approach, both effects have been investigated separately by performing several comparisons for Normandy region:

PESERA model has been run using high resolution data and the results has been compared to validation data (i.e. French expert erosion model with high resolution data);

PESERA model has been applied using low resolution data that are available for the whole Europe and the results has been compared to the results obtained with high resolution data. In the same time, results of French expert erosion model with high and low resolution data have also been compared.

Results of PESERA model and French expert erosion model with low resolution data have also been compared.

This method will allow validating and differentiating between data quality effects, resolution effects and modelling procedure effects on the final results.

5.3.2.2. Results: effect of spatial resolution and data quality

Annual assessment:

Resulting maps and statistics for the four models are presented in Figure 5.1.

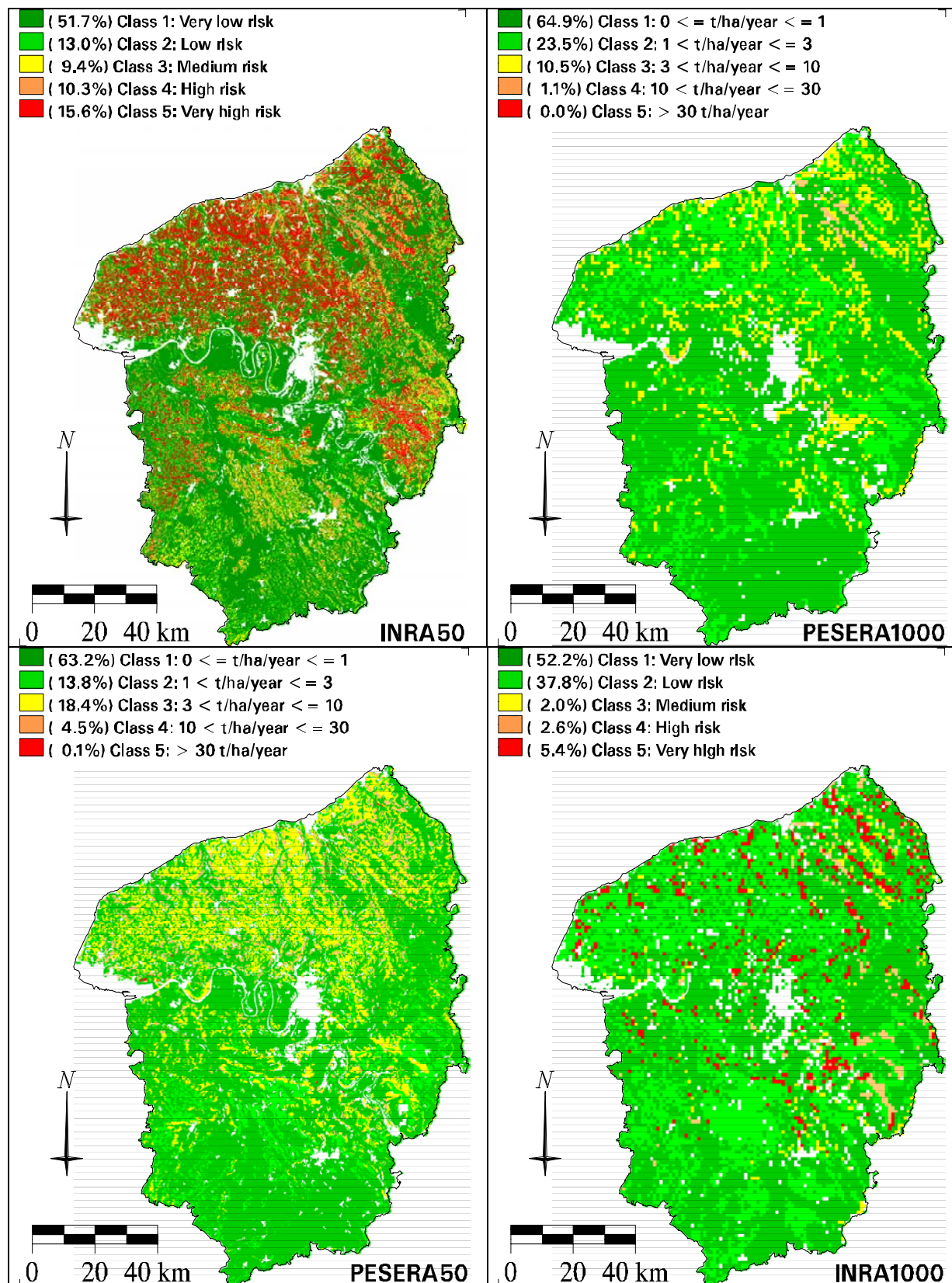


Figure 5.1: The effect of spatial resolution and data quality using the INRA expert model and the PESERA model

If we compare, for the annual erosion risk, PESERA 1000 result, which correspond to the PESERA standard output, with INRA 50 result, which is considered as the validation data, we observe a general similar pattern for the area, with higher risk class in the north of the area and lower risk in the south. However, the proportion of high and very high risk is much lower for PESERA model than for INRA map. This could be due either to the different quality and resolution of data used for both maps or to the model conception and data used. To separate between both effects we can look at the PESERA 50 map and compare it with INRA 50 result, to eliminate resolution and data quality effects (Figure 5.2).

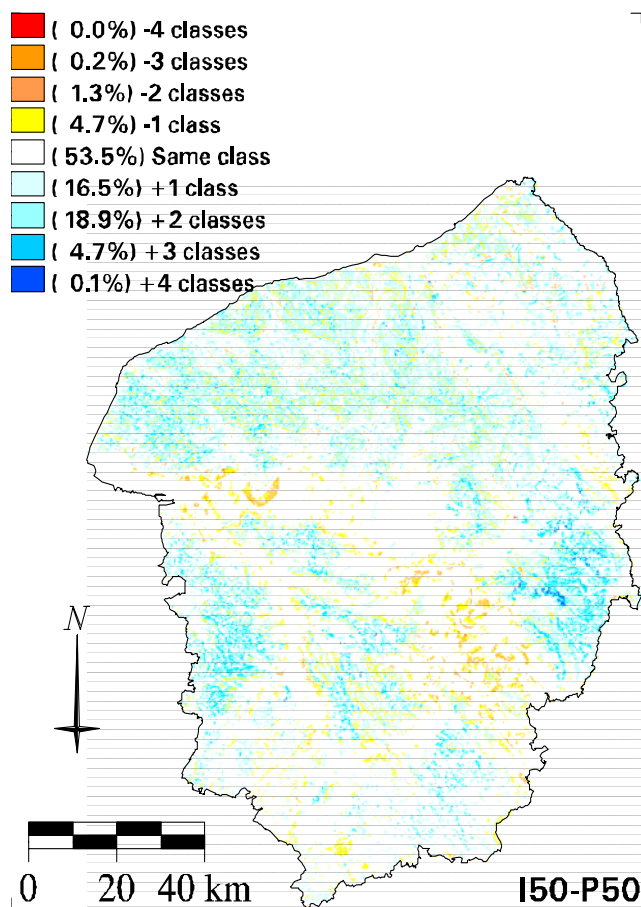


Figure 5.2: Comparison between the INRA expert model and the PESERA model at 50 m resolution.

It is still clear that the PESERA model underestimate the risk in the north of the Normandy region, but the difference is less important and could be due to the lack of real calibration of the model. The INRA 50 map features 26% of class 4 and 5 whereas PESERA 50 features only 4.5% of class 4 and 0.1 % of class 5, and PESERA 1000 only 1.1% of class 4 and no class 5. The geographical comparison is on the following map. It shows that for 75% of the area the classification is the same or differ for one class. Areas over-estimated by PESERA model by two classes or more represent only 1.5% and correspond typically to step slopes talus along the Seine river, which are not considered as erosion areas in INRA assessment but could in fact be subject to erosion due to the slope. So, in this case we can consider that the PESERA model is right. Areas under-estimated by PESERA model by Two

classes or more represent about 24% and they are located everywhere, particularly in areas of high and very high erosion risk according to INRA map. These differences can be attributed either to the model conception and parameterisation itself or to the calibration of both assessment. In fact neither the INRA and PESERA approaches have been really calibrated, because of the limited of field data, so it is very highly probable that a part of the discrepancy results from the bad calibration of both approaches, and therefore the good geographical convergence in the risk trend between both map show the good potential of PESERA model.

Now the second step in the validation process is the PESERA 50 and 1000 comparison, in order to assess the effect of resolution and data quality degradation on the result of the model. The map below shows that 85% of the area is in the same class or neighbouring class. The low resolution and degradation of data quality additionally decrease the proportion of high and medium risk classes. However the same result is observed for the INRA model, with even a more important effect. The main reason for this is probably the influence of pixel size increase which reduce the slope value. Figure 5.3 shows the results of the INRA model with three pixel sizes; it shows that the pattern remains the same between 50 and 250 m whereas the regional discrimination of erosion risk is seriously degraded with the 1000 m pixel size.

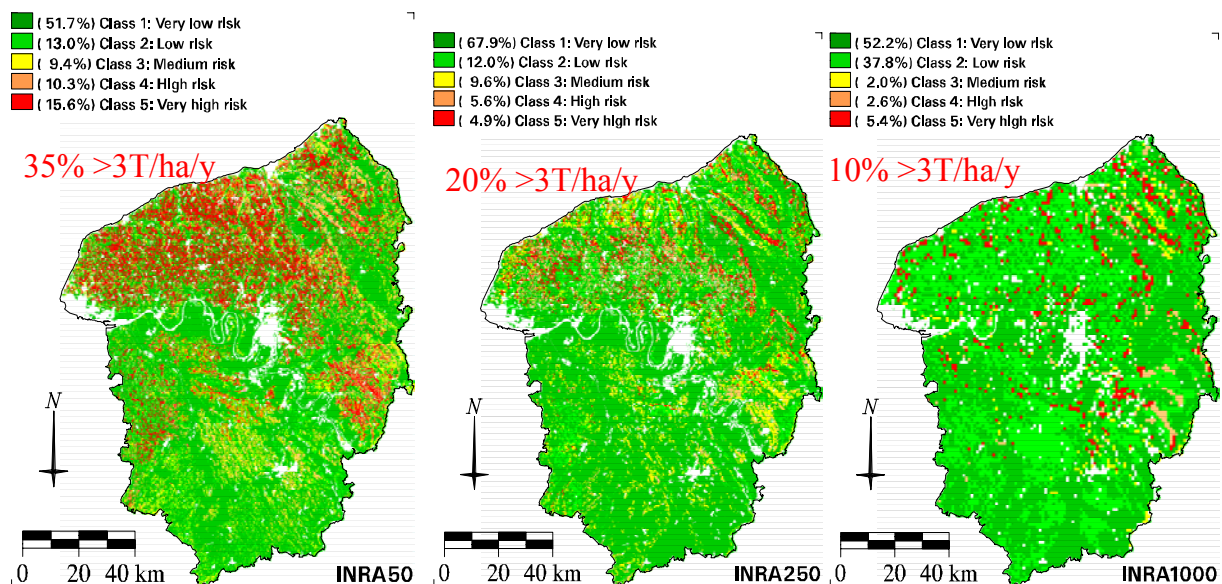


Figure 5.3: Comparison of the INRA expert model at three different resolutions.

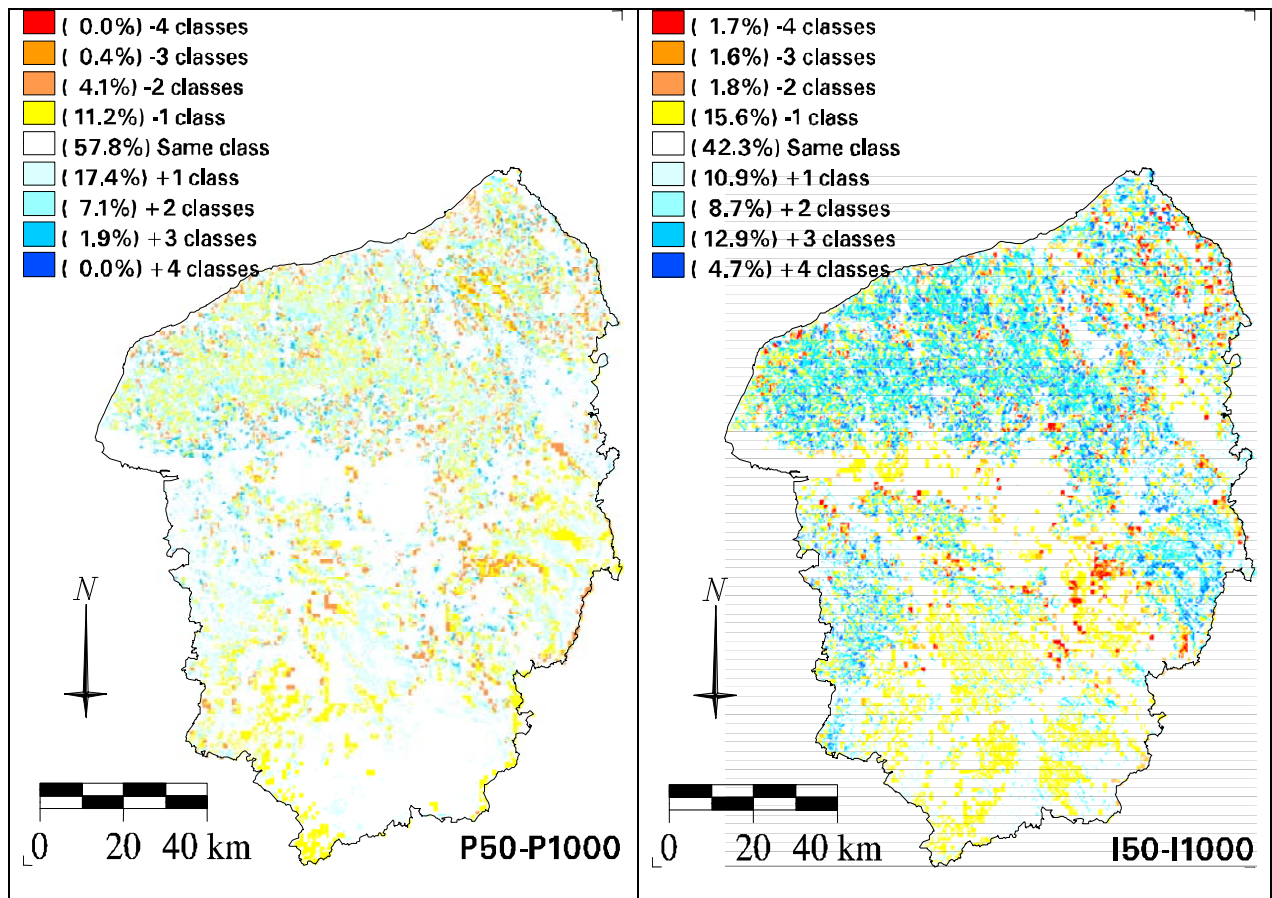


Figure 5.4: Comparison between different resolutions for the INRA expert model (I) and the PESERA model (P).

Seasonal assessment:

We did the same comparison exercise between PESERA 50 and INRA 50 models with seasonal erosion risk results. This will allow to further validate the model by analysing its sensibility to seasonal changes (climate and vegetation). Results are not the same for the different seasons. The histogram below shows the seasonal values for each class of erosion risk for the two models. The general pattern is the same for the two models, with highest risks in Autumn and winter, however, the PESERA model underestimates erosion risk in Spring and Winter. This is probably due to the low quality of the meteorological data used in PESERA model (50 km resolution) compared to data at 5 km resolution in INRA model.

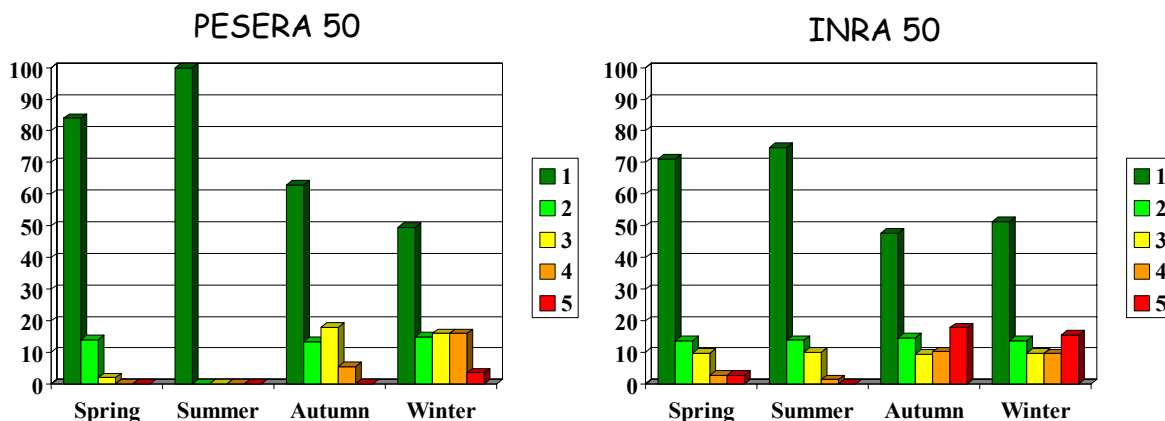
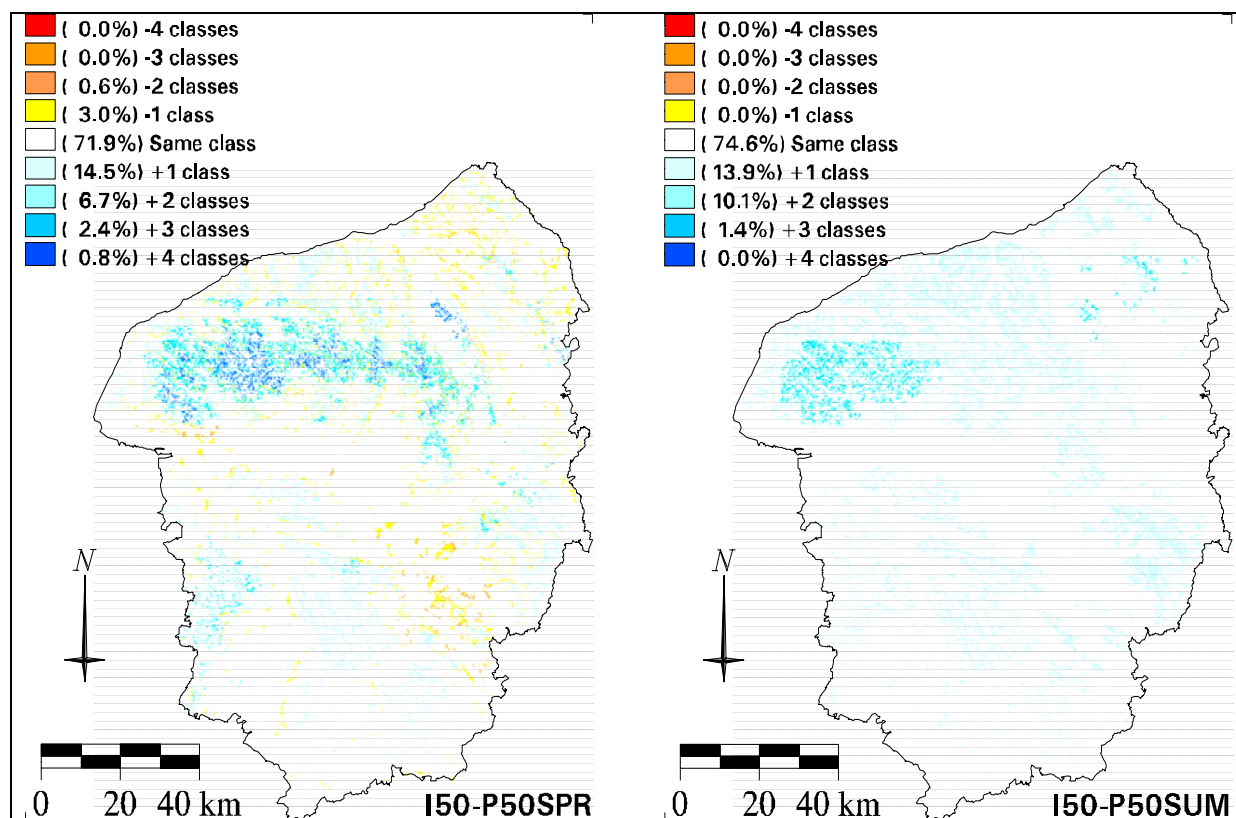


Figure 5.5: Histogram of seasonal values for each class of erosion risk for the two models

The four maps below show the geographical differences between the two models: underestimation of erosion risk by PESERA model is mainly in areas of high and very high erosion risk, in Spring and Summer, whereas it is more widespread in Autumn and winter.



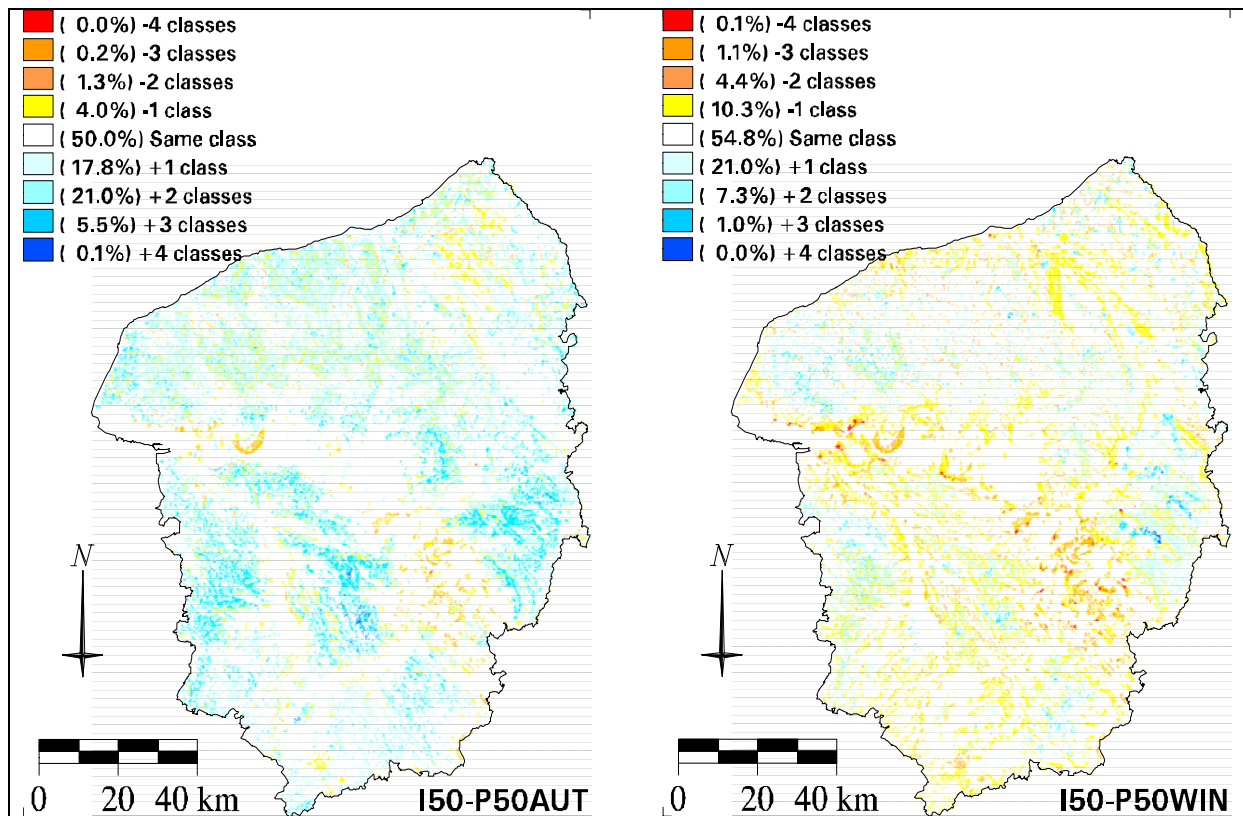


Figure 5.6: Comparison between the INRA expert model and the PESERA model at 50 m resolution for the four seasons.

The main conclusions of this regional validation exercise are:

- a global underestimation of erosion risk by PESERA model, which is reduced by using high resolution data, but still remains, especially for the Spring and Summer seasons. The reason for this could be partly due to global calibration problems, but the seasonal problems are certainly due to the low quality of meteorological data.
- A fairly good seasonal pattern, beside the problems mentioned above.

It can be concluded that the remaining discrepancy between PESERA model and the validation data from INRA model is probably due to data quality and resolution effects rather than model problems, although further calibration of the PESERA model is certainly necessary before the final application to the entire Europe.

5.3.2.3. Validation of PESERA model at regional scale for different areas in Europe

The same exercise was planned for three other test areas in Europe: Flanders (Belgium), Lesbos (Greece), and south of Spain.

For each test area, erosion assessment or measurement data as well as high resolution input data are available. Results will be available for the Wageningen Pesera meeting and will be presented in the final report.

5.4. WORK PACKAGE MANAGEMENT ISSUES

5.4.1. Significant difficulties or delays experienced during the third reporting period

Contributions of our team are in accordance with the work plan. Database have been delivered in due time. However, the results of crusting and erodibility pedotransfer rules should be calibrated on the basis of high resolution validation data set analysis. The current analysis of this data set does not allow to establish significant calibration relationships, therefore the pedotransfer rules have to be used for PESERA model without calibration for the moment.

5.4.2. Sub-contracted work during the third reporting period

no

5.4.3. Deliverables

For WP5: An updated version of the database, taking into account modifications discussed during the ISPRA meeting, has be delivered to all partners:

Database and information on factors affecting erosion: topography, soils, climate, and vegetation cover.

Database and information on pre-processed model input parameters: DEM fromSAR, soil cover, soil storage, soil erodibility, crusting, daily rainfall interpolated at finer resolutions and rainfall intensity.

Software for automated processing of meteorological data.

Meteorological data interpolated to a 1km x 1km grid

For WP4: Validation results at low resolution for Normandy region has been delivered month 36 for Wageningen meeting.

CHAPTER 6 THE EUROPEAN SOIL BUREAU AT JRC

Robert J A Jones, Mirco Grimm and Luca Montanarella

The European Soil Bureau, Soil & Waste Unit, Environment Institute, JRC, Ispra

6.1. ROLE AND CONTRIBUTION

The European Soil Bureau coordinates the application of the PESERA model at the European level (WP5). Together with INRA the ESB have been working on database management, data quality and data availability to fulfill the needs and requirements set by the PESERA model. The work carried out during the reported period consists of the development of the soil water storage capacity.

6.2. SOIL WATER STORAGE CAPACITY

This section describes the estimation of the *available water capacity* and the *drainable pore space* needed to calculate the Soil Water Storage Capacity (SWSC) for input to the PESERA soil erosion model. The SWSC is important because balancing the potential for storing rainwater with the moisture state of the soil at the time of precipitation permits more accurate estimation of when runoff is likely to begin.

6.2.1. Soil Water Storage Capacity (SWSC)

Figure 6.1 shows the main components of the soil-plant-system with respect to the soil water available to plants and the drainable pore space. The results from this component of the PESERA project comprise recalculation of a number of soil physical and hydraulic parameters currently stored in the European Soil Database. Recalculation was necessary to develop a complete database of these parameters because some basic data are missing. A number of new pedotransfer rules have also been constructed to complete the calculations.

The soil water storage capacity, integrated to 1m or to the depth to rock (if smaller) – $SWSC_{profile}$ can be calculated as:

$$SWSC_{profile} = \sum_{0-100} SWAP + \sum_{0-100} k(SPO) \dots\dots\dots (1)$$

Where k is a proportion between 0 and 1: 0.33 and 0.5 have been suggested.

The Soil Water Available to Plants (SWAP), calculated in mm, is defined by Thomasson (1995). The amount of water available to plants depends on the depth of soil into which the plants can extend their roots. In principle, it is the amount of water held between field capacity (5kPa) and permanent wilting point (1500kPa) but the amount available in a soil profile varies for different crops (Jones et al., 2000). In developing the PESERA model, only the SWAP in a 1m depth of soil (or to the depth of rooting if less than 1m) has been

computed. In future, it may be worthwhile computing SWAP for different crops and relating these data to land cover to improve the input data for PESERA.

Assuming the topsoil is 30cm thick, Swap_tot – total SWAP – is calculated as:

$$\text{Swap_tot} = \text{Swap_top} + \text{Swap_sub} \tag{2}$$

Where:

$$\text{Swap_top} = \sum_{0-30} \text{AWC_top} \tag{3}$$

$$\text{Swap_sub} = \sum_{30-100^*} \text{Awc_sub} \tag{4}$$

* or less if rooting is restricted by rock or compaction.

The total drainable pore space (Po_{tot}) can be estimated by integrating the drainable pore space, as a % vol, for the profile to 1m. This is done by partitioning the profile into topsoil and subsoil horizons – see Figure 6.1 and equation (5).

6.2.2. Drainable Pore Space

Po_{Top} and Po_{Sub} are the topsoil and subsoil components of Po , and Po_{tot} , the total drainable pore space, is defined as

$$Po_{tot} = Po_{top} + Po_{sub} \tag{5}$$

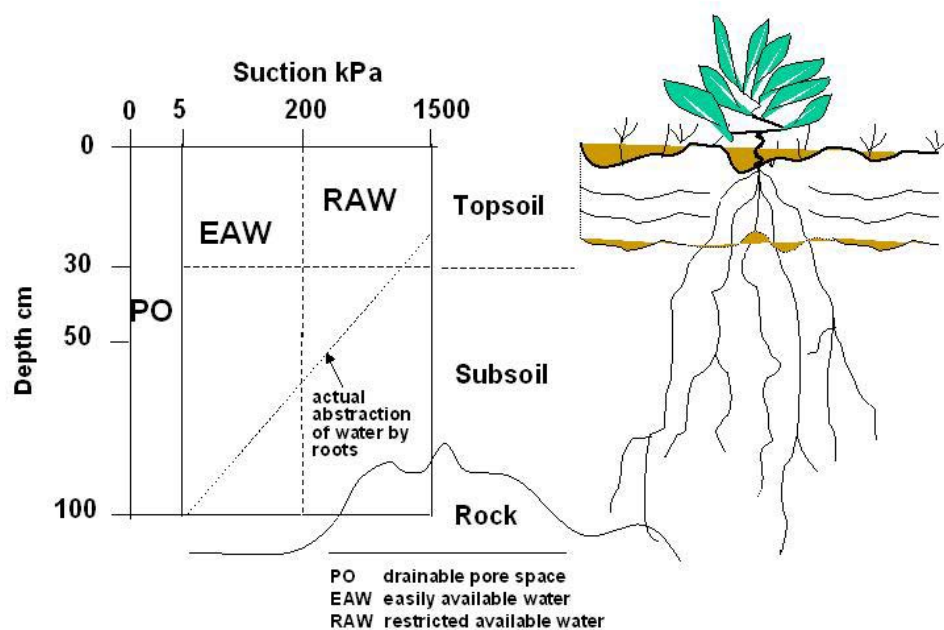


Figure 6.1 Water retention in the soil-plant system

Table 6.1 shows estimates of the drainable pore space (effectively the air capacity), as a % by volume (Hall *et al.*, 1977), for the soil texture classes of FAO (CEC, 1985). The values are given for different packing densities (Jones *et al.*, 2003).

The drainable pore space, **Po_tot** is calculated using equation (5) by referring to Table 6.1. For texture code (TEXT1) and the packing density for the topsoil (PD_TOP), the appropriate drainable pore space is selected from Table 6.1 and multiplied by 30. The integrated drainable pore space in *mm* is calculated for the topsoil using Equation 6.

$$\text{Where } Po_{top} = \sum_{0-30} Po \tag{6}$$

Table 6.1 Drainable Pore Space (Po % vol.)

Texture	TEXT	Po_top %			TD1	Po_sub %		
		PD_TO P	PD_TO P	PD_TO P		PD_SU B	PD_SU B	PD_SU B
Name	COD E	LOW	MED	HIGH	COD E	LOW	MED	HIGH
Coarse	1	30	25	20	1	25	20	18
Medium	2	20	15	10	2	18	15	10
Med-fine	3	15	12	8	3	15	12	8
Fine	4	10	8	5	4	10	8	5
V Fine	5	8	5	3	5	5	3	2
Organic	9	30	25	--	9	30	25	--
None	0	--	--	--	0	--	--	--

For the subsoil, a similar procedure was adopted by selecting the drainable pore space according to the subsoil texture (**TD1**) and the packing density for the subsoil (**PD_SUB**). The drainable pore space was then integrated over the remainder of the profile using equation (7), unless the depth to rock (**DR**) is less than 1m in which case equation (8) was used.

For example:

If DR => 100cm then,

$$Po_{sub} = \sum_{30-100} \frac{Po}{10} \tag{7}$$

If DR <100cm then,

$$Po_{sub} = \sum_{30-DR} \frac{Po}{10} \tag{8}$$

Profile drainable pore space **Po_tot** is then calculated from equation (5).

Before calculating the SWSC for input to the PESERA model, consideration must be given to the proportion of this capacity that is realistically available for absorbing rainfall before runoff begins. This will depend on the moisture content at the time of the precipitation event, the degree of crusting and the permeability of the soil.

For example in the simplest case, if the soil is at permanent wilting point (PWP) the SWSC could be calculated according to equation (1):

$$\text{SWSC} = (\text{Swap_tot}) + k(\text{Po_tot}) \quad (9)$$

Where k is a proportion between 0 and 1; initially k is set to 0.5

However, in practical terms the total SWSC of a soil at PWP moisture content may only be available for storing rainfall if the soil profile to 1m depth is loosely packed and rapidly permeable (ie with a saturated hydraulic conductivity $k_{\text{sat}} > 10 \text{ m d}^{-1}$). Where permeability is slow, for example $k_{\text{sat}} \leq 10 \text{ cm d}^{-1}$, only a proportion, for example 10% or less, of the SWSC will be available for absorbing rainfall. For very slow permeability ($k_{\text{sat}} = 0.1$ to 1 cm d^{-1}) even less (only about 1%) of the SWSC could be accessible.

The SWSC volume that is actually available for absorbing precipitation also depends on the moisture-state at the time of the precipitation. For example, if the soil profile is completely dry then more water will be potentially absorbed than if the soil is moist.

Therefore, the soil water available to plants, in 1m depth of soil, that is *effectively* available for storage (**Swap_totef**) – see equation (10) – needs to be calculated according to equation (10) after the components for topsoil and subsoil have been adjusted according to the factors **p1** and **p2** listed in Table 6.2.

$$\text{Swap_totef} = p1(\text{Swap_top}) + p2(\text{Swap_sub}) \quad (10)$$

Table 6.2 Proportion of the SWAP available for storing precipitation

Texture	TEXT1	p1(Swap_top)			TD1	p2(Swap_sub)		
		PD_TO P	PD_TO P	PD_TO P		PD_SU B	PD_SU B	PD_SU B
Name	COD E	LOW	MED	HIGH	CO DE	LOW	MED	HIGH
Coarse	1	1.0	1.0	0.8	1	1.0	0.8	0.6
Medium	2	1.0	0.8	0.6	2	1.0	0.8	0.6
Med-fine	3	0.8	0.6	0.4	3	0.8	0.6	0.4
Fine	4	0.6	0.4	0.2	4	0.6	0.4	0.2
V Fine	5	0.3	0.2	0.1	5	0.3	0.2	0.1
Organic	9	1.0	0.9	--		1.0	0.9	--

None	0	--	--	--	0	--	--	--
------	---	----	----	----	---	----	----	----

Two values for the effective SWSC can then be calculated using equations (11) and (12):

$$Swsc_eff = p1(Swap_top) + p2(Swap_sub) + k(Po_tot_mmr) \dots (11)$$

$$Swsc_eff_2 = p1(Swap_top) + k(Po_tot_mmr) \dots (12)$$

Where k is a proportion between 0 and 1: k = 0.5 is proposed initially.

6.2.3. Implementation

To calculate the effective soil water storage capacity (SWSC) spatially using the European Soil Database (scale 1:1,000,000) requires a number of further steps.

Firstly, the available water must be recalculated in mm because the database provides only a class code that indicates a range in mm/m. Secondly, the soil water available to plants must be calculated by integrating the available water capacity for a 1m depth of soil (or less if rock is present). Thirdly, drainable pore space must be calculated as described above.

6.2.3.1. Available Water Capacity

Two important input factors for this calculation are the Available Water Capacity in the topsoil (**Awc_top**) and in the subsoil (**Awc_sub**). These parameters have already been estimated by applying the pedotransfer rules (PTR) 553 and 551 respectively (Van Ranst *et al.* 1995). The output parameters from PTR_553 and PTR_551, Awc_top and Awc_sub, are expressed in mm/m or %. However, rule 553 for AWC_SUB was modified to remove depth to rooting restriction (ROO) as an input parameter because this is replaced later by using depth to rock (**Dr**).

In the database table **stu.dbf** (in the folder \ptrdb\ on the distribution CD of the European Soil Database, the results of applying all the pedotransfer rules are given for every STU. It was discovered that for a number of STU's, although AWC_TOP has been estimated for most STUs, AWC_SUB has been assigned # (no data or not applicable) where no data for the fields **Text** and **TD1** or **TD** exist in the database.

Table 6.3 Classes of available water capacity (mm/m)

Class code	Class name	AWC	Water content
VL	Very Low	~ 0 mm/m	20mm/m
L	Low	< 100 mm/m	60mm/m
M	Medium	100 – 140 mm/m	120mm/m
H	High	140 – 190 mm/m	165mm/m

VH	Very High	> 190 mm/m	220mm/m
XH	Extremely High		300mm/m
#	[No data or not applicable]		-999

6.2.3.2. Topsoil Available Water Capacity

The Topsoil Available Water Capacity (**AWC_TOP**) was derived using the input data **Text** (pedotransfer rule on dominant surface textural class **Text1**) and topsoil packing density (**PD_TOP**) following the pedotransfer rule 551. Where no data exist for the **Text** of an STU, texture was estimated (from **Soil**) by expert judgement. The field **TextAWCtop** contains the dominant surface texture class used as Input data for the Topsoil Available Water Capacity and the source of these data are given in **TxAWtpOrig**.

Where the dominant surface texture class is coded '9' (meaning histosols), the **AWC_TOP** was set (by expert judgement) to XH (extremely high) = 300 mm/m for calculating Topsoil Available Water Capacity. The results are given in the column **AWC_TOP_02t** (as char string) and **AWC_TOP_02** (in mm/m).

6.2.3.3. Subsoil Available Water Capacity

The Subsoil Available Water Capacity was derived using texture and subsoil packing density (**PD_SUB**) input and applying the pedotransfer rule shown in the Table 6.4. In the STU-table the results can be found in the column **AWC_SUB02t**. Whereas for the packing density of the subsoil just one set of input data was used (**PD_SUB**), for the texture of the subsoil different Input data had to be used because the dominant sub-surface textural class (**TD1**) is missing for some STU's. The following sequence was used to select the input data for texture:

- TD1 Dominant sub-surface textural class
- TD An applied pedotransfer rule on dominant sub-surface textural class (TD1)
- Text1 Dominant surface textural class
- Text An applied pedotransfer rule on dominant surface textural class (Text1)

It was observed that in a number of cases, **TD1** had a dominant sub-surface textural class of '9' (= No texture (histosols, ...)) whereas the dominant surface textural class (**Text 1**) had a value of between 1 and 5. Since it is not common to have mineral surface horizons overlying organic material, the TD code was taken instead of that for TD1. During compilation of the database, it is possible that a '9' was used instead of '0' where information was not available. The texture of the topsoil (**Text1** and **Text**) was used for that of the subsoil, where **TD1** and **TD** are missing.

For STU's where no information on sub-surface texture class is stored, expert judgement was used to derive it from **Soil**. The new sub-surface textural classes used in the pedotransfer rule (Table 6.4) are given in the column **TextAWCsub** with the source of the data given in **TxAWsbOrig**.

Table 6.4: Estimation of **AWC_SUB02** from texture and subsoil packing density

		PD SUB		
Texture (TextAWCsub)	Texture class	L	M	H
		Low	Medium	High
1	Coarse	M	L	L
2	Medium	VH	H	M
3	Medium fine	VH	VH	M
4	Fine	VH	H	M
5	Very fine	VH	H	M
9	No texture (histosols,...)	XH	XH	N/A
0	No information	#	#	#

The results of applying the pedotransfer rule in Table 6.4 are given in the column AWC_SUB_02t (as char string) and AWC_SUB_02 (in mm/m).

For the further steps in the calculation, the columns **TextAWCtop** and **TextAWCsub** have been used for the dominant surface and sub-surface textural classes respectively.

6.2.3.4. Soil Water Available to Plants (SWAP)

Soil water storage capacity can be calculated by taking into account various combinations of the soil water available to plants (SWAP) and the drainable pore space (Po). The following sections specify the implementation adopted for this database. For the calculation of **Swap_top** it was assumed that there is no restriction to rooting within 30 cm depth whereas for **Swap_sub** any restriction to rooting was derived from the parameter Depth to Rock (**DR**), according to the limits specified in Table 6.5.

Table 6.5: Derived restriction of soil depth by depth to rock (DR)

DR (Depth to Rock)	DR (classes in cm)	DRcm (Restriction in cm)
S(hallow)	0-40	30
M(oderate)	40-80	60
D(eep)	80-120	100
V(ery) D(eep)	>120	200

The proportion of the SWAP available for storing excess water is defined by p1(Swap_top) for the topsoil and p2(Swap_sub) for the subsoil.

6.2.3.5. Drainable Pore Space

The output of the drainable pore space calculations (see equations 6–8) is stored as **Po_top%** and **Po_sub%**, expressing the percentage of air-filled pores in the upper and lower compartments of the soil profile.

Calculating the pore space in mm must also take into account restriction to rooting. For calculating **Po_top_mm**, it was assumed that no restriction to rooting exists within 30 cm of

the surface whereas any restriction relevant to the calculation of **Po_sub_mm** was derived from the depth to rock (**DR**); classes of DR are defined in Table 6.5.

These parameters were calculated as follows:

$$Po_top_mm = 0.3 ((Po_top\%)10)$$

$$Po_sub_mm = ((Po_sub\%)(DR - 30))/10$$

6.2.3.6. Effective Soil Water Storage Capacity

The soil water storage capacity (SWSC) calculated using equation (9) gives a maximum estimate. Alternatively the effective soil water storage capacity (SWSC_{eff}) is calculated using equations 11 and/or 12.

6.2.4. Spatial distribution of SWSC at European level

The resulting SWSC data (total and effective), as described in the previous sections, have been used to generate maps of SWSC at European level, using the ArcView GIS (ver 3.2). Figure 6.2 is presented in an attempt to clarify the differences between the equations proposed for estimating SWSC.

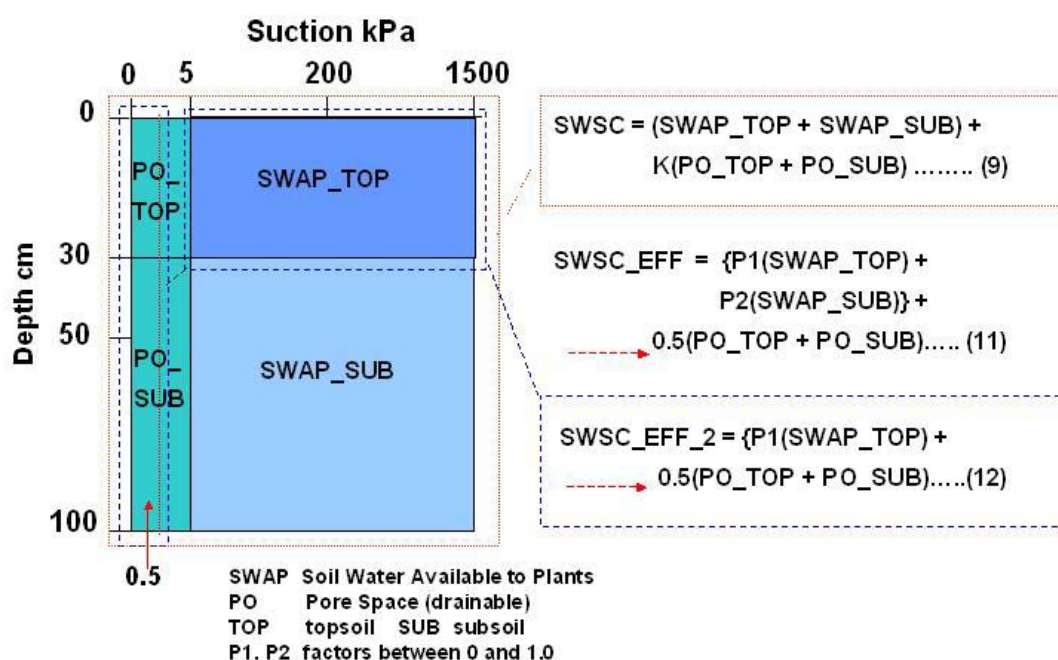


Figure 6.2 Calculating Soil Water Storage Capacity

Figures 3-6 show the distribution of drainable pore space (PO), soil water available to plants (SWAP) and two estimates of soil water storage capacity (SWSC) for Europe.

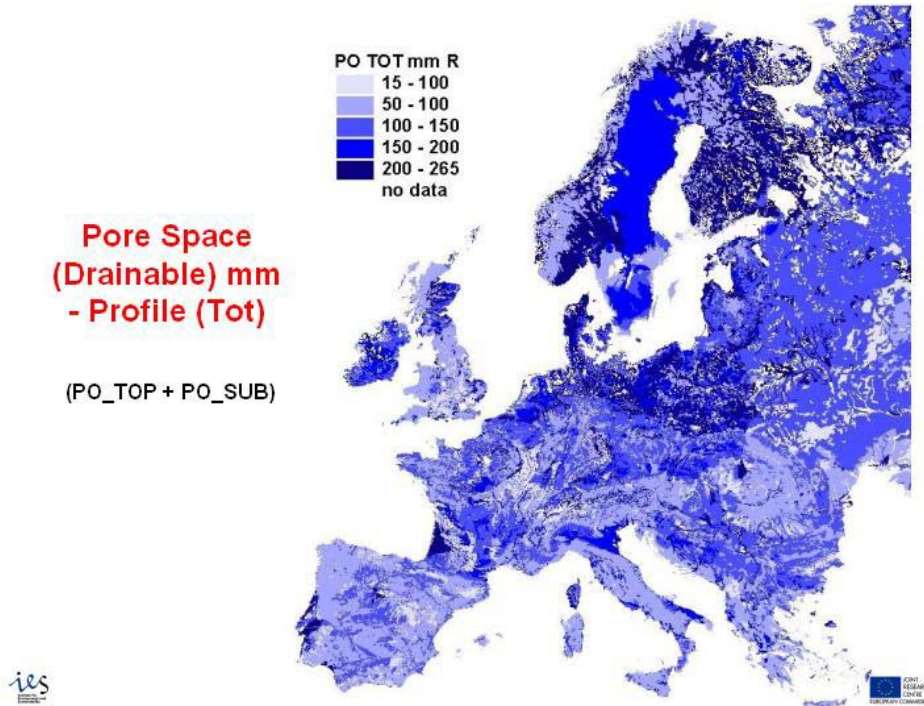


Figure 6.3 Drainable Pore Space, PO (mm)

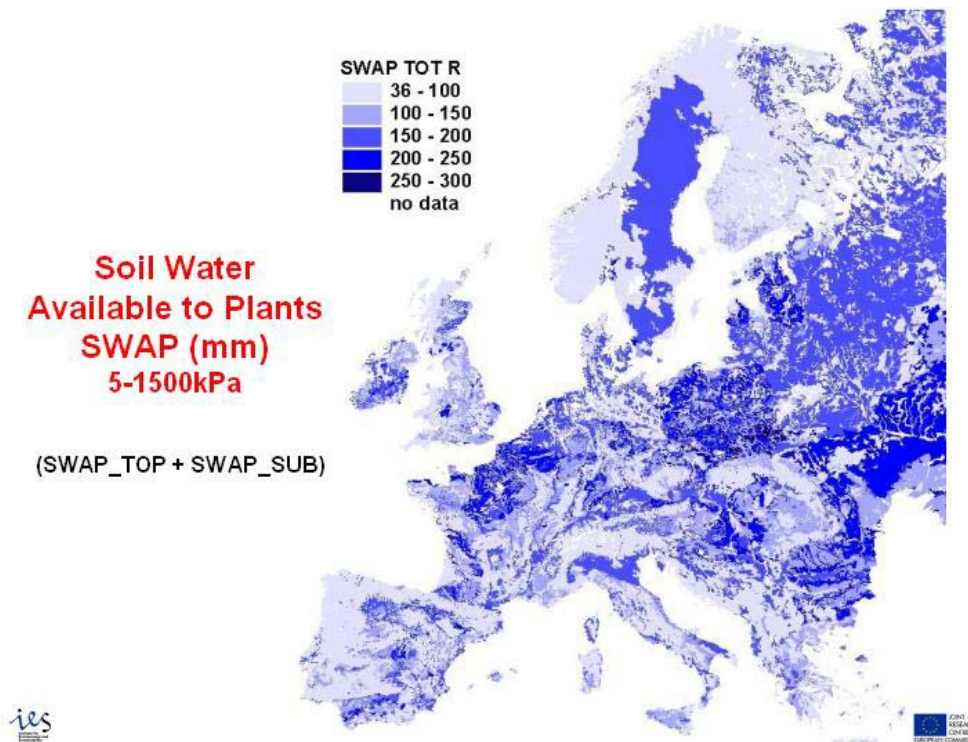


Figure 6.4 Soil Water Available to Plants (SWAP)

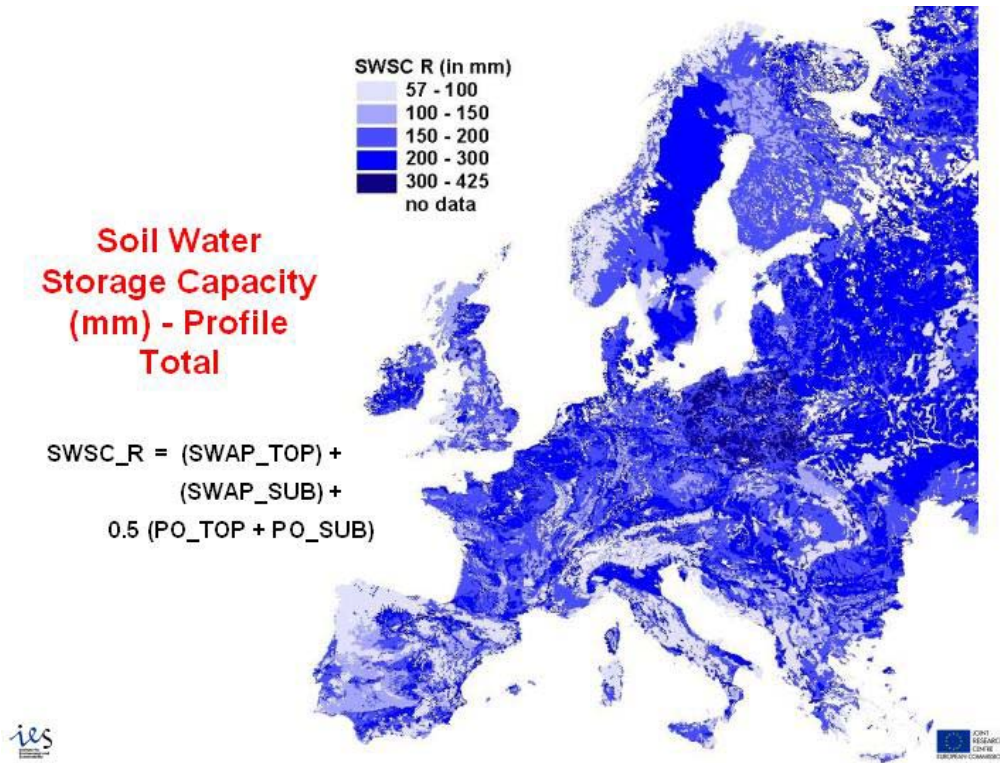


Figure 6.5 Soil Water Storage Capacity mm, k = 1

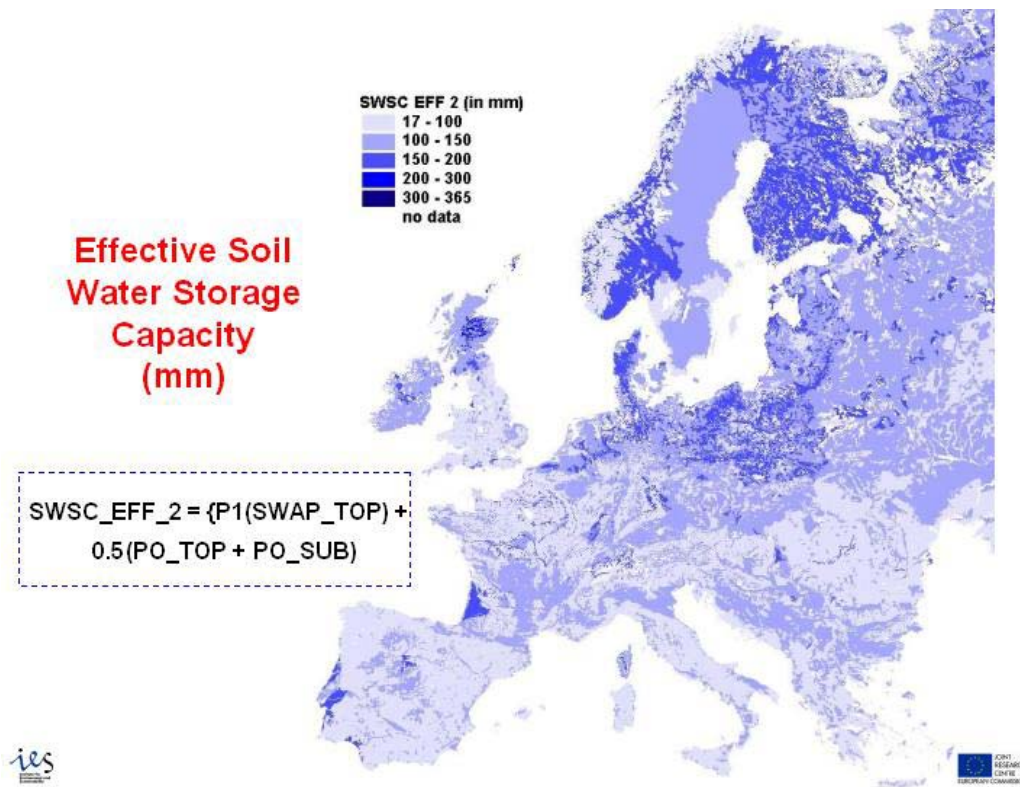


Figure 6.6 Effective Soil Water Storage Capacity mm by Equation 12

6.2.5. Future actions

With respect to the PESERA Project, the soil water storage capacity (SWSC) database will be used to generate erosion risk assessments for Europe at 1km x 1km resolution. These assessments will be validated against actual measurements of sediment loss from catchments in Italy and Belgium.

Depending on the results of the validation studies, the database described here will permit the PESERA model to be rerun using different calculations of ‘effective’ soil water storage capacity ($SWSC_{eff}$), for example by varying the value of ‘k’ used in equations 11 & 12.

Another refinement that could be adopted would be computing SWAP for different crops, relating these data to land cover and computing new estimates of $SWSC_{eff}$.

CHAPTER 7 INTERNATIONAL SOIL REFERENCE AND INFORMATION CENTRE (ISRIC)

Stephan Mantel, Jan Huting, Godert van Lynden
Postbus 353, 6700 AJ Wageningen. The Netherlands

7.1. ROLE AND CONTRIBUTION

In work package 6 the PESERA model will be run for a number of scenarios. Scenarios will be selected so that the impact of both natural changes, such as climate, and anthropogenic changes, such as land use, can be evaluated. The scenarios will be run for a number of representative regions within the European Union.

Special attention will be given to the potential effects of climate change on the soil erosion risk. Climate changes may have important effects in relatively dry Mediterranean areas, which will therefore receive particular attention. Climate change scenarios will be derived from Global Change Models. From these scenarios the necessary input data for PESERA will be derived and model runs will be carried out to investigate the potential effects of climate change on erosion risk. Within this study, it will be necessary to take into consideration the fact that significant climate changes will also be accompanied by land use changes. By running the model for specific crops, policy factors (e.g. CAP) can be taken into account.

7.2. ACTIVITIES DURING REPORTED PERIOD

The International Soil Reference and Information Centre carried out the following work during the period April 2002 to April 2003:

- Test-running the regional model
- Acquisition of scenario layers for climate and land use
- Soil suitability analyses for crops as a way to assess potential distribution of crops

7.2.1. WP6: Data layers for scenario studies

Scenario analysis provides information on erosion risk in a changed climate and the possible impact of erosion. Land use changes within Europe are largely controlled by agricultural and environmental policies. Running PESERA for various land use scenarios supplies information on the potential impact of agricultural policies on erosion risk. The significance of erosion for land use and the effects of climate change on erosion (risk), resulting from scenario analyses, will in turn provide information for policy formulation.

7.2.1.1. Land use scenarios

The assumption for this work package had been that the output of the ATEAM EU project (land use scenarios for Europe) could be used (PESERA, 2002). The output of the ATEAM project is seriously delayed, to the extent that PESERA will effectively not be able to use ATEAM products within the PESERA project period. Alternative scenario data have been explored. The ATEAM and ACCELERATES projects planned to deliver four draft land use scenario's and a comprehensive report in September 2002. It was only in January 2003 that the draft scenarios were completed and the final product is now expected for September 2003. The ATEAM/ACCELERATES creates 10 min. grid land use scenarios with multiple components. The current draft scenarios are not fit for use in PESERA, as they contain five crude land use classes (%) only; arable land, grass land, forest land, urban land, other.

A suitability assessment for crops was made for Europe (1 Km grid) as an input to analyses with climate scenarios. This combination may provide an alternative to the land use change scenario layers. It allows stratification for areas not suitable for particular crops and areas that are potentially suitable.

Decision rules (Boogaard *et al.*, 2002) were used to assess soil and land limitations to crop growth. The following parameters were used in the suitability assessment: rooting depth, soil salinity, soil alkalinity, drainage, soil phase, slope, soil texture. The salinity, alkalinity, and drainage are derived from soil properties in the European soils database, through soil classification code and soil phase indication. Soil phase is obtained directly from the European soils database. Soil texture and rooting depth are obtained from the PESERA grids. Slope is classified from the 1 Km European Digital Elevation model. See Figure 7.1 for an example of drainage limitations to cereal crops.

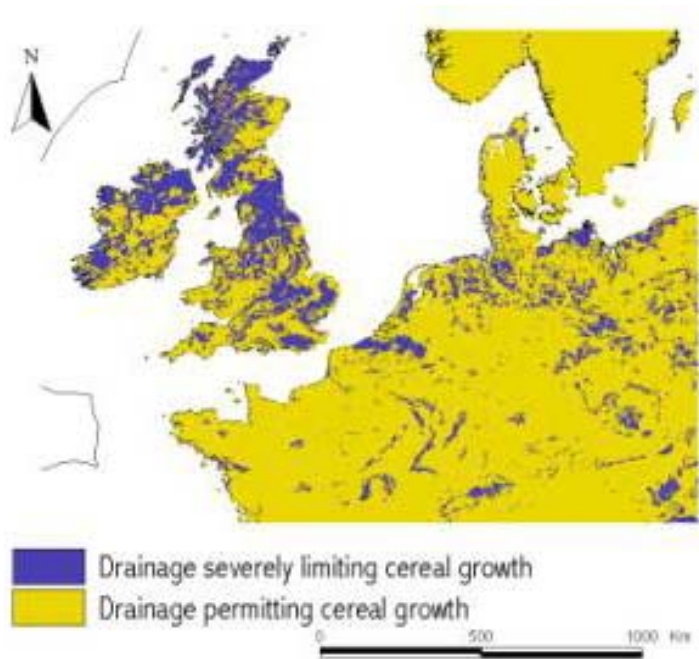


Figure 7.1: Drainage constraints to cereal growth in NW Europe.

The suitability analysis was done for two crop groups and one crop type: root crops, cereals, and maize. In Figure 7.2 a draft map of soil suitability for cereals is presented. Climate limitations will be analysed separately and will be added as an additional layer to the suitability map. That way, the suitability maps can be produced for both actual conditions and for scenarios. The suitability analysis will be verified by comparing maps with actual land use information, such as Corine land use database and higher resolution information for windows, with other existing other land suitability studies for Europe.

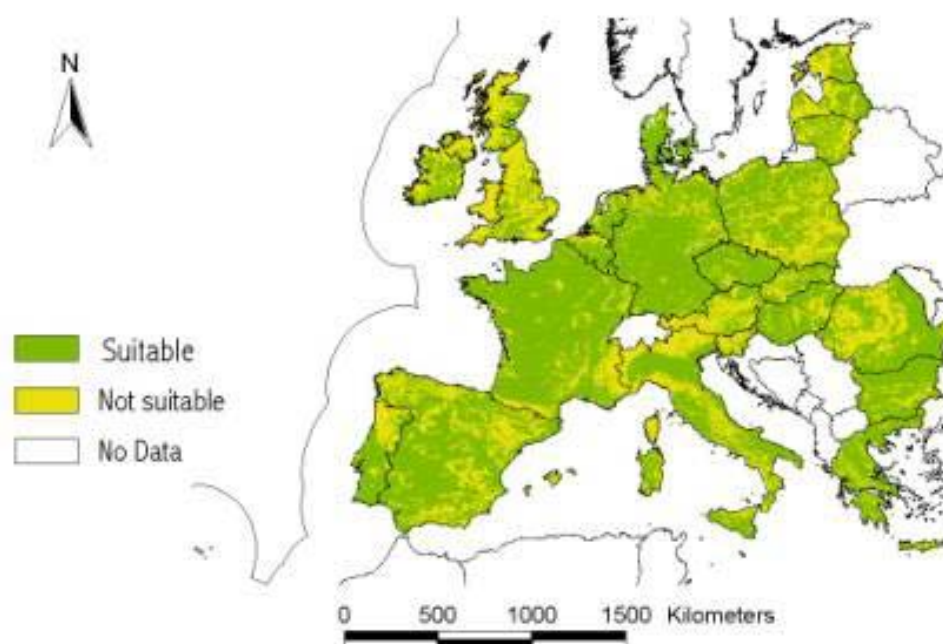


Figure 7.2: Suitable soils for cereals in Europe based on dominant soils.

7.2.1.2. Global Circulation Model climate scenarios

For climate scenarios, the Hadley Centre for climate prediction and research, which is part of the UK Met Office, was contacted. The Hadley Centre runs several computer climate models for climate projections at varying spatial and temporal resolutions, and for different assumptions on socio-economic changes. The Hadley Centre has given PESERA access to climate scenario files of HADRM3, a Regional Climate Model (RCM). The regional Climate Model (RCM) has been developed by the Hadley Centre to help address issues that processes that are below the resolution of the General Circulation Models (GCMs). These models typically have a grid resolution of about 300 kilometres at best. This is considerably less than that required for many impact studies, particularly those involving hydrological processes (Hostetler, 1994). Local features, such as mountains, greatly influence local climate change. These local features are not well represented in global models because of their coarse resolution. Models of higher resolution are unpractical for global simulation of long periods

of time. Therefore, higher resolution (typically 50 km), regional climate models are constructed for limited areas and run for shorter periods (20 years or so). RCMs take their input at their boundaries and for sea-surface conditions from the global Atmosphere General Circulation Models, e.g., HadAM3 (Hadley Centre, 2003). The regional HADRM3 model was selected mainly because of the finer resolution of 50 km. The HADRM3 file format is in rotated pole coordinates and is transformed into a format that can be used as an input to PESERA. The Hadley Centre global change models are run within the framework of the story lines of the Special Report on Emission Scenarios (SRES), produced by the International Panel on Climate Change. Each SRES scenario consists of a typical story line, spanning different possible futures (c.f. globalisation versus regional blocks; growth of material wealth versus environmental protection and equity). The story lines define different demographic, economic and technological developments and lead to strongly different future emissions (based on model calculations), (IPCC, 2003). In principle the A2 and B2 story lines will be used for WP6, as they represent a high case and intermediate case of emission scenarios. Time slices available for the HADRM3 scenarios are: 1961-90 (reference conditions), and 2070-99.

CHAPTER 8 AGRICULTURAL UNIVERSITY OF ATHENS

C. Kosmas, N. Yassoglou, P. Kosmopoulou, D. Kosma

Laboratory of Soils and Agricultural Chemistry
Iera Odos 75, Botanikos 11855, Athens GR

8.1. MAIN WORK CARRIED OUT DURING THE REPORTING PERIOD

The following work was carried out during the period from April 2002 to March 2003:

- Compilation of the draft user's manual for PESERA model (excel version)
- Presentation of the PESERA model to end-users in the MEDRAP workshop held in Troia, Portugal.
- Application of the PESERA model (ArcGIS version) for the island of Lesvos
- Comparison of the erosion rates map (PESERA model) and the degree of soil erosion map estimated from soil surveys data.

8.2. METHODOLOGY AND MAIN RESULTS OBTAINED

8.2.1. WP7: Compilation of the user's manual for the PESERA model

A draft manual for end users of the PESERA model (excel version) was prepared. The manual included a description of the basic concepts and equations used by the model to assess soil erosion rates along a hillslope. The input model parameters for running the model were individually described explaining the format and units used. The model output data were also described. An example of the model calibration and validation was included using existing experimental soil erosion data. Finally, examples of the model application on environmental protection in the region of Sekania Sea Turtle National Park in the island of Zante, were included in the manual. More applications of the PESERA model will be included in the final version of the user's manual.

More specifically, the following chapters were included in the present version of the manual:

1. INTRODUCTION
2. ANALYSIS OF THE MODEL
 - a. Climate

-
- b. Soil
 - c. Topography
 - d. Vegetation
 - e. Integration of erosion parameters
3. USING THE PESERA MODEL
- a. Input model parameters
 - b. Model output
4. CALIBRATION AND VALIDATION OF THE MODEL
- a. Calibration of the model
 - b. Validation of the model
5. EXAMPLES OF APPLICATION OF THE MODEL
- a. The Sekania Sea Turtle National Park
 - b. THE ISLAND OF LESVOS
6. EVALUATION OF THE MODEL
7. CONCLUSIONS
8. REFERENCES

8.2.2. WP7: End-users of the PESERA model

The MEDRAP Concerted Action to Support the Northern Mediterranean Regional Action Plan to Combat Desertification in collaboration with: (a) the Annex IV Committees to Combat Desertification and (b) the Portuguese Focal Point organized a workshop with the title “**Identification of Sensitive Areas to Desertification in the Mediterranean**”. The workshop was held in Troia, Portugal, on 6-8 June 2002. The MEDRAP Concerted Action was funded by the European Commission to support the UNCCD Annex IV countries (Portugal, Spain, Italy, Greece and Turkey) for preparing the regional action plan for Mediterranean Europe (RAP). The workshop participants included end-users from Turkey, Greece, Italy, Spain, Portugal as well as the corresponding Focal Points from South America. The main objective of the Workshop was to derive indicators that can be used to define environmentally sensitive areas to desertification at a regional scale.

In this workshop the PESERA model was presented and the possibilities of application of the model were analyzed for defining environmentally sensitive areas to desertification. Also, the importance of the model in defining rates of soil erosion under different types of land use, climatic conditions, and management characteristics were presented. Finally, the PESERA model was included in the conclusions as a valuable tool for compilation of the Mediterranean Regional Action Plan to Combat Desertification in the Annex IV countries.

8.2.3. WP4: Example of regional model application

The PESERA model was applied in the island of Lesvos using existing vegetation, soil, and climate data. A database was prepared in a grid format (size 250 m by 250 m). More specifically the name and description of the grids used in the model are shown in table 1. The input grids described in Table 8.1 were created in ArcMap using the spatial analyst extension.

Table 8.1: Data in grid format prepared for application of the PESERA model in the island of Lesvos.

Data Source	Grid name	Description
Vegetation data	Rootdepth	Root depth
	Rough0	Initial surface storage
	Rough_red	Roughness reduction
	Use	Land use characteristic
	Cov_jan – cov_dec	Ground cover
Climate data	Meanrf1301-meanrf13012	Monthly rainfall
	Mtmean1- mtmean12	Mean temperature
	Mtrange1- mtrange12	Mean temperature range
	Cvrf21 – cvrf212	Coefficient of variation of rain per rain day
	Meanrf21-meanrf212	Mean rain per rain day
	Meanpet301-meanpet3012	Mean potential Evapo-Transpiration (ET)
Soil data (soil texture)	Soil_stor	Soil storage
	Crust_0702	Crusting
	Erod_0702	Erodibility
	Zm	Scale depth (range 5-30mm)
INRA	Std_eudem2	Standard deviation of elevation

Originally the grid size selected for Europe was set to 1km in order to run the operations and calculations more efficiently. For the island of Lesvos the cell size of the input data was adjusted to 250m. Initially the vegetation and soil data from Lesvos was transformed to match the projection and coordinate system of the INRA data (Lambert- Azimuthal) and then the shape files were converted to grids.

The implementation of the model required ArcMap and ArcInfo while part of the processing scripts were in Arc Macro Programming Language (aml). The final output of the model represented monthly estimated erosion rates and the total annual erosion rates.

Two workspaces were created: 1). The first folder (d:\meteo_grids) where all grids were stored and used as input in the PESERA model, and 2).The second (d:\temp_ascii) where all the scripts, dll, and executables of the model were run. The output grids are stored in a temporary folder (d:\temp_ascii) and include the estimated monthly and total annual erosion measured in tonnes per hectare.

The resulting grids were processed using an aml file, which was edited to select only the extent of Lesvos (xll = 1420000 –860000, yll = 1520000 –790000). The grids were extracted as ascii files to a temporary folder (d:\temp_ascii). In this pre-processing stage (Fortran90) the ascii files created previously were beheaded and merged. The PESERA code runs through

an executable file in order to make all the calculations using as input the previous ascii files while the output of this stage is also in ascii format.

The post-processing stage converts the resulting ascii files into grids. In the final stage an aml script was used to estimate the monthly erosion and total annual erosion grids. One grid was created for each month (sedi_jan ...sedi_dec), representing monthly erosion rates in tones per hectare and the total estimated annual erosion (sedi_tot) representing the total estimated erosion rate in tones per hectare per year. The model flow chart application is given in Figure 8.1.

8.2.3.1. Comparison of soil erosion rates and degree of soil erosion

The soil erosion rate for the island of Lesvos estimated by the PESERA model were divided into the following five classes:

- No soil erosion: annual soil losses (ASL)<0.1 t/ha
- Slight soil erosion rates: 0.1<ASL<0.5 t/ha
- Moderate soil erosion rates: 0.5<ASL<3.0 t/ha
- Severe soil erosion rates: 3.0<ASL<5.0 t/ha
- Very severe high soil erosion rates: ASL>5 t/ha

The first class of soil erosion rates covers an area of 13.2% of the island. It includes mainly plane areas, wetlands and hilly areas covered with dense evergreen perennial vegetation. The second class covers an area of 11% of the island. It includes hilly areas with moderate deep soils with moderately dense evergreen perennial vegetation. Areas with moderate soil erosion rates cover 40% of the island. This class includes hilly areas with shallow soils partially vegetated with shrubs and olives. Areas with severe erosion rates cover 17.5% of the island. This class includes very steep slopes with shallow soils partially vegetated with annual or perennial shrubby vegetation. The last class of soil erosion rates represents an area of 17,5 % of the total area of the island. It includes areas with very steep slopes, shallow soils and poor vegetative cover.

Based on the above classification of the soil erosion rates estimated by the PESERA model the soil erosion map of the island of Lesvos was compiled (Fig. 3). This map was compared with the degree of soil erosion map (Fig. 2) compiled during the MEDALUS III project (Mediterranean Desertification and Land Use) (Kosmas *et al.*, 1999). The degree of soil erosion map includes five classes described as in Table 8.2.

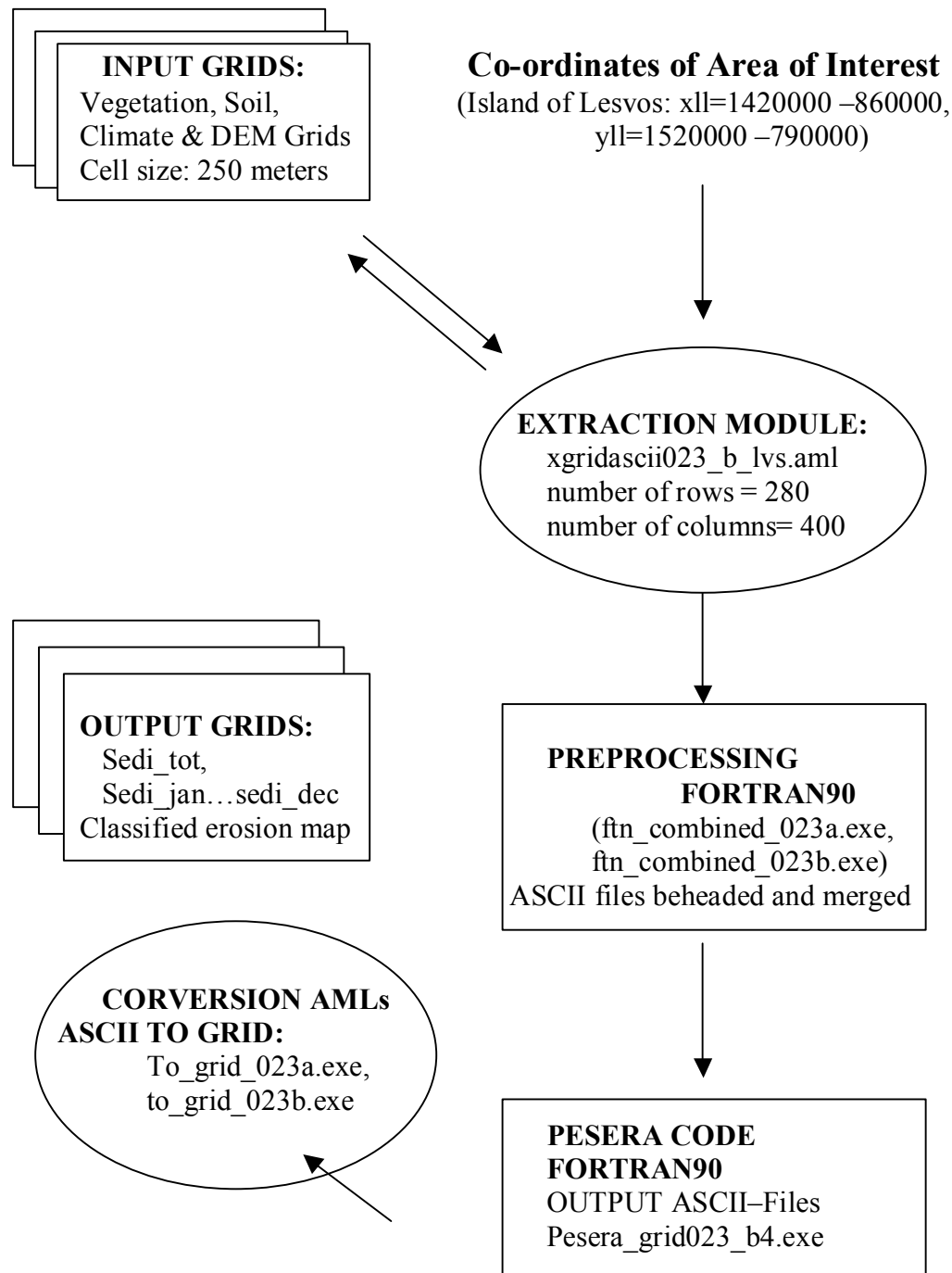


Figure 8.1: PESERA model flow chart for application in the island of Lesvos

Table 8.2. Classification of the various classes used to compile the degree of soil erosion map of the island of Lesvos.

Erosion class	Description
No	No erosion features are present
Slight	Parts of the A horizon have been eroded, so that usually less than 20% of the initial A horizon is present with current scattered spots of erosion.
Moderate	Soils that present an intricate pattern of current spots of erosion ranging on the average from 20 to 50% on the original A horizon.
Severe	Soils that show an intricate pattern of eroded spots ranging from 50 to 80% of the original A horizon. In most areas of this class the parent material is exposed at the surface.
Very severe	Soils that have lost more than 80% of the A horizon and some or all of the deeper horizons throughout most of the area. Original soil can be identified only in spots. Some areas may be smooth, but most have an intricate pattern of gullies and the parent material is exposed at the soil surface.

The comparison of both maps (Fig. 2 and 3) shows several similarities. In both cases the western part of the island is characterized as very severely eroded. The erosion rates estimated by the PESERA model are the highest for this area (Fig. 3). Areas in the central and eastern part of the island are characterized as slightly to moderately eroded (Fig. 2), while the PESERA model gave mostly moderate erosion rates (Fig. 3).

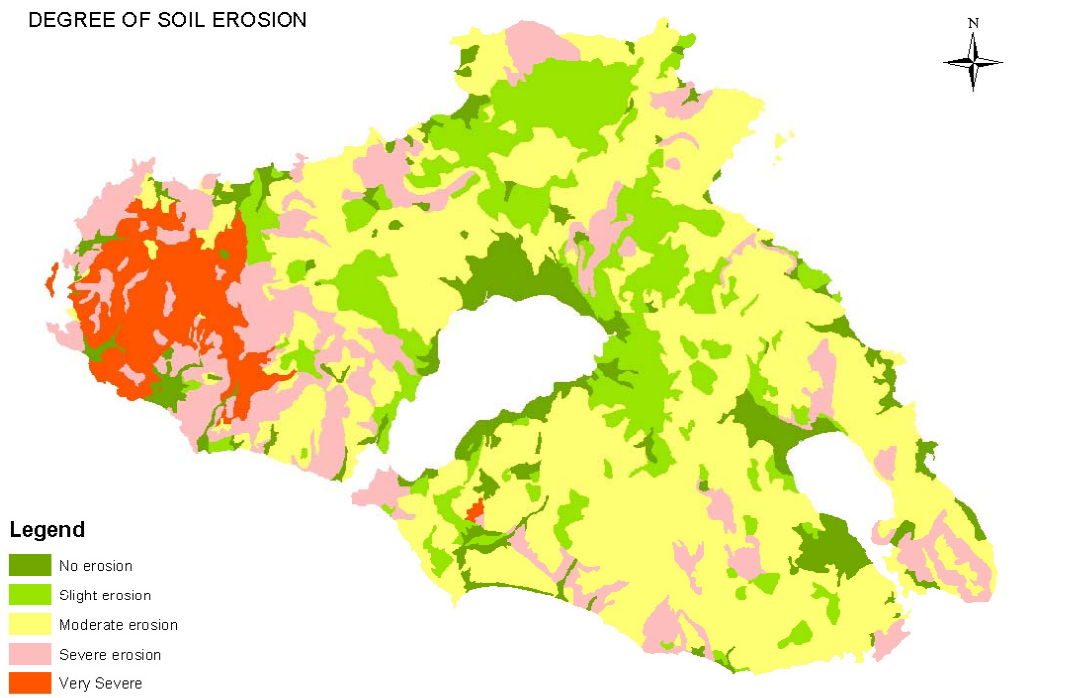


Figure 8.2: Map of Degree of Soil Erosion of Lesvos (MEDALUS III, project)

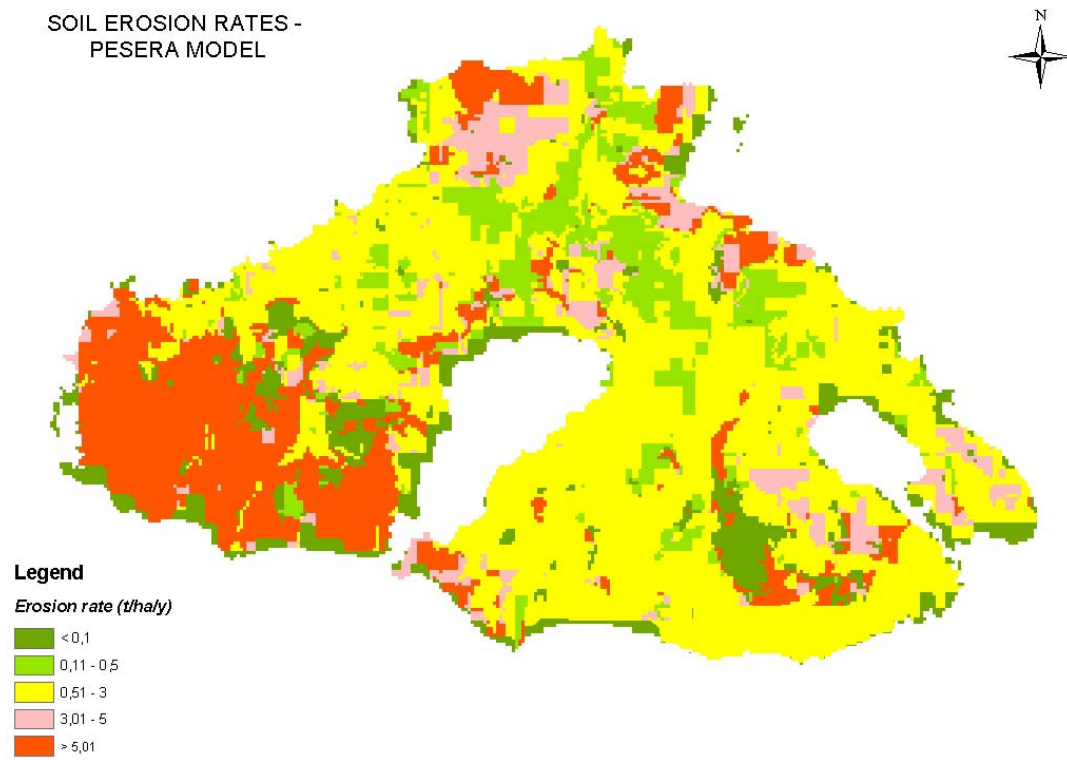


Figure 8.3: Map of Soil Erosion Rate estimated by the PESERA model.

Figures 8.4 and 8.5 represent the distribution (area %) of the various classes of erosion rates estimated by the PESERA model and the degree of soil erosion estimated in the soil survey. The obtained results show a similar distribution for all classes of soil erosion. Therefore, by using the appropriate database the PESERA model can be used for estimating soil erosion rates under different soil, climate, and vegetation conditions.

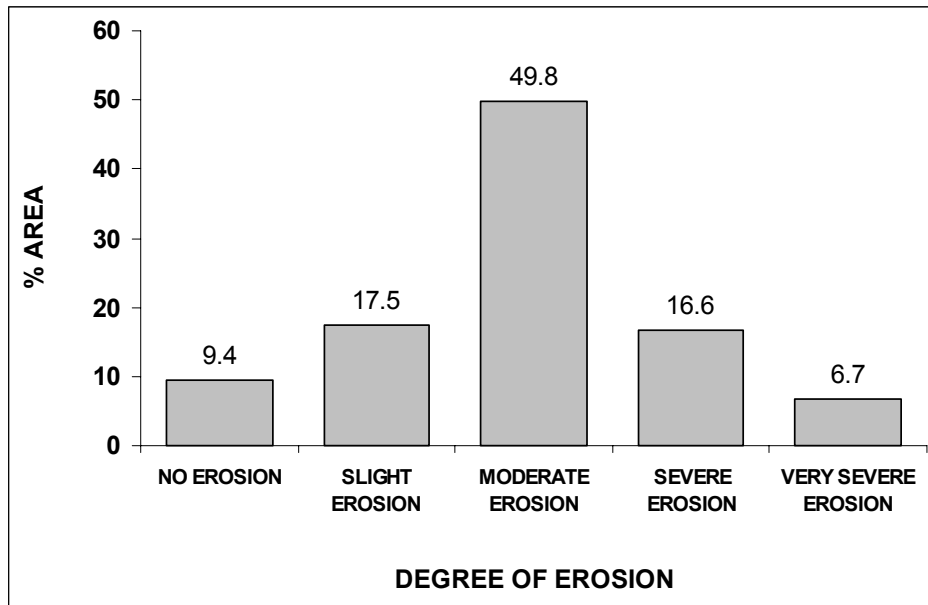


Figure 8.4: Degree of erosion versus percent of area

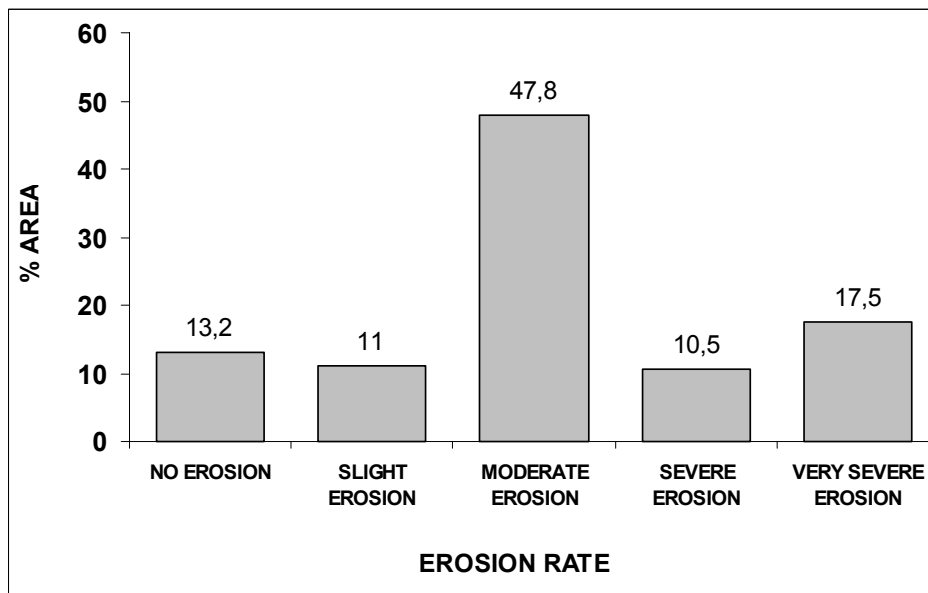


Figure 8.5: Erosion rate classes versus percent area

CHAPTER 9 CONCLUSIONS

9.1. OVERALL CONCLUSIONS

The PESERA Project has made very substantial progress during the third year. In addition to two plenary workshops, held in Leeds, Ispra and Wageningen respectively, one additional workshop is planned to take place in Wageningen to discuss scenario analysis and Project finalisation. Potential end-users and external interested scientists were invited to the plenary meetings. The involvement and cooperation with Syngenta has been very successful and synergetic. The workshops enabled those teams involved in the modelling part of the project to discuss modelling efforts in more detail.

The PESERA Project and approach will continue to play a vital role in several other Projects, notably in MEDRAP, SOWAP, ENRISK, DISMED, COP6 and DESERTLINKS. The PESERA methodology was also presented at the OECD meeting on soil erosion in Rome, at several COST623 action (erosion and global change) workshops held in Brussels, Helsinki, Möncheberg and Budapest, and at the EGS conference in Nice. At these international conferences and meetings, several scientific colleagues and stakeholders were identified and co-operations were established with a number of them to safeguard the future of the Project methodology. The communications held by several members of the PESERA team are now being compiled and transformed in a series of peer-reviewed publications.

9.2. SPECIFIC CONCLUSIONS

9.2.1. WP1: Modelling Strategy

There has been substantial progress in the finalisation of the model code for grid applications and in making the model operational for other partners. ARC GRID is used for visualisation and input manipulation, and FORTRAN for executing the model code

The finalisation of the model code has triggered off numerous model runs at both higher resolutions case studies and at the Pan-European scale. On the basis of the several validation and calibration exercises at different scales, the PESERA model is currently being fine-tuned.

An interface module has been developed, which allows the public open web-access to the model, run it for a window of up to about 100x100 km in a reasonable time, and perform simple land use or climate change scenarios. Fuller assessment of intermediate model components is required, such as water deficits and vegetation cover, to assess intermediate model performance.

The plant growth model was finalised but it was decided not to include it entirely into the PESERA grid version since model runs and memory requirements would be too high to handle. Several components were incorporated in the final grid version of the model: planting dates, the water use efficiency and the refinement of the cover look-up table.

9.2.2. WP2: Spatial and temporal resolution linkages

Synergetic effects of spatial and temporal variation in land attributes on hillslope erosion rates and the implications for the PESERA soil erosion model were further investigated using simulation experiments, carried out with an existing spatially distributed soil erosion model (LISEM) at the Rambla Honda Field Site (SE Spain).

Within the simulated environment, effects of temporal variability in rainfall intensity were much greater than those of spatial variation in vegetation and soil attributes. At the event scale, effects of spatio-temporal variation in land attributes decrease with the amount and intensity of the rainfall, and with slope gradient.

The implications for low-resolution soil erosion models are that ignoring spatial and particularly temporal patterns of land attributes may cause substantial uncertainty in the predictions of soil loss rates, even more pronounced in environments with strongly non-linear relationships between vegetation cover fraction and soil hydrological/erosional properties.

9.2.3. WP3: Calibration and validation at high resolution

The long-term erosion measurement database was used to test the underlying equations to simulate runoff and sediment transport in the PESERA model and to calibrate values for k (erodibility) and h (storage capacity).

A separate database of erosion rate measurements and observations across Europe was compiled on the basis of literature reports and contacts with authors. The 1 km² PESERA map was validated through a visual, numerical and categorical comparison between measured and observed erosion rates. Results show a general underprediction of 52% for observed erosion rates above 1 t.ha⁻¹.yr⁻¹ and an overprediction of 69% for observed erosion rates below 1 t.ha⁻¹.yr⁻¹.

The PESERA point-model was tested at Rambla Honda (11 year record) under natural degraded land cover with plot-specific relief and standard cover table or plot specific cover. The model predictions for long-term runoff and soil loss are in reasonable agreement with observed values. Long-term predictions deviate more from the observed values when plot-specific cover is used. The model seems to undervalue the effect of vegetation cover.

9.2.4. WP4: Validation at low resolution

A regional approach has been developed for validation at low resolutions. The approach differentiates between data quality effects, resolution effects and modelling procedure effects when comparing different map results. Results show an overall underprediction of the PESERA estimates, but good seasonal patterns. The differences in results are attributed to data quality and resolution effects rather than model problems.

The PESERA model was applied for the island of Lesbos using existing data layers for vegetation, soil, and climate at a 250 m by 250 m resolution. Comparison of the PESERA erosion rates map and the degree of soil erosion map estimated from soil surveys data showed a satisfactory result.

9.2.5. WP5: Application at the European scale

The preparation of European wide datasets has been completed. The model input grids have been recalculated with the very latest datasets available.

An algorithm was developed to derive soil water storage capacity in combination with soil depth.

Agricultural land use was spatialised through the coupling of the Farm Structure Survey Census data per harmonised NUTS region and CORINE Land Cover. This enabled the identification of the most dominant arable crops across Europe.

The hybrid system ARC-FORTRAN has been tested for the whole of Europe. Some adaptations are still needed to incorporate the latest land cover and soil water storage databases.

9.2.6. WP6: Scenario analysis

Existing land use change data layers produced by other scientific groups seemed unfit for use within the PESERA context mainly due to lack of detail. Therefore, it was concluded that model runs could be performed under three different land cover scenarios of arable land: (1) worst case scenario (all arable=maize), (2) dominant land use and (3) 2nd dominant land use.

Concerning climate change scenarios, the Hadley Centre has given PESERA access to climate scenario files of HADRM3, a Regional Climate Model (RCM). Time slices available for the HADRM3 scenarios are: 1961-90 (reference conditions), and 2070-99.

9.2.7. WP7: End-user Involvement

A synergetic cooperation with the company Syngenta has been continued.

Documents are regularly uploaded to the PESERA website (<http://pesera.jrc.it>).

The approach and achievements of the PESERA Project were presented and discussed at the MEDRAP workshop in Portugal, at several COST623 (soil erosion and global change) workshops and at international conferences.

The active involvement of the PESERA team with other EU Projects (ENRISK, SOWAP, DesertLinks, MEDRAP) will ensure the use of the PESERA results and methodology beyond the Project's lifetime.

9.3. PERSONNEL, TIMEFRAME AND FINANCES

This section deals with personnel and minor difficulties with regard to timeframe and finances encountered during the reported project period. The majority of the problems have been resolved within the team or solutions have been worked out to face some of the difficulties.

The complexity of the model has required a different coding strategy to be used for the grid-version. Initially a simplified version of the at-a-point Visual Basic code was developed in AML. Numerical iterations, finer temporal analysis and the incorporation of a plant growth model in forecasting mode required the model to be re-coded in FORTRAN to save computer time.

Further simplifications for the grid version of the PESERA Model included the replacement of the plant growth model with a cover look-up table, and making the model user-friendly. Although the current model is performing well, in practical terms it has meant a delay in regional applications to be started.

A further consequence to the complexity of the PESERA model is that a simple Graphic User Interface cannot be developed. Instead a web-based interface has been developed. This web-based application allows the public to access the model on the web, and run it for a window of up to about 100x100 km in a reasonable time. The replacement of the GUI with a web-based application ensures dissemination of the Project methodology and results after funding has ceased.

The EEZA/CSIC budget for equipment included money for purchasing a balloon-borne photography system to obtain data on the spatial structure of plant cover. Since the beginning of the project, high-resolution satellite systems have become available that allow observations over larger areas with less instrumental and technical involvement from the user. The Commission has allowed to change the concept of this expenditure from equipment to consumables.

Personnel-wise, no major changes have taken place. At JRC, Mirco Grimm has left the PESERA team. Anton Van Rompaey is on secondment from LEG-KULeuven to the ESB-JRC. At the University of Leeds, two persons have strengthened the team to help with coding and the web-based interface.

CHAPTER 10 REFERENCES

- Abrahams, A. D., Parsons, A. J. & Luk, S. 1991. The effect of spatial variability in overland flow on the downslope pattern of soil loss on a semiarid hillslope, Southern Arizona. *Catena* 18: 255-270.
- Abrahams, A. D., Parsons, A. J. & Wainwright, J. 1995. Effects of vegetation change on interrill runoff and erosion, Walnut Gulch, southern Arizona. *Geomorphology* 13: 37-48.
- Aguiar, M. R. & Sala, O. E. 1999. Patch structure, dynamics and implications for the functioning of arid ecosystems. *Trends in Ecology & Evolution* 14: 273-277.
- Bergkamp, G. J. J. 1996. Mediterranean Geoecosystems: hierarchical organisation and degradation 1996. Dissertation Laboratory of Physical Geography and Soil Science, University of Amsterdam.
- Beven, K. 1995. Linking parameters across scales: subgrid parameterization and scale dependent hydrological models. *Hydr. Processes* 9: 507-525.
- Beven, K. 2002. Runoff generation in semi-arid areas. In: Bull, L. J. & Kirkby, M. J. (eds.) *Dryland rivers: hydrology and geomorphology of semi-arid channels*, pp. 57-105. John Wiley & Sons, Chichester.
- Blöschl, G. & Sivaplan, M. 1995. Scale issues in hydrological modelling: a review. *Hydr. Processes* 9: 251-290.
- Bochet, E., Rubio, J. L. & Poesen, J. 1999. Modified topsoil islands within patchy Mediterranean vegetation in SE Spain. *Catena* 38: 23-44.
- Boer, M. M. & Puigdefabregas, J. (2003) Effects of spatially-structured vegetation patterns on hillslope erosion rates in semiarid Mediterranean environments: a simulation study. (in review, *Earth Surface Processes and Landforms*).
- Boer, M. M. 1999. Assessment of dryland degradation: linking theory and practice through site water balance modelling. Dissertation Dept. Phys. Geography, Utrecht University, Utrecht, The Netherlands.
- Bolton, J., Smith, J. L. & Link, S. O. 1993. Soil microbial biomass and activity of a disturbed and undisturbed shrub-steppe ecosystem. *Soil Biol. Biochem.* 25: 545-552.
- Boogaard, H.L., Eerens, H.L., Supit, I., Van Diepen, C.A., Piccard, I., Kempeneers, P., 2002. Description of the MARS Crop Yield Forecasting System (MCYFS). METAMP-report 1/3, ALTERRA and VITO, JRC-contract 19226-2002-02-F1FED ISP NL.
- CEC. (1985). Soil Map of the European Communities, 1:1,000,000. CEC Luxembourg, 124pp., 7 maps.
- Cross, A. F. & Schlesinger, W. H. 1999. Plant regulation of soil nutrient distribution in the northern Chihuahuan Desert. *Plant Ecology* 145: 11-25.
- de Ploey, J., Kirkby, M.J. and Ahnert, F., 1991. Hillslope erosion by rainstorms - a magnitude-frequency analysis. *Earth Surface Processes & Landforms* 16, 399-409.
- De Roo, A. P. J., Offermans, R. J. E. & Cremers, N. H. D. T. 1996a. LISEM: a single event physically-based hydrologic and soil erosion model for drainage basins: II. Sensitivity analysis, validation and application. *Hydr. Processes* 10: 1119-1126.
- De Roo, A. P. J., Wesseling, C. G. & Ritsema, C. J. 1996b. LISEM: a single event physically-based hydrologic and soil erosion model for drainage basins: I. Theory, input and output. *Hydr. Processes* 10: 1107-1117.

- Gobin, A. 2002. The Plant Growth Model, Presentation from PESERA Second Annual Meeting.
- Gobin, A., Govers, G. (Eds.), 2002. PESERA, Pan-European Soil Erosion Risk Assessment. Second annual report to the European Commission, 1 April 2001 - 2 April 2002.
- Govers, G. 1990. Empirical relationships on the transporting capacity of overland flow. International Association of Hydrological Sciences Publication 189: 45-63.
- Hadley Centre, 2003. <http://www.met-office.gov.uk/research/hadleycentre/models/modeltypes.html>
- Hall, D.G.M., Reeve, M.J., Thomasson, A.J., Wright, V.F. (1977). Water retention, porosity and density of field soils. Soil Survey Technical Monograph No. 9, Harpenden, UK, 75pp.
- Hargreaves, G. H. & Samani, Z. A. 1982. Estimating potential evapotranspiration. ASCE Journal of Irrigation and Drainage 108: 225-230.
- Hostetler, S.W. (1994): Hydrologic and atmospheric models: the (continuing) problem of discordant scales. Climate Change 7, pp. 85-95.
- IPCC, 2003. The Intergovernmental Panel on Climate Change (IPCC). Source: <http://ipcc-ddc.cru.uea.ac.uk/asres/a1/SRESA1background.html>
- Jetten, V. LISEM - Limburg Soil Erosion Model. User manual for Windows version 2.x. 1-64. 2002. Utrecht, The Netherlands, Utrecht Centre for Environment and Landscape Dynamics, Utrecht University.
- Jones, R., Grimm, M. and Montanarella, L. 2002. Soil Water Storage Capacity for input to the PESERA Soil Erosion Model, Technical Report, JRC Ispra.
- Jones, R.J.A., Spoor, G. and Thomasson, A.J. (2003). Vulnerability of subsoils in Europe to compaction: a preliminary Soil & Tillage Research [In press]
- Jones, R.J.A., Zdruli, P. and Montanarella, L. (2000). The estimation of drought risk in Europe from soil and climatic data. In: Drought and Drought Mitigation in Europe. J.V. Vogt and F. Somma (eds.): 133-146. Kluwer Academic Publishers. the Netherlands.
- Kirkby, M. J., Imeson, A. C., Bergkamp, G. J. J. & Cammeraat, L. H. 1996. Scaling up processes and models from the field plot to the watershed and regional areas. Journal of Soil and Water Conservation 391-396.
- Kirkby, M.J. and Cox, N.J. 1995. A climatic index for soil erosion potential (CSEP) including seasonal and vegetation factors. Catena 25, 333-52.
- Kirkby, M.J. and Neale, R.H., 1987. A soil erosion model incorporating seasonal factors. International geomorphology, II, John Wiley, 289-210.
- Kirkby, M.J., Le Bissonais, Y., Coulthard, T.J., Daroussin, J. and McMahon, M.D., 2000. The development of Land Quality Indicators for Soil Degradation by Water Erosion. Agriculture, Ecosystems and Environment.
- Kosmas, C., Yassoglou, N., Karavitis, C., Gerontidis, S., Briasouli, H., Mizara, A., 1999. Mediterranean Desertification and Land Use- MEDALUS III final report, Target Areas. Commission of the European Communities, Contract Number ENV4-CT95-0119, pp. 479 - 528.
- Musgrave, G.W., 1947. Quantitative evaluation of factors in water erosion- a first approximation. Journal of Soil and Water Conservation 2, 133-38.
- Nicolau, J. M., Solé-Benet, A., Puigdefábregas, J. & Gutiérrez, L. 1996. Effects of soil and vegetation on runoff along a catena in semi-arid Spain. Geomorphology 14: 297-309.
- Pebesma, E. J. GSTAT user's manual, version 2.3.3. [2.0]. 2001. Utrecht, Dept. of Physical Geography, Utrecht University.

- PESERA, 1999. Final version of the Technical Annex of the Pan-European Soil Erosion Risk Assessment Project (5th framework Project QLRT-1999-1323 / Key Action n° 1.1.1.-5.4.).
- Puigdefábregas, J. & Sanchez, G. 1996. Geomorphological implications of vegetation patchiness on semi-arid slopes. In: Anderson, M. G. & Brooks, S. M. (eds.) *Advances in hillslope processes*, pp. 1027-1060. John Wiley & Sons Ltd., Chichester.
- Puigdefábregas, J., Alonso, J. M., Delgado, L., Domingo, F., Cueto, M., Gutiérrez, L., Lázaro, R., Nicolau, J. M., Sánchez, G., Solé, A. & Vidal, S. 1996. The Rambla Honda field site: interactions of soil and vegetation along a catena in semi-arid Spain. In: Brandt, J. & Thornes, J. B. (eds.) *Mediterranean desertification and land use*, pp. 137-168. John Wiley & Sons, Ltd., Chichester.
- Puigdefábregas, J., Del Barrio, G., Boer, M. M., Gutiérrez, L. & Solé, A. 1998. Differential responses of hillslope elements to rainfall events in a semi-arid area. *Geomorphology* 23: 337-351.
- Puigdefábregas, J., Solé, A., Gutiérrez, L., Del Barrio, G. & Boer, M. M. 1999. Scales and processes of water and sediment redistribution in drylands: results from the Rambla Honda field site in Southeast Spain. *Earth Science Reviews* 48: 39-70.
- Renard, K.G., G.R. Foster, G.A. Weesies and J.P. Porter (1991). RUSLE: Revised Universal Soil Loss Equation. *J. Soil and Water Conservation* 46(1):30-33.
- Renard, K.G., G.R. Foster, G.A. Weesies, D.K. McCool and D.C. Yoder, coordinators (1997). *Predicting Soil Erosion by Water: A Guide to Conservation Planning with the Revised Soil Loss Equation (RUSLE)*. U.S. Dept. of Agriculture, Agric. Handbook No. 703, 404 pp.
- Sanchez, G. 1995. *Arquitectura y dinámica de las matas de esparto (Stipa tenacissima L.), efectos en el medio e interacciones con la erosión*. Dissertation Universidad Autónoma de Madrid, Spain.
- Thomasson A.J. (1995). Assessment of soil water reserves available for plants (SWAP): a review. In: *European Land Information Systems for Agro-environmental Monitoring*. D. King, R.J.A. Jones and A.J. Thomasson (Eds.). EUR 16232 EN (1995) 115-130. Office for Official Publications of the European Communities, Luxembourg.
- Van Orshoven, J., Terres, J.-M., Willekens, A., Feyen, J., 1999. Transfer procedures for model-based agricultural monitoring. Symposium organised by the European Society of Agronomy regarding "Modelling Cropping Systems". Lleida, June 21-23, 1999: 2p.
- Van Ranst, E., Thomasson, A.J., Daroussin, J., Hollis, J.M., Jones, R.J.A., Jamagne, M., King, D., Vanmechelen, L., (1995). Elaboration of an extended knowledge database to interpret the 1:1,000,000 EU Soil Map for environmental purposes. In: . King, D., Jones, R.J.A. and Thomasson, A.J., (Eds). *European Land Information Systems for Agro-environmental Monitoring*, EUR 16232 EN, Office for Official Publications of the European Communities, Luxembourg, pp.71-84.
- Virginia, R. A. & Jarrell, W. M. 1983. Soil properties in a Mesquite-dominated Sonoran Desert ecosystem. *Soil Sci. Soc. Am. J.* 47: 138-144.
- Wezel, A., Rajot, J.-L. & Herbrig, C. 2000. Influence of shrubs on soil characteristics and their function in Sahelian agro-ecosystems in semi-arid Niger. *J. Arid Env.* 44: 383-398.

11.2. DATA REQUIREMENTS FOR THE PESERA/RDI MODEL (*VER. EROS022/PESERA-GRID023*)

INPUT is required for each cell.

Model Parameter	Range of values	Units	Source	Description/Source
Erod	(0-10) x 0.00011	-		Erodibility
Crust	0-12(100)	mm		Crust storage
soil_stor	24-109	mm	SOIL DB	Soil storage
Zm	5,10,15,20,30	mm	SOIL DB	Scale depth (TOPMODEL)
rough0	0,5,10	mm	USE/COVER	Initial surface storage
rough_red	0,50	%	USE/COVER	Surface roughness reduction per month
rootdepth	5,30,50,100	mm	USE/COVER	
Wue	0-1		USE/COVER	Water use efficiency (Currently set at 1.0. Data desirable)
Use	-	-	USE/COVER	Land cover type/management option
cov_	0-100	%	USE/COVER	Initial ground cover
std_eudem2	-	m	DEM	Standard deviation of elevation for all points within 1.5 km radius
meanrf130_	-	mm	CLIMATE	Mean monthly rainfall
meanrf2_	-	mm	CLIMATE	Mean monthly rainfall per rain day
cvrf2_	-		CLIMATE	Monthly standard deviation of rainfall per rain day.
mtmean_	-	°C	CLIMATE	Mean monthly temperature
mtrange_	-	°C	CLIMATE	Monthly temperature range (max – min)
meanpet30_	-	mm	CLIMATE	Mean monthly PET
veg_erod	0.5 x 0.00011	-	SOIL DB	Reduced erodibility due to cover
Iplant%	-	-	COVER	Planting data
iharv%	-	-	COVER	Harvesting date

SOIL DB: derived from soil mapping units, interpreted as textural data (e.g. from European Soils Data Base or Equivalent), and converted to parameter values using pedo-transfer rules. Additional information for some soil profiles, including moisture properties, is also desirable.

COVER: derived from land cover type (e.g. CORINE) and/or from remote sensing data (e.g. AVHRR or Vegetation). Best results where both data sources are available.

DEM: Currently using Gtopo30, available from EROS data base in USA, at approximately 1km resolution. Better data bases will be available in the future, and it would be preferable to use 250 m or 100 m resolution data

CLIMATE: Currently using the JRC MARS data base, which is interpolated data at 50 km resolution, although the poor spatial resolution of this data is the most critical shortcoming of the model. Preferred data consists of daily values over up to 50 years of record, for individual stations. A high density of actual rainfall station data is particularly important.

11.3. RUNNING MODULAR COMPONENTS OF PESERA-RDI_GRID

When operating on large grids, large volumes of data are generated. (Figures quoted are for the European grid)

Create a new workspace d:\meteo_grids and extract annual and stationary grids from pesera_grids.zip (93no') (Table 1) **(3.5GB unzipped)**

Create a further workspace d:\temp_ascii and extract perera_grid023_b.zip to d:\temp_ascii

11.3.1. EXTRACTING

The aml file xgridascii023_b.aml can be edited to select different areas of interest windows. Current default is to Europe but can be readily changed.

To run xgridascii023_b.aml

open arc GRID, set workspace as d:\meteo_grids

ArcGIS > ArcInfo Workstations > Grid

At the GRID: prompt set workspace

GRID: arc w d:\meteo_grids

Run xgridascii.aml

GRID: &run d:\temp_ascii\xgridascii023_b.aml

Ascii files will be extracted to d:\temp_ascii (**6GB**)

11.3.2. PREPROCESSING

‘nrows’ and ‘ncols’ must be known before executing the preprocessing unit, this can be verified from the header files from the extracted grids. Grids can be opened in excell or wordpad.

(Europe: ‘nrows’ = 2724 and ‘ncols’ = 3199)

Currently ‘nrow’ max is 4000 and ‘ncol’ max is 3200.

To run ftn_combined_023a.exe

Ensure salflibc.dll file and executable are available at d:\temp_ascii

Double click on ftn_combined_023a.exe. (reformats data + **12GB**)

Enter data requested, ‘nrows’ and ‘ncol’. Program runs from 1 to 93

Double click on ftn_combined_023b.exe. (compiles data into grid_data.dat +**12GB**) **Do not delete 2use.dat this is used as a template.** Program runs from 1 to (‘nrows’ x ‘ncols’)

Enter data requested, ‘nrows’ and ‘ncol’

11.3.3. PESERA_GRID

‘nrows’ and ‘ncols’ must be known before executing the PESERA code.

To run pesera_grid023.exe

Ensure salflibc.dll file and executable are available at d:\temp_ascii

Double click pesera_grid023_a.exe. Enter data requested, ‘nrows’ and ‘ncol’

11.3.4. POST-PROCESSING

Double click to _grid_023a.exe. Enter data requested, ‘nrows’ and ‘ncol’

Double click to _grid_023b.exe.

Enter data requested, ‘nrows’, ‘ncol’, ‘cellsize’, ‘xll’ and ‘yll’

Ensure file 2use.dat remains available

(Europe: ‘xll’ = -1594713.25 and ‘yll’ = -1312168.125)

(‘cellsize’ = 1000)

11.4. OUTPUT GRIDS

open arc GRID, set workspace as d:\temp_ascii

GRID: arc w d:\temp_ascii

Run xasciigrid023_b.aml

GRID: &run xasciigrid023_b.aml

sedi_jan to sedi_dec (12no) + (sedi_tot) can be viewed in ArcMap.

Ensure projection files are defined.

When operating on large grids large volumes of data are generated.

Annual data files (7 no')

Monthly Source data GRIDS (annual data derived from monthly data)	Source
cvrf21 to cvrf212	INRA data
meanpet301 to meanpet3012*	INRA data (x no' days in month)
meanrf1301 to meanrf13012*	INRA data (x no' days in month)
meanrf21 to meanrf212	INRA data
mtmean1 to mtmean12	INRA data
mtrange1 to mtrange12	INRA data
cov_jan to cov_dec*	Land cover

(initial cover derived from land-use and assumed cultivation)

Stationary data files (9 no')

Source data GRIDS	Source
crusting	INRA data
erodibility	INRA data
rootdepth	Land cover
rough0	Land cover
rough_red	Land cover
soil_stor	texture
Std_eudem2	INRA data
Use	INRA data
Zm	texture

The above data is for the current model, additional parameters maybe added.

CHAPTER 12 APPENDIX 2 – DESCRIPTION OF EUROPEAN WIDE DATASETS

This appendix provides a description of European wide data sets to serve as input to the final version of the PESERA model.

Spatial resolution and registration: all data layers to be produced at 1x1 Km grid cells registered to the Land use data source.

Spatial extent: list of countries for which all data layers are available

Projection system: GISCO standard for the EU

Data sources:

Land use	CORINE Land Cover, 250 m raster, MARS database, SAI/JRC Ispra
Relief	GTOPO30 30 arc seconds DEM (~1 Km), USGS HYDRO1K database, except France: 250 m DEM, Institut Géographique National, and Italy: 250 m DEM, source
Meteorology	50 km grid daily meteorological database for 25 years, MARS database, SAI/JRC Ispra
Soil	Soil Geographical Database of Eurasia at scale 1:1,000,000, European Soil Bureau, SAI/JRC Ispra

Data layers and methods of production:

Software: ESRI ArcInfo, and ESRI ArcInfo Grid module.

12.1. GENERAL

Grid MASK

Description: area of interest.

Method: determine area with available data from all data sources.

Coverage COUNTRY

Description: country boundaries.

12.2. RELIEF PARAMETERS

Grid ALT

Description: altitude (in meters).

Method:

1. Project GTOPO30 and DEMs for France and Italy to GISCO standard projection system and resample to 1 Km resolution with bilinear interpolation.
2. Then for each 1 Km cell that is covered by a 250 m resolution DEM (France and Italy), compute a mean altitude from the underlying 250 m altitudes and replace the GTOPO30 cell value.

Grid SLOPE

Description: slope intensity (in percentage).

Method: ALT → slope function → SLOPE

Grid STD_EUDEM2

Description: 3x3 Km window relief index (in meters).

Method: ALT → focal standard deviation within 3x3 Km moving window → STD_EUDEM2

12.3. METEOROLOGICAL PARAMETERS

The SPLINE TENSION method for interpolating from 50 Km spaced points of the MARS meteo database to 1 Km grid cells was chosen (see elements for making this choice in Appendix 1).

For temperature parameters only, the following corrective factor for altitude was chosen:

Each 50 Km grid cell of the MARS meteorological database is provided with its altitude.

Interpolate that altitude to a 1 Km resolution raster using the same method as for meteorological parameters.

For each 1 Km cell compute the difference between that interpolated altitude and the corresponding altitude from grid ALT here considered as a reference.

For each 1 Km cell compute the temperature correction as ± 0.6 °C per 100 m in altitude difference.

For each 1 Km cell apply this correction to temperature parameters MEANTMIN, MEANTMAX, MEANT

Grids NBDATA1 to NBDATA12

Description: total number of days of available data per month.

Method: count of days with available data in the month over all years.

This applies to MEANPET, MEANRF1, MEANT, MEANTRANGE, MEANTMIN, MEANTMAX and NBRZ with no care about days with incoherent temperature data (where MINIMUM_TEMPERATURE > MAXIMUM_TEMPERATURE).

Grids MEANPET1 to MEANPET12

Description: mean per month of daily potential evapotranspiration (in mm).

Method:

1. (sum of available daily PETs in the month over all years) / NBDATA
2. Then interpolate to 1 Km.

Grids MEANRF11 to MEANRF112

Description: mean per month of daily rainfall (in mm).

Method:

1. (sum of available daily RFs in the month over all years) / NBDATA
2. Then interpolate to 1 Km.

Grids MEANTMIN1 to MEANTMIN12

Description: mean per month of minimum temperature (in °C).

Method:

1. (sum of available daily MINIMUM_TEMPERATUREs in the month over all years) / NBDATA
2. Then interpolate to 1 Km.
3. Then apply correction for altitude.

Grids MEANTMAX1 to MEANTMAX12

Description: mean per month of maximum temperature (in °C).

Method:

1. (sum of available daily MAXIMUM_TEMPERATUREs in the month over all years) / NBDATA
2. Then interpolate to 1 Km.
3. Then apply correction for altitude.

Grids MEANTRANGE1 to MEANTRANGE12

Description: mean per month of daily temperature range (in °C).

Method:

1. Compute daily TRANGE = MAX_TEMPERATURE - MIN_TEMPERATURE
2. Then compute MEANTRANGE from TRANGE as (sum of available daily TRANGEs in the month over all years) / NBDATA
3. Then interpolate to 1 Km.

Grids MEANT1 to MEANT12

Description: mean per month of daily temperature (in °C).

Method:

1. Compute daily TEMPERATURE = (MAX_TEMP + MIN_TEMP) / 2
2. Then compute MEANT from TEMPERATURE as (sum of available daily TEMPERATUREs in the month over all years) / NBDATA
3. Then interpolate to 1 Km.
4. Then apply correction for altitude.

Grids NBFRZ1 to NBFRZ12

Description: total number of days below freezing per month.

Method:

1. Count of days with TEMPERATURE < 0 in the month over all years.

Recall that $TEMPERATURE = (MAXIMUM_TEMPERATURE + MINIMUM_TEMPERATURE) / 2$

2. Then interpolate to 1 Km.

Grids NBPROPFRZ1 to NBPROPFRZ12

Description: total number of days of available data per month where minimum_temperature <= maximum_temperature.

Method:

count of days with available and coherent min-max temperature data in the month over all years used for MEANPROPFRZ calculation:

1. Compute PROPFRZ

= proportion of the day with a temperature bellow freezing

= if MAX < 0 then

PROPFRZ = 1

else if MIN > 0 then

PROPFRZ = 0

else if (MAX + MIN) = 0

PROPFRZ = 0.5

else /* i.e. MAX >= 0 >= MIN and (MAX + MIN) <> 0 */

PROPFRZ = 1 - 1 / pi * atan(sqrt(-MAX * MIN) / (MAX + MIN))

with the arc tangent interpreted to give an angle in the range 0 to pi.

NB: records with (minimum_temperature > maximum_temperature) are excluded.

2. Then compute NBPROPFRZ and MEANPROPFRZ

3. Then interpolate to 1 Km.

Grids MEANPROPFRZ1 to MEANPROPFRZ12

Description: mean per month of the proportion of the day with a temperature bellow freezing.

Method:

1. (sum of available daily PROPFRZs in the month over all years) / NBPROPFRZ

2. Then interpolate to 1 Km.

Grids NBRF21 to NBRF212

Description: total number of rain days per month.

Method:

1. Count of days with RF (rainfall) > 0 in the month over all years.

2. Then interpolate to 1 Km.

Grids MEANRF21 to MEANRF212

Description: mean per month of rainfall per rain day (in mm).

Method:

1. (sum of available daily RFs > 0 in the month over all years) / NBRF2

2. Then interpolate to 1 Km.

Grids STDRF21 to STDRF212

Description: standard deviation per month of rainfall per rain day (in mm).

Method:

1. Standard deviation of available daily RFs > 0 in the month over all years.
2. Then interpolate to 1 Km.

12.4. SOIL PARAMETERS

Grid CRUSTING

Description: soil sensitivity to surface crusting index.

Method:

1. Apply Pedotransfer Rules to infer the crusting class of each Soil Typological Unit (STU) in the Soil Geographical Database of Europe at scale 1:1,000,000 from its FAO74-CEC85 soil name, surface textural class and parent material.
2. Then compute the crusting index for each Soil Mapping Unit (SMU) as the average of all composing STUs crusting class weighted by their respective within SMU proportion.
3. Then rasterise.

Grid ERODIBILITY

Description: soil sensitivity to erodibility index.

Method:

1. Apply Pedotransfer Rules to infer the erodibility class of each Soil Typological Unit (STU) in the Soil Geographical Database of Europe at scale 1:1,000,000 from its FAO74-CEC85 soil name, surface textural class and parent material.
2. Then compute the erodibility index for each Soil Mapping Unit (SMU) as the average of all composing STUs erodibility class weighted by their respective within SMU proportion.
3. Then rasterise.

Grid ROO

Description: depth class of an obstacle to roots.

Method:

1. Compute the depth class for each Soil Mapping Unit (SMU) as the dominant depth class from all composing STUs according to their respective within SMU proportion.
2. Then rasterise.

12.5. WATER CONTENT:

See appendix 4 on water content

The following parameters are available:

Water content at saturation (reservoir is full)

Drainable pore storage (DPS) in mm??? (grid SOIL_STOR???)

Water content at field capacity (after 48 hours, all the water that was in the drainable pores has flown out by gravity)

Available water capacity for plants (AWC)

Water content at wilting point

12.6. LAND COVER PARAMETERS

Grid USE

Description: land cover classes.

Method:

1. Re-class CORINE land cover classification according to following table:

CORINE land cover classification		PESERA land cover classification	
Code	Description	Code	Description
111	Continuous urban fabric	100	Artificial land
112	Discontinuous urban fabric	100	Artificial land
121	Industrial or commercial units	100	Artificial land
122	Road and rail networks and associated land	100	Artificial land
123	Port Areas	100	Artificial land
124	Airports	100	Artificial land
131	Mineral extraction sites	100	Artificial land
132	Dump sites	100	Artificial land
133	Construction sites	100	Artificial land
141	Green urban areas	100	Artificial land
142	Sport and leisure facilities	100	Artificial land
211	Non-irrigated arable land	210	Arable land
212	Permanently irrigated land	210	Arable land
213	Rice fields	400	Water surfaces and wetland
221	Vineyards	221	Vineyards
222	Fruit trees and berry plantations	222	Fruit trees and berry plantations
223	Olive groves	223	Olive groves
231	Pastures	231	Pastures and grassland
241	Annual crops associated with permanent crops	240	Heterogeneous agricultural land
242	Complex cultivation patterns	240	Heterogeneous agricultural land
243	Land principally occupied by agriculture, with significant areas of natural vegetation	240	Heterogeneous agricultural land
244	Agro-forestry areas	240	Heterogeneous agricultural land
311	Broad-leaved forest	310	Forest
312	Coniferous forest	310	Forest
313	Mixed forest	310	Forest
321	Natural grassland	231	Pastures and grassland
322	Moors and heathland	310	Forest
323	Sclerophyllous vegetation	320	Scrub
324	Transitional woodland-scrub	320	Scrub
331	Beaches, dunes, sands	330	Bare land
332	Bare rocks	330	Bare land

333	Sparsely vegetated areas	334	Degraded natural land
334	Burnt areas	334	Degraded natural land
335	Glaciers and perpetual snow	330	Bare land
411	Inland marshes	400	Water surfaces and wetland
412	Peat bogs	400	Water surfaces and wetland
421	Salt marshes	400	Water surfaces and wetland
422	Salines	400	Water surfaces and wetland
423	Intertidal flats	400	Water surfaces and wetland
511	Water courses	400	Water surfaces and wetland
512	Water bodies	400	Water surfaces and wetland
521	Coastal lagoons	400	Water surfaces and wetland
522	Estuaries	400	Water surfaces and wetland
523	Sea and ocean	400	Water surfaces and wetland

2. Then change resolution of raster to 1 Km by keeping dominant value.

CHAPTER 13 APPENDIX 3 – FARM STRUCTURE SURVEY

13.1. SPATIAL LINK OF FARM STRUCTURE SURVEY (FSS) DATA

The nomenclature of territorial units for statistics (NUTS) serves as a base map of regional boundaries covering the entire EU territory. The nomenclature subdivides the EU economic territory into 6 administrative levels, from country (level 0), through regional (level 1,2,3) to local (level 4,5) level. At present, 3 versions (V5, V6 and V7) for three scale ranges (1M, 3M and 10M) are maintained at GISCO.

The NUTS provide the means to spatially present agricultural statistical survey and census data. The Farm Structure Survey (FSS), Farm Accountancy Data Network (FADN) and agricultural statistics data cover all member states and include information of crop type and area, farm size, farming income, crop yields, livestock type and number at the NUTS 2 and 3 levels. Trends in livestock numbers and composition, crop areas and farm produce can be related to the corresponding product prices at the NUTS 2 level. The latest available datasets are from 2000 for FSS.

13.2. CLASSIFICATION

Areal data are collected in ha and concern the principal following classes: arable land (D), kitchen gardens (E), meadows and pasture (F), permanent crops (G), others (e.g. wood, roads, buildings,...) (H). The holding or Agricultural Area (AA) is the sum of D+E+F+G areas, and the total area of the holding is the sum of AA + H area. Besides this, in the category I irrigated arable areas, area under glass, comprising successive crops as well as the annual crops associated with the permanent crops are entered. More details are given in the Table 13.1.

Table 13.1: FSS Classification of agricultural land use.

Code	Principal FSS Class	Code	Level 2 FSS Class
D	Cereals	D1	wheat and spelt
		D2	durum wheat
		D3	rye
		D4	barley
		D5	oats
		D6	grain maize
		D7	rice
		D8	other cereals
	Dried vegetables	D9a	pure crops for fodder
		D9b	others

	Root crops	D10	potatoes
		D11	sugar beets
		D12	fodder roots and brassicas
	Industrial plants	D13a	tobacco
		D13b	hops
		D13c	cotton
		D13d	Oilseeds
	fresh vegetables, melons, strawberries	D14	outdoor
		D15	under greenhouse
	Flowers and ornamental plants	D16	outdoor
		D17	under greenhouse
	Forage plants	D18a	temporary grass
		D18b	other forage plants
	Other crops of arable land	D19	arable land seeds and seedlings
		D20	other arable land crops
		D21	fallow land
E	Kitchen gardens	E	Kitchen gardens
F	Permanent pastures and meadows	F	Permanent pastures and meadows
G	Permanent crops	G/01	fruit and berry plantations
		G/02	citrus plantations
		G/03	olive plantations
		G/04	vineyards
		G/05	nurseries
		G/06	other permanent crops
		G/07	permanent crops under glass
H	Unutilised agricultural land	H/01 & H/03	unused Agricultural Area
		H/02	woodland
I	Successive secondary crops	I/01	successive secondary crops
		I/02	mushrooms
		I/03	irrigable and irrigated area ground area covered by greenhouses in use
		I/04	use
		I/05	combined crops

CHAPTER 14 APPENDIX 4 - WATER CONTENT LAYERS

The following sections list the parameters included in the SWSC database.

Stu Soil typological unit number: Identifier of Soil Typological Unit

Awc_top Topsoil Available Water Capacity obtained by applying the pedotransfer rule 551 (old version), where:

Code	Class	Awc_top
L	Low	< 100 mm/m
M	Medium	100 – 140 mm/m
H	High	140 – 190 mm/m
VH	Very High	> 190 mm/m
#		No data or not applicable

Awc_sub Subsoil Available Water Capacity obtained by applying the pedotransfer rule 553 (old version), where:

Code	Class	Awc_top
VL	Ver Low	~ 0 mm/m
L	Low	< 100 mm/m
M	Medium	100 – 140 mm/m
H	High	140 – 190 mm/m
VH	Very High	> 190 mm/m
#		No data or not applicable

Soil Full 1974 (modified CEC 1985) FAO-Unesco legend name

TEXT_SRF_D Dominant surface textural class

TEXT_SUB_D Dominant sub-surface textural class

Where:

1	Coarse (clay < 18% and sand > 65%)
2	Medium (18% < clay < 35% and sand > 15%, or clay < 18% and 15% < sand < 65%)
3	Medium fine (clay < 35% and sand < 15%)
4	Fine (35 % < clay < 60 %)
5	Very fine (clay > 60%)
9	No texture (histosols,...)
0	No information

Text Pedotransfer rule 1: Dominant surface textural class (completed from dominant STU).

Td Dominant sub-surface textural class (Pedotransfer rule 421)

Where:

1	Coarse (clay < 18% and sand > 65%)
2	Medium (18% < clay < 35% and sand > 15%, or clay < 18% and 15% < sand < 65%)
3	Medium fine (clay < 35% and sand < 15%)
4	Fine (35 % < clay < 60 %)
5	Very fine (clay > 60%)
9	No texture (histosols,...)
0	No information

The output from the pedotransfer rule for TEXT, for version 4.0 SGDBE, has been modified to include the following texture codes:

7	No texture (because of rock outcrop)
8	No texture (because of organic layer)
6	No texture (other cases)

Dr Depth to rock (pedotransfer rule)

Where:

Class	Depth
S(hallow)	0-40 cm
M(oderate)	40-80 cm
D(eep)	80-120 cm
V(ery) D(eep)	>120 cm

Dr_rest restriction of soil depth by depth to rock (Dr)

Dr code	Dr (classes in cm)	Dr_rest (Restriction in cm)
S(hallow)	0-40	30
M(oderate)	40-80	60
D(eep)	80-120	100
V(ery) D(eep)	>120	200

Where FAO85_FULL= “222” [urban], “444” [water], “555”[glacier] or “666” [rock outcrop], then Dr_rest = 0

Dr_rest_10 In cases where Dr_rest = 200 cm Dr_rest was set to 100 cm, whereas other depths remained as in Dr_rest.

Dr code	Dr_rest (Restriction in cm)	Dr_res_10t (Restriction in cm)
S(hallow)	30	30
M(oderate)	60	60
D(eep)	100	100
V(ery) D(eep)	200	100

Ro_o Depth class of an obstacle to roots

Where:

Code	Description
0	No information
1	No obstacle to roots between 0 and 80 cm
2	Obstacle to roots between 60 and 80 cm depth
3	Obstacle to roots between 40 and 60 cm depth
4	Obstacle to roots between 20 and 40 cm depth
5	Obstacle to roots between 0 and 80 cm depth

Pd_{top} Topsoil Packing density

Pd_{sub} Subsoil Packing density

Where:

Class	PD
L(ow)	1.4 g/cm ³
M(edium)	1.4 – 1.75 g/cm ³
H(igh)	> 1.75 g/cm ³

14.1. NEW CALCULATIONS

Textawctop Dominant surface textural classes that are used as Input data for calculating the Topsoil Available Water Capacity

Textawcsub Dominant sub-surface textural classes that are used as Input data for calculating the Subsoil Available Water Capacity

Where:

1	Coarse (clay < 18% and sand > 65%)
2	Medium (18% < clay < 35% and sand > 15%, or clay < 18% and 15% < sand < 65%)
3	Medium fine (clay < 35% and sand < 15%)
4	Fine (35 % < clay < 60 %)
5	Very fine (clay > 60%)
6	No texture (other cases)
8	No texture(because of organic layer)
9	No texture (histosols,...)
0	No information

Where **Text** = 8 [No texture(because of organic layer)] then **Textawctop** = 0

Txawtporig Sources of the data given in **Textawctop**

Where:

Text	Pedotransfer rule 1: Dominant surface textural class
Expert judgement	Expert judgement done mainly using information out of Soil
No texture	No information

Txawsborig Sources of the data given in Textawcsub

Where:

TEXT_SUB_D	Dominant sub-surface textural class
TD	Pedotransfer rule 421: Rule inferred subsoil texture
TEXT_SRF_D	Dominant surface textural class
Text	Pedotransfer rule 1: Dominant surface textural class
Expert judgement	Expert judgement done mainly using information out of Soil
No texture	No information

Awc_top2s, Awc_top2mm

Topsoil Available Water Capacity in mm/m (new version)

Awc_top_2 was derived using the input data Text (Pedotransfer rule 1: Dominant surface textural class) and topsoil packing density (Pd_top) following the pedotransfer rule 551. For STU's with no **Text**, an expert judgement for the texture was made based on **Soil**.

The results are presented in character form in **Awc_top_2s** and in numeric form in **Awc_top_2** mm (in mm/m)

Where:

String	Number
VL (Very Low)	20mm/m
L (Low)	60mm/m
M (Medium)	120mm/m
H (High)	165mm/m
VH (Very High)	220mm/m
XH (Extremely High)	300mm/m
# (No information)	-999

Awc_sub2s and Awc_sub2mm

Subsoil Available Water Capacity mm/m (new vers)

The Subsoil Available Water Capacity was derived using the input data texture and subsoil packing density (**Pd_sub**) and applying the pedotransfer rule shown in the table. Whereas for the packing density of the subsoil just one input data was used (**Pd_sub**) for the texture of the subsoil different Input data had to be used due to the fact that dominant sub-surface textural class (Td1) doesn't cover all STU's. Therefore in a sequence data were used one after the other trying to cover as many STU's as possible. The sequence is the following:

No.	Parameter	Description
1	TEXT SUB D	Dominant sub-surface textural class
2	Td	Dominant sub-surface textural class (Pedotransfer rule 421)
3	TEXT SRF D	Dominant surface textural class
4	Text	Dominant surface textural class (Pedotransfer rule 1)

For a number of soils, TD1 has been given coded '9' (= No texture (histosols,)) whereas the dominant surface textural class (Text1) has a class of 1 until 5. This was assumed to be an error and in such cases, the value of Td was used instead of Td1. It is possible that some contributors to the database used the code '9' for no information instead of '0'.

Where neither Td1 nor Td is available, it was assumed that the texture for the topsoil and subsoil are the same and Text1 and Text were used.

For the STU’s where the sub-surface textural class is not specified, expert judgement was used to derive it from **Soil**.

The new sub-surface textural classes that are used for applying the pedotransfer rule (Table) are given in the column **TextAWCsub** with the source of the data given in **TxAWsbOrig**.

14.2. AWC_SUB2 DERIVED FROM TEXTURE AND SUBSOIL PACKING DENSITY

Texture (TextAWCsub)	Texture class	Pd_sub		
		L	M	H
		Low	Medium	High
1	Coarse	M	L	L
2	Medium	VH	H	M
3	Medium fine	VH	VH	M
4	Fine	VH	H	M
5	Very fine	VH	H	M
9	No texture (histosols,...)	XH	XH	N/A
0	No information	#	#	#

The results of the applied pedotransfer rule (table above) are given in the column Awc_sub2s (as char string) and Awc_sub2mm (in mm/m).

Where:

String	Number
VL (Very Low)	20mm/m
L (Low)	60mm/m
M (Medium)	120mm/m
H (High)	165mm/m
VH (Very High)	220mm/m
XH (Extremely High)	300mm/m
# (No information)	-999

Swap_top Soil Water Available to Plants in the topsoil (0 - 30 cm) in mm

For the calculation of Swap_top it was assumed that there is no restriction within 30 cm depth. The calculation was made as follows, and ‘-999’ indicates no information:

$$\text{Swap_top} = 0.3(\text{Awc_top2mm})$$

Swap_sub Soil Water Available to Plants in the subsoil (30 – 100 cm) in mm

For the calculation of **Swap_sub** soil depth was assumed to be 100 cm, with no restriction to rooting between 30 and 100 cm depth:

$$\text{Swap_sub} = 0.7(\text{Awc_sub2mm})$$

For no information **Swap_sub** = -999.

Swap_sub_r Soil Water Available to Plants in the subsoil (30 – 100 cm) in mm including restriction of soil depth by depth to rock (Dr), is calculated as follows:

$$\text{Swap_sub_r} = (\text{Awc_sub2mm})(\text{Dr_rest}_{10} - 30)/100$$

Where $\text{Dr_rest} = 200$ cm, the soil depth for calculating **Swap_sub_r** is set to 100 cm and the result is in mm. ‘-999’ indicates no information.

Swap_tot Soil Water Available to Plants in the top- and subsoil (0 – 100 cm) in mm

Swap_tot_r Soil Water Available to Plants in the top and subsoil (0 – 100 cm) in mm including restriction of soil depth by depth to rock (Dr)

The calculations were made as follows:

$$\text{Swap_tot} = \text{Swap_top} + \text{Swap_sub}$$

$$\text{Swap_tot_r} = \text{Swap_top} + \text{Swap_sub_r}$$

The results are shown in mm for the depth of 0 – 100cm of soil. A value ‘-999’ indicates no information.

Po_top_% Drainable Pore Space of topsoil (0 – 30 cm) [in % vol.]

Po_sub_% Drainable Pore Space of subsoil (30 – 100 cm) [in % vol.]

These two components of the drainable pore space are derived from the pedotransfer rule below:

		Po_top_%				Po_sub_%		
Texture	Text1	Pd_top	Pd_top	Pd_top	Td1	Pd_sub	Pd_sub	Pd_sub
Name	CODE	LOW	MED	HIGH	CODE	LOW	MED	HIGH
Coarse	1	30	25	20	1	25	20	18
Medium	2	20	15	10	2	18	15	10
Med-fine	3	15	12	8	3	15	12	8
Fine	4	10	8	5	4	10	8	5
V Fine	5	8	5	3	5	5	3	2

Organic	9	30	25	--	9	30	25	--
None	0	--	--	--	0	--	--	--

The results are in % vol; ‘-999’ indicates no information. The drainable pores space is then converted to mm water storage.

Po_top_mm Drainable Pore Space in the topsoil (0 – 30 cm) in mm

For the calculation of Po_top_mm it was assumed that there is no within 30 cm depth.

Po_top_mm was calculated as following:

$$Po_top_mm = ((Po_top_%)10)0.3$$

The result are in mm for a soil depth of 0 – 30cm of soil; ‘-999’ indicates no information.

Po_sub_mm Drainable Pore Space in the subsoil (30 – 100 cm) in mm

For the calculation of Po_sub_mm it was assumed that there is no restriction to rooting within 100 cm depth.

$$Po_sub_mm = ((Po_sub_%)10)0.7$$

The results are shown in mm for a soil depth of 30 - 100cm, with ‘-999’ indicating no information.

Po_sub_mmr Drainable Pore Space in the subsoil (30 – 100 cm) in mm including restriction of soil depth by rock (Dr)

The calculation is as follows:

$$Po_sub_mmr \text{ (in mm)} = (Po_sub_%) (Dr_rest_{10-30})/10$$

The results are in mm for the 30 – 100cm depth of soil; ‘-999’ indicates no information.

Po_tot_mm Drainable Pore Space (0 – 100 cm) in mm including restriction of soil depth by rock (Dr)

The calculation is as follows:

$$Po_tot_mm = Po_top_mm + Po_sub_mm$$

$$Po_tot_mmr = Po_tot_mm + Po_sub_mmr$$

The results are in mm for 0 - 100cm depth of soil; '-999' indicates no information.

P1swap_top Proportion of the SWAP available for storing precipitation in the topsoil (0 – 30 cm)

P2swap_sub Proportion of the SWAP available for storing precipitation in the topsoil (30 – 100 cm)

P1swap_ awc and P2swap_ awc are derived from:

		P1swap_top			P2swap_sub			
Texture	Text1	Pd_top	Pd_top	Pd_top	Td1	Pd_sub	Pd_sub	Pd_sub
Name	CODE	LOW	MED	HIGH	CODE	LOW	MED	HIGH
Coarse	1	1.0	1.0	0.8	1	1.0	0.8	0.6
Medium	2	1.0	0.8	0.6	2	1.0	0.8	0.6
Med-fine	3	0.8	0.6	0.4	3	0.8	0.6	0.4
Fine	4	0.6	0.4	0.2		0.6	0.4	0.2
V Fine	5	0.3	0.2	0.1	5	0.3	0.2	0.1
Organic	9	1.0	0.9	--		1.0	0.9	--
None	0	--	--	--	0	--	--	--

Swsc Soil Water Storage Capacity; this includes Drainable Pore Space.

The calculation is as follows:

$$Swsc = Swap_tot + (0.5(Po_tot_mm))$$

The results are in mm for 0 – 100cm depth of soil; '-999' indicates no information.

Swsc_r Soil Water Storage Capacity. This includes Drainable Pore Space and any restriction of soil depth by rocks.

The calculation is as follows:

$$Swsc_r = Swap_tot_r + (0.5*(Po_tot_mmr))$$

The results are in mm for 0 – 100cm depth of soil; '-999' indicates no information.

Swap_totef Soil Water Available to Plants (SWAP)effectively available for storing precipitation and including restriction of soil depth by rock

The calculation is as follows:

$$Swap_totef = (P1swap_top)(Swap_top) + (P2swap_sub)(Swap_sub_r)$$

For k the factor 0.5 was assumed.

The results are in mm for 0 – 100cm depth of soil; '-999' indicates no information.

Swsc_eff Effective Soil Water Storage Capacity, including drainable pore space, restriction of soil depth by rock and a proportion of the SWAP available for storing precipitation.

The calculation is as follows:

$$\text{Swsc_eff} = ((\text{P1swap_top}) (\text{Swap_top})) + ((\text{P2swap_sub}) (\text{Swap_sub_r}) + k(\text{Po_tot_mmr}))$$

Where k is initially assigned a value of 0.5.

The results are shown in mm for the depth of 0–100cm of soil, ‘-999’ indicates no information.

Swsc_eff_2 Effective Soil Water Storage Capacity – 2; this includes drainable pore space and the proportion of the SWAP available in the topsoil for storing precipitation.

The calculation is as follows:

$$\text{Swsc_eff_2} = (\text{P1swap_top}) (\text{Swap_top}) + k(\text{Po_tot})$$

Where k is initially assigned a value of 0.5.

The results are in mm for 0 – 100cm depth of soil; ‘-999’ indicates no information.